SUBTYPE-SPECIFIC ROLES FOR PRESYNAPTIC NMDA RECEPTORS IN EXPERIENCE-DEPENDENT PLASTICITY AND VISUAL CORTICAL DEVELOPMENT

Rylan Scott Larsen

A dissertation submitted to the faculty of the University of North Carolina at Chapel Hill in partial fulfillment of the requirements for the degree of Doctor of Philosophy in the Department of Cell Biology and Physiology.

Chapel Hill
2013

Approved By

Benjamin Philpot

Ken McCarthy

Mark Zylka

Paul Manis

Richard Weinberg

Serena Dudek

ABSTRACT

Rylan Scott Larsen: Subtype-specific roles for presynaptic NMDA receptors in experience-dependent plasticity and visual cortical development
(Under the direction of Dr. Benjamin Philpot)

A defining property of the brain is its ability to modify neuronal circuits in response to sensory stimuli to allow for adaptive responses to the environment. In the visual cortex, sensory stimuli shape cortical circuitry through activity-dependent processes. These processes are diverse, however one such mechanism for sensory experience-induced changes in cortical function is Hebbian plasticity. NMDA-type glutamate receptors (NMDARs) are critical to many forms of Hebbian plasticity including LTP and LTD and therefore likely contribute significantly to the development of sensory cortices. NMDARs canonically are postsynaptic receptors, however recent evidence also demonstrates roles for presynaptic NMDARs in synaptic plasticity and modulating synaptic transmission.

In L2/3 of the visual cortex, the molecular identity of presynaptic NMDARs had been explored, but previous findings did not explain how these receptors functioned in manners distinct from their postsynaptic counterparts. I found that the NMDAR subunit GluN3A (NR3A) was critical for the function of presynaptic NMDARs in the visual cortex. Subsequently, I observed that presynaptic NMDARs and GluN3A were regulated by visual experience. The reexpression of

presynaptic NMDARs following visual experience resulted in restoration of the contribution of these receptors to spike timing-dependent plasticity and to glutamate release from L4 inputs. These findings suggest an important role for presynaptic, GluN3A-containing NMDARs in the function of the visual cortex and its modification by sensory experience.

To my mother, whose personal dedication to her own higher education in the face of adversity and her willingness to let her children explore has engendered in me the skepticism and curiosity that drives my interest in science.

Acknowledgements

Most importantly, I wish to thank my mentor Dr. Ben Philpot whose willingness to have me as a student has allowed me to have many fulfilling experiences. In particular, I wish to thank Ben for allowing me to influence the trajectory of my research, perform risky and sometimes expensive experiments, collaborate with amazing scientists (including those in our own lab), and explore the possibilities of a career in science through attending the MBL Neurobiology course and many scientific conferences. I have little doubt that one of the best decisions of my scientific career will always be joining the Philpot lab. Similarly, I should thank Ben for hiring many wonderful people which I have worked with over the years. I wish to thank, Koji Yashiro, Adam Roberts, Hsien-Sung Huang, Thorfinn Riday, Mike Wallace, Janet Berrios, Maile Henson, Jaya Miriyala, Matt Judson, Angie Mabb, and Ji Eun (Hanji) Han for teaching me a great deal and for being great to work with. In particular, I wish to also thank Rebekah Corlew, whose research provided the basis of my projects and who taught me the basics of electrophysiology.

Much of my research would not have been possible without the generosity of collaborators which have provided time, reagents, and mice to my projects. I must especially thank Richard Weinberg and the members of his lab for being

willing to look for NMDA receptors on the wrong side of the synapse. I also must thank all the members of my graduate committee for providing expertise that helps ensure I do the best experiments to address my hypotheses. I wish to thank Paul Manis for providing his vast knowledge of electrophysiology to me and for serving as a supportive additional mentor and dissertation chair. I also wish to thank Ann Stuart who provided me with considerable advice from her many years as a neuroscientist and whose presentation class was a critical component of my graduate education.

I wish to thank my family, and in particular, my parents for being supportive of my many years spent being a student. My parents' personal pursuit of higher education has been a constant positive example for me through my life. I also wish to thank Elyse Dankoski, whose companionship and understanding as a fellow scientist has made my life far better in the last few years.

Table of Contents

List of Tables

List of Figures

LIST OF ABBREVIATIONS

NMDAR, N-methyl-D-aspartate receptor

GluN1, NR1, or *Grin1*- N-methyl-D-aspartate receptor subunit 1 (*Grin* is gene)

GluN2A, NR2A, or *Grin2a* - N-methyl-D-aspartate receptor subunit 2A

GluN2B, NR2B, or *Grin2b* - N-methyl-D-aspartate receptor subunit 2B

GluN2C, NR2C, or *Grin2c* - N-methyl-D-aspartate receptor subunit 2B

GluN2D, NR2D, or *Grin2d* - N-methyl-D-aspartate receptor subunit 2D

GluN3A, NR3A, or *Grin3a* - N-methyl-D-aspartate receptor subunit 3A

GluN3B, NR3B, or *Grin3b* - N-methyl-D-aspartate receptor subunit 3B

AMPAR, alpha-amino-3-hydroxyl-5-methyl-4-isoxazole-propionate receptor

GluR1,alpha-amino-3-hydroxyl-5-methyl-4-isoxazole-propionate receptor subunit

SCNN1A sodium channel, non-voltage-gated 1 alpha subunit

PKA, protein kinase A

PKC, protein kinase C

PP2A, protein phosphatase 2A (calcineurin)

CaMKII, calcium/calmodulin-dependent kinase II

P, postnatal day

ER, endoplasmic reticulum

LTP, long-term potentiation(typically used to refer to frequency-dependent forms)

tLTP, spike timing-dependent LTP

LTD, long-term depression(typically used to refer to frequency-dependent forms)

tLTD, spike timing-dependent LTD

mEPSC, miniature excitatory postsynaptic current

EPSP, excitatory postsynaptic potential

EPSC, excitatory postsynaptic current

IPSC, inhibitory postsynaptic current

mo, months

yr, year

VC, visual cortex

ACSF, artificial cerebrospinal fluid

V1, Primary visual cortex

PNS, postnuclear supernatant

LM, light membranes fraction

CYT, cytosolic fraction

P2, second pellet fraction, crude synaptosomes

P3, third pellet fraction, lysed synaptosomal membranes

TSF, triton-soluble fraction

SPM, purified synaptic plasma membranes

PSD, postsynaptic density

CNS, central nervous system

Ca^{2+}, calcium

Mg^{2+}, magnesium

pre, presynaptic

post, postsynaptic

iMK801, internal MK801

APV or AP5, (2R)-amino-5-phosphonovaleric acid

GABA(A)R GABA(A) receptor

KO, knockout

OE, overexpressor

Chapter 1: Spike Timing-Dependent Plasticity (STDP) in the Developing Sensory Neocortex

1.1 Introduction

A fundamental property of the brain is its ability to change in response to sensory stimuli. These adaptations to changes in either the sensory environment or sensory receptor function provide a substrate for the memory of sensory experiences and perceptual learning. A long-term goal of neuroscience research has been to determine the molecular mechanisms that underlie the formation of cortical responses to environmental stimuli. Changes in synaptic strength have been modeled *in vitro* using low- or high-frequency stimulation to produce long-term depression (LTD) and long-term potentiation (LTP), respectively (Bliss & Lomo, 1973; Dudek & Bear, 1992). While frequency-dependent plasticity has provided a wonderful tool to study the mechanism for the strengthening and weakening of cortical synapses during early stages of development, frequency-dependent plasticity is not sufficient to explain many modifications in synaptic strength that result from changes in sensory experience. Manipulations that produce synaptic plasticity *in vivo* are not always associated with significant changes in firing rates, and changes in firing rates that induce plasticity *in vitro* do not always produce plasticity when occurring naturally *in vivo* (Carandini & Ferster, 2000; Celikel, Szostak, & Feldman, 2004; Fox & Wong, 2005). The discovery that the precise temporal precision of spiking between pre- and post-

synaptic neurons in the hippocampus can dictate whether a synapse is strengthened or weakened raised great excitement, as this timing-dependent plasticity mechanism could readily account for changes observed *in vivo* that were not readily explained by frequency-dependent forms of plasticity (Levy & Steward, 1983; Magee & Johnston, 1997).

Since the initial discoveries of STDP (Bell, Han, Sugawara, & Grant, 1997; Bi & Poo, 1998; Debanne, Gahwiler, & Thompson, 1998; Levy & Steward, 1983; Magee & Johnston, 1997; Markram, Lubke, Frotscher, & Sakmann, 1997), it has been proposed as a mechanism by which receptive field maps and sensory selectivity can be formed and modified *in vivo* (Clopath, Busing, Vasilaki, & Gerstner, 2010; Song & Abbott, 2001). STDP has been observed in sensory cortices just following birth, and is also thought to provide a mechanism for modifying synaptic strength in adulthood (Banerjee et al., 2009; Fu et al., 2002; Pellicciari, Miniussi, Rossini, & De Gennaro, 2009). Although synaptic plasticity can occur throughout life, the induction and expression mechanisms of both frequency-dependent plasticity and STDP are believed to change over development. For example, adult plasticity in response to sensory deprivation is believed to result primarily from the potentiation of spared (sensory-driven) inputs and not by depression of the lost (sensory-independent) inputs (Glazewski & Fox, 1996). Similarly, both frequency- and spike timing-dependent LTD (tLTD) are difficult to induce following postnatal day 30 (P30) in rodents (Banerjee et al., 2009; Corlew, Wang, Ghermazien, Erisir, & Philpot, 2007; Dudek & Bear, 1993; Fox, 2002). This suggests that while the ability to strengthen and weaken

sensory synapses remains throughout life, changes in synaptic proteins that occur throughout development may influence how plasticity is induced or expressed. Herein, we describe mechanisms by which STDP can be shaped through development via the expression of synaptic proteins in the cortices of the somatosensory, visual, and auditory systems (**Table 1**). Although STDP has been observed in many neocortical layers (Egger, Feldmeyer, & Sakmann, 1999; Kampa & Stuart, 2006; Letzkus, Kampa, & Stuart, 2006; Sjostrom, Turrigiano, & Nelson, 2003), for simplicity we focus on the synaptic connection between cortical layer (L) 4 and L2/3 neurons and between L2/3 neurons. These synapses represent the major site of intracortical processing for inputs arriving from the thalamic relays. In addition, STDP in L2/3 synapses has been observed throughout development, is relatively well characterized *in vitro*, and occurs in response to sensory deprivation (Diamond, Huang, & Ebner, 1994; Drew & Feldman, 2009). We also consider the contribution of neuromodulation to the expression and development of cortical STDP. Although we emphasize changes in synaptic proteins between excitatory cortical connections that may influence STDP expression, considerable evidence demonstrates that STDP exists at inhibitory connections (Haas, Nowotny, & Abarbanel, 2006; Holmgren & Zilberter, 2001) and that there are considerable changes in inhibitory circuitry during development (Yazaki-Sugiyama, Kang, Cateau, Fukai, & Hensch, 2009) that are likely to be shaped by STDP.

1.2 STDP in somatosensory cortex

STDP in rodent primary somatosensory cortex (S1) has been proposed to underlie refinement of receptive fields in response to changes in whisker stimulation (Feldman, 2009; Fox & Wong, 2005). In support of this idea, whisker trimming during early life alters the firing sequence of L4-L2/3 synaptic connections *in vivo* to produce timing patterns known to weaken synapses *in vitro*, and this change in the temporal precision of spiking precedes the degradation of L2/3 receptive field maps (Celikel et al., 2004; Feldman, 2000). Response depression can also be produced *in vivo* by pairing natural spike trains with coincident whisker deflection to mimic the timing requirements for inducing tLTD *in vitro* (V. Jacob, Brasier, Erchova, Feldman, & Shulz, 2007). Such findings suggest that STDP is likely to occur naturally during receptive field refinements through development and even into adulthood (Clark, Allard, Jenkins, & Merzenich, 1988). Below, we discuss the molecular mechanisms underlying STDP and how they may be regulated to produce and tune STDP in developing S1.

1.2.1 tLTP in S1

In general, the induction of timing-dependent LTP (tLTP) in cortical areas requires glutamate binding of NMDA receptors (NMDARs) coincident with arrival of a back-propagating action potential (BAP) into the postsynaptic dendrite (Froemke, Poo, & Dan, 2005; Letzkus et al., 2006; Magee & Johnston, 1997). The pairing of glutamate binding with the BAP causes the removal of Mg^{2+} from NMDARs and produces a supralinear summation of calcium entering through

NMDARs and voltage-gated calcium channels (VGCCs) (Kampa & Stuart, 2006; Koester & Sakmann, 1998; Nevian & Sakmann, 2006). Despite the importance of both VGCCs and NMDAR activation for tLTP induction, postsynaptic NMDARs are believed to act as the sole coincidence detector for tLTP within the neocortex (Froemke et al., 2005; Froemke, Tsay, Raad, Long, & Dan, 2006; Rodriguez-Moreno & Paulsen, 2008).

S1 pyramidal cells maintain the ability to express tLTP into adulthood, and many of the induction parameters appear to be similar throughout life. For example, the timing requirements for tLTP induction are largely unchanged across development, as pre-post pairings with positive intervals of ~10 ms readily induce tLTP from P6-P100 (Banerjee et al., 2009; Bender, Bender, Brasier, & Feldman, 2006; Feldman, 2000; Rodriguez-Moreno & Paulsen, 2008). The requirement for postsynaptic NMDAR activation is also maintained across development, because intracortical tLTP is blocked by the NMDAR antagonist APV in S1 in both younger (<P20) and older (>P35) rodents (Banerjee et al., 2009; Frey, Sprengel, & Nevian, 2009; Rodriguez-Moreno & Paulsen, 2008). The induction of tLTP between S1 L4-L2/3 synapses requires postsynaptic NMDARs, because selectively loading the postsynaptic recording pipette with the NMDAR antagonist MK-801 is sufficient to abolish tLTP (Bender et al., 2006; Rodriguez-Moreno & Paulsen, 2008). In addition to having many similar induction requirements across development, the magnitude of tLTP expression also does not correlate with age in rats across the P18-P32 developmental period (Feldman, 2000).

While many aspects of tLTP induction are similar throughout life, there are also likely to be important developmental differences. Because postsynaptic NMDARs are thought to be the sole coincidence detector for tLTP, developmental changes in NMDAR functions may by one important modulator of the properties of tLTP induction. In the neocortex, postsynaptic NMDARs undergo a developmental switch from primarily GluN2B-containing to GluN2A-containing receptors. In rodent S1, this switch to predominately GluN2A-containing receptors occurs ~P9 in L2/3 pyramidal cells (Flint, Maisch, Weishaupt, Kriegstein, & Monyer, 1997; Liu, Murray, & Jones, 2004). As would be predicted based on this expression pattern in S1, GluN2A-, but not GluN2B-containing, receptors are required for tLTP induction at L4-L2/3 synapses in P11-P15 mice (Banerjee et al., 2009). The contribution of GluN2B to tLTP induction has not been studied at young ages (<P6), thus it is not yet clear how the developmental switch from GluN2B to GluN2A influences tLTP induction. There are currently two ideas as to how an increased GluN2A/GluN2B ratio would affect tLTP, with one prediction suggesting that a higher ratio would compress the tLTP timing window (Shouval, Bear, & Cooper, 2002) and the other suggesting that it will make tLTP less likely to be induced (Gerkin, Lau, Nauen, Wang, & Bi, 2007). Both predictions suggest that a shift in the GluN2A/GluN2B ratio would adjust the balance between tLTD and tLTP. Thus, further studies are warranted to determine how changes in S1 postsynaptic NMDAR composition and downstream signaling cascades at different ages influence the expression, magnitude, and timing requirements of tLTP.

1.2.2 tLTD in S1

While postsynaptic NMDARs act as a coincidence detector for tLTP, they have not been shown to act as the coincidence detector for tLTD between L4 and L2/3 synapses. Instead, the near-simultaneous activation of postsynaptic mGluRs coincident with both postsynaptic depolarization and activation of VGCCs is thought to constitute a separate coincidence detector for tLTD (Bender et al., 2006; Karmarkar & Buonomano, 2002). In this model, tLTD is induced when postsynaptic group 1 mGluRs (likely mGluR5) are activated with T- or L-type VGCCs to increase PLC activity (Bender et al., 2006; Nevian & Sakmann, 2006). Activation of PLC leads to generation of inositol 1,4,5-triphosphate (IP_3) and intracellular release of calcium from IP_3-mediated internal stores (Bender et al., 2006; Nevian & Sakmann, 2006). This calcium, along with the calcium released from VGCCs, combines to trigger release of the endocannabinoid 2-arachidonyl glycerol (2-AG) from the postsynaptic neuron (Bender et al., 2006). Activation of presynaptic CB1 receptors and presynaptic NMDARs results in lasting reductions in release probability from the presynaptic neuron, although the time course and pathways by which this occurs remains to be determined. This type of LTD can become manifest with post-before-pre action potential pairings occurring with intervals up to 50 ms (Bender et al., 2006; Feldman, 2000; Nevian & Sakmann, 2006), which is much longer than the 10-20 ms pre-before-post timing window required for tLTP induction. It should be noted that tLTD in the visual cortex can also be induced in a manner thought to rely on

postsynaptic NMDARs as the coincidence detector (Froemke et al., 2005; Urakubo, Honda, Froemke, & Kuroda, 2008), and a similar mechanism is likely to occur in S1. Exactly how these two forms of tLTD cooperate or are segregated is not clear, and it is possible that development influences tLTD in a location or spike-dependent manner.

While tLTP is thought to be inducible throughout life, a dramatic reduction in the ability to induce tLTD *in vitro* between L4-L2/3 synapses in rodent S1 occurs by P25 (Banerjee et al., 2009). This decrease in tLTD magnitude is reminiscent of the developmental loss of frequency-dependent LTD in CA1 of the hippocampus (Dudek & Bear, 1993) and to the loss of LTP at S1 thalamocortical synapses (Crair & Malenka, 1995). A developmental reduction in tLTD magnitude has also been observed in L4-L2/3 synapses in primary visual cortex, and this loss is curiously dependent on inhibition (Corlew et al., 2007). This suggests that a developmental increase in inhibition might limit tLTD induction, perhaps through shunting inhibition, but this hypothesis has yet to be rigorously tested. Since standard experimental protocols do not reliably induce tLTD in mature neocortex, it is possible that the requirements for tLTD induction are different, and will require increasing the number or adjusting the timing of the pairings. In support of this idea, a very narrow window for inducing tLTD has been observed in adult rats *in vivo* (V. Jacob et al., 2007).

Before P25 in rodents, it is remarkable that the magnitude of tLTD is similar at all ages tested (P6-P32; (Banerjee et al., 2009; Feldman, 2000), despite large changes in many of the proteins involved in tLTD induction. Among

these proteins, mGluRs and their downstream effectors are developmentally upregulated before P15. The requirement for group 1 mGluRs for tLTD at L2/3 synapses has been shown at P13-P23, when mGluR expression begins to plateau (Bender et al., 2006; Nevian & Sakmann, 2006). In S1, mGluR5 expression is uniform in all layers by P16 and remains constant at these levels through adulthood (Blue, Martin, Brennan, & Johnston, 1997). Similarly, the expression of group 1 mGluR's downstream effector, PLC, reaches stable expression in S1 by P14 (Hannan, Kind, & Blakemore, 1998). The early developmental upregulation of mGluR5 and PLC expression do not seem to influence the magnitude or induction of tLTD, because mice aged P6-P8 show tLTD with a similar magnitude to mice at P11-P25 (Banerjee et al., 2009). This suggests that mGluRs do not developmentally gate tLTD induction, but may influence tLTD in other ways. It is clear that mGluRs and their downstream effectors play an important role in S1 development because the genetic deletion of mGluR5 or PLC causes barrels to form improperly (Hannan et al., 2001), yet whether this is a direct consequence of altered tLTD remains unknown.

Synaptic proteins involved in tLTD induction have also been suggested to be segregated based on synapse. For example, the requirement both for endocannibinoid signaling and specific preNMDAR subunits differs by synaptic pathway. In mice, CB1Rs are not required for tLTD between L4-L2/3 synapses at either P11-P15 or P28-P42 but are required between L2/3-L2/3 synapses at P11-P15 (Banerjee et al., 2009; Hardingham, Wright, Dachtler, & Fox, 2008). In contrast, CB1Rs and postsynaptic endocannabinoid synthesis are required for

tLTD induction between L4-L2/3 rat neurons at P16-P23 (Bender et al., 2006). These differences may reflect laminar and species-specific differences in the activation of CB1Rs or their downstream signaling. The expression of CB1Rs reaches stable adult levels by P16 in rats and CB1R function is required during this period for barrel receptive field formation (Bodor et al., 2005; Deshmukh et al., 2007). Chronically blocking CB1Rs with the *in vivo* administration of the antagonist AM251 between P13-P16 disrupts whisker tuning and results in the loss of experience-dependent plasticity in L2/3 rat S1 (L. Li et al., 2009). This demonstrates the importance of CB1R signaling in rats at a time when tLTD is readily inducible both *in vivo* and *in vitro* by CB1R activation, suggesting that there may be a causal relationship between tLTD induction and receptive field tuning in S1.

In a similar fashion to the segregation of endocannabinoid signaling across cortical layers, there are differing layer-dependent requirements for presynaptic NMDAR subunits. Moderately selective GluN2C/D antagonists, but not GluN2B or GluN2A antagonists, block the induction of tLTD between L4-L2/3 S1 synapses (Banerjee et al., 2009). In contrast, L2/3-L2/3 synapses show a requirement for GluN2B-containing receptors, but not GluN2C/D (Banerjee et al., 2009). The segregation of presynaptic NMDAR subunits may permit differential modulation of tLTD depending on the synaptic pathway, which is consistent with previous findings that the induction requirements and timing windows of STDP depend on dendritic location (Froemke et al., 2005; Letzkus et al., 2006). The mechanisms by which STDP are induced appear diverse and synapse-specific.

Due to the wide variety of synaptic mechanisms for induction, tLTD may be developmentally regulated in a unique way at each synapse. Studies that compare the pathway-specific tLTD mechanisms could determine the exact requirements for tLTD induction at each S1 synapse. The existing evidence suggests that the molecular mechanisms of tLTD are not universal across synapses within sensory cortices.

1.3 STDP in visual cortex

The importance of coordinated activity in the developing visual cortex was first demonstrated in groundbreaking experiments by Hubel and Wiesel where binocular receptive fields were converted to monocular receptive fields by changing the synchrony of visual inputs in kittens with artificial strabismus (Hubel & Wiesel, 1965). STDP within the visual cortex likely follows constraints unique to the environmental stimuli it receives, allowing this form of plasticity to modulate synaptic connectivity in a manner that is different from S1. Like plasticity in S1, STDP in V1 is a relevant mechanism for synaptic strengthening and weakening. Indeed, pairing action potentials with precisely timed visual stimuli induces STDP *in vivo* (Meliza & Dan, 2006). In further support of the idea that STDP can shape visual processing, manipulating the temporal order of spiking in V1 neurons is sufficient to change orientation preferences and receptive fields *in vivo,* and these modifications can occur in a bidirectional manner similar to STDP timing rules observed *in vitro* (Schuett, Bonhoeffer, & Hubener, 2001). For example, when visual stimuli of a particular orientation are paired with electrical stimulation of a neuron, the orientation preference of that

neuron shifts towards that of the given stimuli (Schuett et al., 2001). Reversing the pairing order (so that the neuron fires before the visual stimuli) weakens the orientation preference away from the given orientation in a tLTD-like manner. Additionally, the pairing of visual stimuli at two orientations shifts the orientation preference of V1 neurons depending on the temporal order of the pairings and can be predicted based on the temporal windows of STDP induced *in vitro* (H. Yao & Dan, 2001). The ability to modify visual responses via STDP learning rules exists through adulthood, as the pairing of visual stimuli can rapidly modify receptive fields and orientation preferences in adult cats (Fu et al., 2002; H. Yao & Dan, 2001). Lastly, STDP learning rules have been shown to be sufficient to segregate sensory inputs onto specific dendritic branches, underscoring how STDP may be essential for shaping cortical connectivity (Froemke et al., 2005). Overall these observations suggest that STDP provides a powerful mechanism by which visual cortical circuitry can be modeled and by which neurons can rapidly adapt to an ever-changing visual environment throughout life. Many synaptic proteins implicated in STDP induction or expression are developmentally regulated between P10-P35 in rodents, overlapping with periods of receptive field development and the visual cortical critical period (Hensch, 2005b; Smith & Trachtenberg, 2007). The regulation of these synaptic proteins may therefore favor the development and stability of visual circuits through adulthood by modulating STDP.

A surprising observation, which we will discuss below, is that the mechanisms of STDP appear largely similar between S1 and V1. The most

pronounced differences in STDP between these regions are due to a developmental delay in V1 development compared to S1 development, and this delay is likely due to a delay in sensory-driven activity in V1.

1.3.1 tLTP in V1

Similar to tLTP observed in the somatosensory cortex, tLTP in V1 is believed to rely on the interaction of BAPs with calcium influx through postsynaptic NMDARs and L-type VGCCs (Froemke et al., 2005; Froemke et al., 2006). NMDARs are required for tLTP induction between P12-P35 at both L5 and L2/3 V1 synapses (Froemke et al., 2006; Markram et al., 1997; Zilberter et al., 2009). Unlike S1, the exact postsynaptic NMDAR subunits required for tLTP have not been investigated. Postsynaptic NMDARs in V1 show a developmental shift from GluN2B to GluN2A at a period later in development (~P25) as compared to other cortical areas (de Marchena et al., 2008). This suggests that a greater proportion of GluN2B-containing receptors may participate in tLTP induction before P25 in the visual cortex compared to somatosensory cortex, although it has been reported that the GluN2B antagonist ifenprodil does not have a major impact on the NMDA:AMPA ratio in L5 neurons of P14-P15 rats (Sjostrom et al., 2003). How the switch in NMDAR subunits during the visual critical period influences STDP induction and expression is not known, but it may involve temporal changes in NMDAR glutamate binding (Laurie & Seeburg, 1994), magnesium sensitivity (Clarke & Johnson, 2006), or allosteric interactions (Urakubo et al., 2008) that could alter dendritic calcium and shape the temporal window for inducing STDP (Shouval et al., 2002).

Surprisingly little is known about how the properties of tLTP adjust over development in the visual cortex, but some assumptions can be made based on known tLTP mechanisms. In addition to the aforementioned changes in NMDAR subunit expression, there are other developmental changes in tLTP-related proteins that can affect tLTP induction across the length of the dendrite. The magnitude of tLTP in L2/3 pyramidal neurons varies with location of the stimulated inputs, such that stimulation of synapses on the proximal dendrite produce a larger magnitude of tLTP than stimulation of synapses on more distal dendrites (Froemke et al., 2005). This effect probably depends on the attenuation of the BAP along the extent of the dendrite (Froemke et al., 2005; Magee & Johnston, 1997; Sjostrom & Hausser, 2006), which would be predicted to affect the supralinear potentiation of calcium that has been observed with tLTP induction (Nevian & Sakmann, 2006). Such an interpretation is consistent with studies in the somatosensory cortex showing that voltage-gated sodium channel dependent action potentials, in turn activate VGCCs (Kampa & Stuart, 2006; Komai et al., 2006). Consequently, any developmental changes in the magnitude or localization of dendritic sodium or calcium channels would be expected to alter the timing requirements and magnitude of tLTP, perhaps by changing the resulting calcium transient. Developmental changes in other dendritic proteins that can affect the shape or size of the BAP, such as A-type potassium channels (Froemke et al., 2005; Hoffman, Magee, Colbert, & Johnston, 1997), would likewise be expected to alter tLTP induction and expression.

1.3.2 tLTD in V1

Like tLTP, NMDAR activation is required for the induction of tLTD. Unlike tLTP, there appears to be both a presynaptic and a postsynaptic contribution of NMDARs. The relative contribution of pre- and post-synaptic NMDARs may vary by age and pathway. Initial studies using bath-applied APV to globally block NMDARs led to the assumption that the NMDARs relevant to tLTD were exclusively postsynaptic (Feldman, 2000; Markram et al., 1997). Later studies in ~P14-P18 rodents found that tLTD could still be induced when postsynaptic (but not presynaptic) NMDARs were blocked (Corlew et al., 2007; Sjostrom et al., 2003). This form of tLTD appeared to have a dual requirement for presynaptic NMDAR and CB1R activation, similar to what has been described for S1 (Bender et al., 2006; Rodriguez-Moreno & Paulsen, 2008; Sjostrom et al., 2003), although whether preNMDARs are acting on a rapid or slow time scale has been debated (Bender et al., 2006; Sjostrom et al., 2003).

While some studies have shown that tLTD at L5-L5 and L4-L2/3 synapses requires presynaptic NMDAR activation (Corlew et al., 2007; Sjostrom et al., 2003), others have shown that tLTD is fully blocked by postsynaptic inhibition of NMDARs in L2/3 V1 neurons (Froemke et al., 2005; Urakubo et al., 2008). This apparent discrepancy might be explained by age-related modifications in the mechanisms of tLTD. Presynaptic NMDARs, which are required for tLTD during early life, are sharply downregulated between P16 and P27 (Corlew et al., 2007). Remarkably, this anatomical reduction in presynaptic NMDARs coincides with the loss of presynaptically-expressed tLTD between L4-L2/3 synapses, which

occurs around three weeks of age, suggesting that there may be a causal relationship between the two events. In support of this idea, studies showing a requirement for presynaptic NMDARs in tLTD have been performed in P14-P18 rodents, while those that support a postsynaptic requirement for NMDARs have been performed in rodents including ages >P21. The form of tLTD involving postsynaptic NMDARs requires activation of the phosphatase calcineurin (Froemke et al., 2005; Urakubo et al., 2008), but it is not known if this is a requirement in younger rodents (**Figure 1.1**).

In addition to developmental changes in the contribution of presynaptic NMDARs to tLTD, there are also likely to be differences in the role that inhibition plays in tLTD. A developmental loss of tLTD at L4-L2/3 synapses is evident in V1 by ~P23 (Corlew et al., 2007), similar to that observed in S1 by ~P25 (Banerjee et al., 2009). However, the induction of tLTD can be restored in older mice by performing the post-before-pre pairing protocol in the presence of $GABA_A$ receptor antagonists (Corlew et al., 2007). When inhibition is blocked at these older ages, tLTD requires *post*synaptic NMDARs instead of *pre*synaptic NMDARs. This suggests development may shape the mechanism by which tLTD is induced from one that is predominately presynaptic to one that is predominately postsynaptic. It is interesting that tLTD that relies on postsynaptic NMDAR activation in older animals is smaller in magnitude than that induced at younger ages, suggesting development may also subtly affect tLTD magnitude in V1 (Corlew et al., 2007). As the loss of presynaptically expressed tLTD coincides with a period of rapid inhibitory development (Hensch, 2005b), it

suggests that inhibition may influence the mechanisms underlying tLTD. An unresolved issue is whether tLTD requires one or two coincidence detectors. While inhibition is one factor that influences tLTD induction mechanisms, others such as dendritic location (Froemke et al., 2005) and dendritic calcium buffering (Kampa & Stuart, 2006; Nevian & Sakmann, 2006) may also influence how tLTD is induced.

1.4 STDP in auditory cortex

Sounds in the acoustic environment have complex temporal structures that overlap in time, space, and frequency content. Cortical lesion studies demonstrate the importance of the auditory cortex in the perception of time-varying sounds across a large range of time scales (Whitfield, 1980). As in visual cortex, coordinated activity may play a role in plasticity in auditory cortex. Raising rats in a noisy environment devoid of structured spectral and temporal cues delays the refinement of the tonotopic map in primary auditory cortex (A1), and this can be reversed by experience in an acoustic environment with tonal structure (Chang and Merzenich, 2003). Neurons in A1 can fire with millisecond precision to the fine temporal structure of acoustic stimuli (for example, Tomita and Eggermont, 2007), and it was recently shown that millisecond differences in neural activity in A1 can be exploited to guide decisions (Y. Yang, DeWeese, Otazu, & Zador, 2008). Given the robust plasticity, importance of temporal features in sound identification and discrimination, and the precision of spiking timing in A1 (Bao, Chang, Woods, & Merzenich, 2004; Kudoh & Shibuki, 1994; Recanzone, Schreiner, & Merzenich, 1993), it is natural to wonder whether A1

has unique timing rules for STDP. Although surprisingly few studies of STDP have been performed in A1, the studies to date suggest that the properties of STDP in A1 are fundamentally similar to those observed in other sensory cortices.

STDP-like rules have been observed in a variety of species (Gerstner, Kempter, van Hemmen, & Wagner, 1996) throughout the auditory pathway, including brainstem (Tzounopoulos, Kim, Oertel, & Trussell, 2004) and cortical areas (Schnupp, Hall, Kokelaar, & Ahmed, 2006). STDP in the dorsal cochlear nucleus appears to follow Hebbian and anti-Hebbian patterns in a cell-specific manner (Tzounopoulos et al., 2004). In contrast, STDP in the auditory cortex, at least at some synapses onto pyramidal cells, appears to follow a traditional Hebbian rule. In P12-P18 rat auditory cortical slices, repetitive pairing of pre-before-post spiking activity at 10 ms intervals produces tLTP and post-before-pre intervals at 40 ms produces tLTD at L2/3-L2/3 synapses (Karmarkar et al 2002). Although the entire STDP window in A1 was not investigated in this study, the results are consistent with findings at similar synapses in P10-P35 rat V1 (Froemke et al., 2006) and in P13-P15 rat S1 (Nevian & Sakmann, 2006). These data suggest that, at least *in vitro*, STDP rules between L2/3 neurons appear roughly similar in all sensory cortices.

In vivo studies also support a role for STDP in A1. In anesthetized and awake adult ferrets, repetitive and asynchronous pairings of pure tones of different frequencies produce shifts in the frequency selectivity of neurons recorded extracellularly (Dahmen, Hartley, & King, 2008), and the temporal

specificity of these shifts is similar to that observed *in vitro*. In this study, a non-preferred tone frequency was paired with a preferred tone frequency with an 8-12 ms time delay between the two tones. When the non-preferred tone was presented before the preferred tone, there was a shift in the neuronal best frequency towards the non-preferred tone frequency. Conversely, when the non-preferred tone frequency was played after the preferred tone frequency, then the neuronal best frequency shifted away from the non-preferred tone. The duration of STDP in A1 observed *in vivo* is similar to that reported in visual receptive fields of V1 in anesthetized cats (H. Yao & Dan, 2001) and for STDP in whisker-evoked responses of barrel cortex in rats (V. Jacob et al., 2007). Interestingly, in A1, the shifts in cortical frequency tuning are restricted to cortical L2/3 and L4 (Dahmen et al., 2008). These observations highlight that the temporal relationships among the components of acoustic stimuli on a millisecond scale to influence auditory processing and suggest that STDP is a relevant mechanism for plasticity in the auditory cortex.

To date, little is known about the mechanistic pathway or developmental modifications of STDP in A1. As STDP displays components of frequency-dependent LTP and LTD, it is rational to speculate that it may use the same mechanisms known to underlie associative LTP and LTD (Malenka & Bear, 2004). Indeed, many of the mechanisms for frequency-dependent plasticity in S1 and V1 are similar to those demonstrated for STDP, it is reasonable to assume that the same may be true for A1. In A1, frequency-dependent LTP and LTD have been demonstrated at thalamocortical synapses and at excitatory

intracortical synapses (Bandrowski, Ashe, & Crawford, 2001; Kudoh & Shibuki, 1994, 1996, 1997). The induction of frequency-dependent LTP is regulated by age and experience (Speechley, Hogsden, & Dringenberg, 2007), suggesting that the same may be true for tLTP. Frequency-dependent LTP of thalamocortical synapses requires activation of NMDARs (Kudoh & Shibuki, 1994, 1996), while LTD at the same synapse requires activation of mGluRs receptors and protein kinase C (Bandrowski et al., 2001). It might be expected in A1 that tLTD requires mGluR activation and activation of a PKC pathway, while tLTP may involve the classic postsynaptic NMDAR pathway. While such a finding would be consistent with tLTP and tLTD mechanisms in V1 and S1, there is not yet experimental evidence that this is true.

1.5 Neuromodulation of STDP in sensory cortices

Neuromodulators alter receptive field plasticity in sensory cortices by expanding the cellular representation of sensory stimuli (Weinberger, 2003). Examples thought to engage neuromodulators include the observations that (1) classical conditioning using whisker stimuli expands the representation of trained whiskers in S1 (Siucinska & Kossut, 2004), (2) perceptual training on visual stimulus orientation discrimination tasks alters V1 tuning for the trained feature (Fu et al., 2002), and (3) activation of cholinergic or dopaminergic inputs during tonal stimuli increases A1 responses to the tone frequency (Bakin & Weinberger, 1996; Bao, Chan, & Merzenich, 2001; Weinberger, Miasnikov, & Chen, 2006). At the cellular level, neuromodulators have both facilitating and depressing effects

on cortical activity that depend on the type of neuromodulators and the pattern of neuromodulator receptors expressed in sensory cortices (Spehlmann, 1971).

The effects of neuromodulators on receptive field plasticity appear to depend on the engagement of STDP-like mechanisms. The properties of STDP can be powerfully adjusted by neuromodulators, which can control the polarity, magnitude, or even the ability to induce STDP through development. In the absence of neuromodulators, tLTD and tLTP can be induced in L2/3-L2/3 synapses in developing V1 by temporally pairing EPSPs to β or γ oscillations produced by injected sinusoidal currents, such that EPSPs synchronous with hyperpolarizing and depolarizing membrane potentials produced tLTD and tLTP, respectively (Wespatat, Tennigkeit, & Singer, 2004). This form of tLTP is impaired in V1 slices from older rats (>P21), but it can be rescued when pairings are made while muscarinic receptors are activated (Wespatat et al., 2004). Similarly, both tLTP and tLTD are impaired at L4-L2/3 synapses in older rat V1, but both tLTD and tLTP can be recovered when AP-EPSP pairings are made in the presence of M1 muscarinic or β-adrenergic receptor activation, respectively (Seol et al., 2007). These results demonstrate that neuromodulators gate STDP in the adult brain. In addition to their role as permissive gatekeepers for STDP induction, neuromodulators are also likely to control the polarity and temporal requirements for inducing STDP plasticity in sensory cortices, as such roles for neuromodulators have been observed in other areas of the brain. For example, in L2/3-L5 synapses in prefrontal cortex, nicotine application converts tLTP to tLTD (Couey et al., 2007). In hippocampal CA1, a β-adrenergic receptor agonist

broadens the tLTP window from 3-10 ms to 15 ms without affecting tLTP magnitude (Y. W. Lin, Min, Chiu, & Yang, 2003). Also at hippocampal synapses, dopamine agonists not only extends the tLTP window from 20 ms to at least 45 ms but, also converts tLTD to tLTP (Zhang, Lau, & Bi, 2009). Thus, neuromodulators can adjust multiple aspects of STDP induction, and the precise effects of neuromodulators on STDP induction likely depend on the neuromodulator, receptor types, synaptic pathway, and age.

How might neuromodulators alter the properties of STDP? Although there are many targets of neuromodulators, the common denominator for most of these mechanisms is that they ultimately influence local calcium levels associated with AP-EPSP pairings. There are several mechanisms by which neuromodulators bring about their effects on calcium levels. First, neuromodulators can activate kinases and phosphatases that regulate the kinetics and availability of dendritic ion channels, such as transient (I_A) and Ca^{2+}-activated K^+ channels (Watanabe, Hoffman, Migliore, & Johnston, 2002). Such modulation brings about profound changes in the width and amplitude of BAPs, ultimately influencing dendritic calcium (Froemke et al., 2006; Magee & Johnston, 1997). For example, β-adrenergic and muscarinic receptor agonists enhance spike backpropagating efficacy by phosphorylating protein kinase A and protein kinase C that result in reduction of I_A channel availability (Hoffman & Johnston, 1998, 1999; Tsubokawa & Ross, 1997). Such changes in I_A might contribute to the observations that M1 muscarinic receptors promote tLTD induction through a PLC-dependent pathway, while β-adrenergic receptor activation promotes tLTP

through the adenylyl cyclase cascade (Seol et al 2007). Second, neuromodulators can target IP_3 receptors and activate calcium-induced-calcium-release from intracellular stores, thereby influencing polarity and input-specificity of STDP (Nishiyama, Hong, Mikoshiba, Poo, & Kato, 2000). Third, neuromodulators can facilitate NMDAR currents (Brocher, Artola, & Singer, 1992; Kirkwood, Rozas, Kirkwood, Perez, & Bear, 1999) and presumably directly regulate STDP induction. Although it has not yet been investigated, developmental changes in neuromodulator influences are also likely to affect the timing rules for inducing STDP in sensory cortices and could play a role in defining critical periods. In support of this possibility, the expression of certain neuromodulator receptor families, such as alpha 7 nicotinic receptors and 5HT receptors, exhibit dramatic regulation around the critical period for receptive field plasticity in sensory cortices (Aramakis & Metherate, 1998; Basura et al., 2008; Broide, O'Connor, Smith, Smith, & Leslie, 1995; Broide, Robertson, & Leslie, 1996).

1.6 Conclusion

The studies discussed here support the argument that STDP is a key mechanism used in sensory processing in somatosensory, visual, and auditory cortices, both for the establishment of circuits during development, and for the storage and processing of sensory information later in life. At a cellular level, STDP is shaped by, but also modifies, specific synapses to produce refinements in neuronal responses to sensory stimuli. While we have emphasized the role of synaptic proteins in shaping STDP, very little is known about how these changes

influence the exact characteristics of induction, expression, and timing of STDP. As STDP depends not just on timing, but on spike patterning (Froemke & Dan, 2002; Froemke et al., 2006; Nelson, Sjostrom, & Turrigiano, 2002; Sjostrom, Turrigiano, & Nelson, 2001), dendritic location (Froemke et al., 2005; Letzkus et al., 2006; Sjostrom & Hausser, 2006), and previous neuronal activity (Zilberter et al., 2009), the roles of specific synaptic proteins in regulating STDP are likely both state- and context-dependent. These changes likely coincide with developmental changes in inhibition and neuromodulation that also shape how STDP learning rules are applied to sensory information (Kirkwood et al., 1999; Meredith, Floyer-Lea, & Paulsen, 2003). Therefore, STDP refines sensory inputs in a manner that is dependent on the developmental context while providing feedback that further changes cortical structure and function.

It is clear that there are large gaps in our knowledge regarding STDP in sensory cortices as well. For example, STDP timing windows, as measured experimentally, are quite noisy, which may reflect either the basal state of synapses prior to the experimental measurement, or the specific selection of synaptic pathways during recording. This variability makes it difficult to discern whether the timing windows are truly different between sensory areas or within different local circuit pathways, as might be predicted from the different temporal dynamics of the incoming sensory information versus the temporal dynamics of local and long-distance intracortical pathways. This biological variability is confounded by inevitable discrepancies in experimental approaches. Second, the reversibility of STDP in sensory cortex has not been investigated. In one of

the first investigations of STDP (Bell et al., 1997) in the electrosensory lobe of mormyrid fish, STDP could be induced rapidly and was readily reversed within minutes with appropriate pairing patterns. Reversibility of timing-dependent plasticity has also been observed in the xenopus retinotectal system (Zhou, Tao, & Poo, 2003). Is STDP in sensory cortex similarly reversible? Such rapid and reversible plasticity would seem to have clear utility in sensory processing, independent of a role in establishing longer sensory memory or shaping response maps. Third, the role of STDP in the inhibitory network is far from understood. Developmental changes in inhibition help drive the establishment of cortical circuits, and may involve STDP (Kanold & Shatz, 2006). Within established cortical networks, both inhibition and excitation exhibit plasticity (Froemke, Merzenich, & Schreiner, 2007; Galindo-Leon, Lin, & Liu, 2009; Lu, Li, Zhao, Poo, & Zhang, 2007), but it is not known whether this *in vivo* plasticity is spike-timing based or not. Given the critical role of inhibition in shaping response maps and spike timing, the role of STDP at inhibitory synapses merits greater investigation. Fourth, the role of STDP in the development and establishment of sensory response maps, while an attractive hypothesis supported by computational studies (Song & Abbott, 2001) and consistent with the available data, has not yet been unequivocally tested. To clarify the role of STDP, rate-based versus timing-based plasticity mechanisms must be disentagled to identify their respective roles in receptive field plasticity *in vivo*. Experimental approaches that allow manipulation of spike trains with millisecond precision *in vivo* are just emerging (Boyden, Zhang, Bamberg, Nagel, & Deisseroth, 2005;

Chow et al., 2010; Gunaydin et al., 2010). These technologies can be leveraged in cleverly-designed experiments and carefully-posed questions to answer the major issues outstanding in the field of STDP.

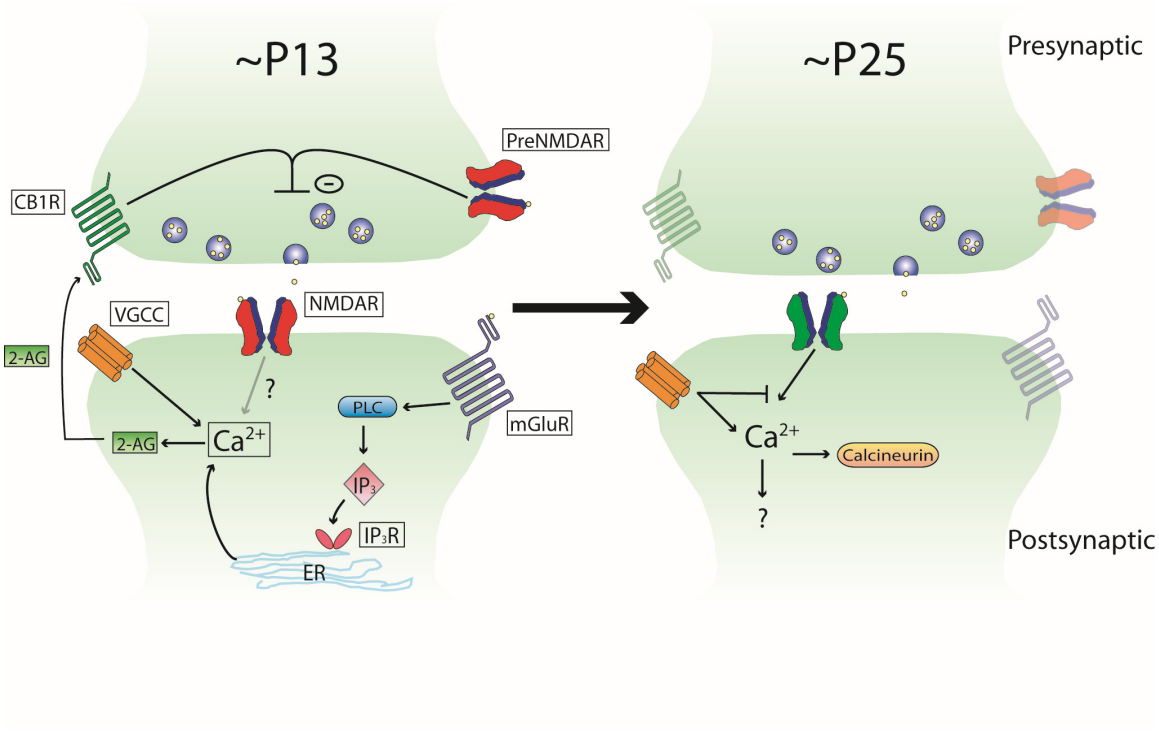

Fig 1.1: Schematic depicting developmental changes in known tLTD induction mechanisms at L4-L2/3 synapses in rodent sensory neocortex. Note that the mechanisms are very similar between the different sensory areas, and that this scheme could apply to primary visual cortex as well as primary somatosensory cortex (see text for details).

Table 1 - Excitatory STDP in Sensory Neocortices

Author	Area	Species	Pathway	Method	Age	*In vivo / in vitro*	tLTP Δt (ms)	tLTD Δt (ms)	NMDARs	Pre-NMDARs	Postsynaptic Ca^{2+}	mGluRs	Ca^{2+} Stores	Endo-cannabinoid	Other
Karmarkar, 2002	A1	Rat	L2/3-L2/3	whole-cell, extra. stim.	P12-18	*in vitro*	10	-40							
Dahmen, 2008	A1	Ferret	?	single units	adult	*in vivo*	8 to 12	-12 to -8							
Jacob, 2007	S1	Rat	L2/3, L5, L6	single units, whole-cell	P27-32, adult (single units)	*in vivo*		-17 to -7							
Frey, 2009	S1	Mouse	L2/3-L2/3	whole-cell, extra. stim.	P39-100	*in vitro*	10		tLTP		tLTP				GluR1 NR
Feldman, 2000	S1	Rat	L4-L2/3	whole-cell, extra. stim.	P18-31	*in vitro*	3 to 15	-50 to 0	tLTP, tLTD						
Banerjee, 2009	S1	Mouse	L4-L2/3, L2/3-L2/3	whole-cell, extra. stim.	P6-8, P11-15, P19-25, P25-42	*in vitro*	10	-15 to -10	tLTP L4-L2/3 (NR2A)	tLTD L4-L2/3 (NR2C/D) L2/3-L2/3 (NR2B)				tLTD - (L2/3-L2/3, NR at L4-L2/3)	
Hardingham, 2008	S1	Mouse	L4- L2/3	whole-cell, extra. stim.	P28-42	*in vitro, in vivo*	10	-50						NR	
Rodriguez-Moreno, 2008	S1	Mouse	L4-L2/3	paired, extra. stim.	P9-14	*in vitro*	10	-15	tLTP (post)	tLTD					
Bender, 2006	S1	Rat	L4-L2/3	whole-cell, extra. stim.	P16-23	*in vitro*	5	-25	tLTP (post)	tLTD	tLTP, tLTD- (T- & L-type)	tLTD - (mGluR5)	tLTD- IP_3R , CICR NR	tLTD - (2-AG & CB1Rs)	
Egger, 1999	S1	Rat	L4-L4	paired	P12-14	*in vitro*		<25	NR		tLTP	tLTP - (group 2)			
Nevian, 2006	S1	Rat	L2/3-L2/3	whole-cell, focal stim.	P13-15	*in vitro*	10	-50 to -10	tLTP	tLTD	tLTP, tLTD - (T-type)	tLTD - (group 1), tLTP - NR	tLTD - IP_3R NR	tLTD - CB1Rs	tLTD - PLC
Letzkus, 2006	S1	Rat	L2/3-L5	paired	P21-42	*in vitro*	-10 (distal) 10 (proximal)	-10 (proximal) 10 (distal)	tLTP, tLTD (distal)		tLTP - (T- or R-type)				
Kampa, 2006	S1	Rat	L5-L5	paired, extra. stim.	P21-28	*in vitro*	10 (3 APs) -15 (3 APs)	-40 (3 APs)	tLTP		tLTP - (T- or R-type)				
Yao, 2001	V1	Cat Human	?	single units	adult	*in vivo*	~0 to ~45	~-20 to ~-5							
Seol, 2007	V1	Mouse	L4-L2/3	whole-cell, extra. stim.	P21-28	*in vitro*	no tLTP *	no tLTD *							
Sjöström, 2003	V1	Rat	L5-L5	paired	P12-21	*in vitro*		-10 and -25		tLTD NR2B	tLTD			tLTD- CB1Rs	
Zilberter, 2009	V1	Rat	L2/3-L2/3	paired	P14-21	*in vitro*	3 to 5 (10 APs)	2 to 10 (1 AP) -12 to -5 ms (10 APs)	tLTP, tLTD - NR		tLTD, tLTP - (L-type)	tLTD - (group 1/2)		tLTP or tLTD - NR	
Corlew, 2007	V1	Mouse	L4-L2/3	whole-cell, extra. stim.	P13-17, P23-30	*In vitro*		-25 to -5	tLTD (P23-30, post)	tLTD (P13-17)					
Markam, 1997	V1	Rat	L5-L5	paired	P14-16	*in vitro*	-10	5 to 10	tLTP						
Froemke, 2005	V1	Rat	L2/3	whole-cell, focal stim.	P14-28	*in vitro*	0 to 30	-100 to 0 (distal) -50 to 0 (proximal)**	tLTD		tLTD - (L-type)				tLTD - calcineurin
Froemke, 2002	V1	Rat	L2/3-L2/3	whole-cell, extra. stim.	P14-35	*in vitro*	0 to 20	-50 to 0 (proximal)							
Froemke, 2006	V1	Rat	L2/3	whole-cell, focal stim.	P10-35	*in vitro*	-15 to -2	2 to 15	tLTP, tLTD		tLTP, tLTD - (L-type)				
Wespatat, 2004	V1	Rat	L2/3-L2/3	whole-cell, extra. stim.	P13, P18-33	*in vitro*	9 to 10 γ peak pairing ***	-13, -5 γ peak pairing	tLTP ***		tLTD				
Urakubo, 2008	V1	Rat	L2/3	whole-cell, focal stim.	P14-28	*in vitro*		-10	tLTD (post)						
Schuett, 2001	V1	Cat	L2/3, L4, L5	single units, extra. stim.	P56-77	*in vivo*	~18	~11							
Sjöström, 2001	V1	Rat	L5-L5	paired	P12-21	*in vitro*	10 (10 Hz)	-10 (0.1 to 20 Hz)	tLTP, tLTD						
Sjöström, 2006	V1	Rat	L5-L5 L5-L2/3	paired, extra. stim.	P21-28	*in vitro*	10 (L5-L5)	10 (L5-L2/3)						LTD (distal) w/o spiking	
Meliza, 2006	V1	Rat	?	whole-cell	P16-21	*in vivo*	1 to 50	-65 to -1			tLTP, tLTD				
Fu, 2002	V1	Cat Human	?	single units	adult	*in vivo*	8 (Cat) 20 (Human)	-8 (Cat) -20 (Human)							

Abbrevations: **Post**=Postsynaptic, **NR**=Not Required, **VGCC**=voltage-gated calcium channnels, **CICR**=calcium-induced calcium release, **2-AG**= 2-arachidonyl glycerol, **extra.**=extracellular, **stim.**=stimulation, **paired**=paired whole-cell recordings, **γ**=gamma oscillation, **proximal**=proximal dendrite, **distal**=distal dendrite.

* β-adrenergic agonist induces tLTP. Muscarinic receptor M1 agonist induces tLTD, at - and + pairing intervals.
** Blockade of voltage-gated potassium channels broadened tLTD window of proximal dendrites up to ~ -100ms
*** Only in the presence of cholinergic agonists at P21-33.

Chapter 2: GluN3A-containing NMDA receptors promote neurotransmitter release and spike timing-dependent plasticity

2.1 Introduction

Postnatal modifications in the properties of synaptic plasticity allow the environment to sculpt neocortical networks for optimal processing of sensory information (Hensch, 2005b; Philpot, Sekhar, Shouval, & Bear, 2001). To ensure greater synaptic stability after maturation, some forms of synaptic plasticity are restricted to early life. This is exemplified by the developmental reduction in the expression of long-term depression (LTD) and in the increased threshold for sensory cortices to compensate for deprivation of a sensory input (Banerjee et al., 2009; Corlew et al., 2007; Dudek & Bear, 1993; Hensch, 2005b) . Although orchestrated shifts in many proteins determine the features of synaptic signaling and plasticity, changes in neurotransmitter receptors may be particularly important, since they shape the initial synaptic response. For example, experience-driven changes in postsynaptic NMDA receptor (NMDAR) subunit composition are known to shift the threshold of neuronal activity required to modify glutamatergic synaptic strength (Philpot et al., 2001).

NMDARs are crucial for many types of learning and memory, and their dysfunction contributes to a large variety of neurological disorders, including schizophrenia, epilepsy, and pain (Cull-Candy & Leszkiewicz, 2004; Kemp & McKernan, 2002). Although most research has assumed that these receptors act postsynaptically, presynaptic-acting NMDARs (preNMDARs) may provide a

powerful complement to their postsynaptic-acting counterparts (Corlew, Brasier, Feldman, & Philpot, 2008; Rodríguez-Moreno, Banerjee, & Paulsen, 2010). PreNMDARs in the neocortex acutely enhance neurotransmitter release (Bender et al., 2006; Berretta & Jones, 1996; Brasier & Feldman, 2008; Corlew et al., 2007; Sjostrom et al., 2003), but under certain circumstances their activation can lead to LTD of neurotransmitter release (Banerjee et al., 2009; Bender et al., 2006; Corlew et al., 2007; Rodriguez-Moreno & Paulsen, 2008; Sjostrom et al., 2003). To date, little is known about the functional mechanisms and developmental regulation of preNMDARs. Interestingly, preNMDARs influence spontaneous release in the absence of strong depolarization. Tonic activation is a unique feature of preNMDARs, as most postsynaptic NMDARs are blocked by magnesium (Mg^{2+}), and therefore require depolarization in conjunction with glutamate binding to become fully active. In the primary visual cortex (V1), preNMDARs are tonically active during early development, but this tonic function is lost by the third postnatal week in mice (Corlew et al., 2007). The loss of tonic preNMDAR function coincides with a reduction in the ability to induce spike timing-dependent LTD (tLTD) at layer (L) 2/3 neocortical synapses (Banerjee et al., 2009; Corlew et al., 2007), a form of plasticity known to rely on preNMDARs (Bender et al., 2006; Corlew et al., 2007; Rodriguez-Moreno & Paulsen, 2008; Sjostrom et al., 2003). What underlies the developmental loss in the ability of preNMDARs to tonically enhance glutamate release and to promote tLTD is unknown.

To determine how preNMDARs contribute to neurotransmitter release and synaptic plasticity, we investigated the molecular composition of preNMDARs, and how this influences the conditions under which these receptors function. We found that the developmental downregulation of GluN3A subunits, which impart Mg^{2+}-insensitivity to NMDARs, correlates with the loss of tonic preNMDAR activity. We also found that GluN3A-containing preNMDARs are required both for the ability of preNMDARs to enhance glutamate release and for the induction of tLTD in the juvenile visual cortex. These observations support a previously unappreciated role for GluN3A-containing NMDARs in regulating presynaptic neurotransmitter release and plasticity during a formative period of neocortical development.

2.2 Results

2.2.1 GluN3A downregulation coincides with the loss of preNMDARs

We first examined whether shifts in the subunit composition of synaptic NMDARs could explain the observed loss of tonic preNMDAR function late in development. NMDARs are tetramers composed of two obligatory GluN1 subunits and two other subunits, either GluN2A-D or GluN3A-B (Cull-Candy & Leszkiewicz, 2004). Since the loss of the obligatory NMDAR subunit GluN1 from the presynaptic terminal could explain the loss of tonic preNMDAR function, which occurs between postnatal day 14 (P14) and P26 in mice (Corlew et al., 2007), we first investigated changes in presynaptic GluN1 expression through development, using immunogold labeling of GluN1. Similar to our previous findings using immunoperoxidase labeling (Corlew et al., 2007), we observed a

decrease in the expression of GluN1 located less than 20 nm from the presynaptic membrane between P14 and P26, but no change in postsynaptic GluN1 (**Fig. 2.1a-f**). However, despite the developmental downregulation of presynaptic GluN1, about 20% of GluN1-labeled synapses still contained presynaptic labeling at P26 (**Fig. 2.1e)**. This finding suggested that the developmental loss in tonic preNMDAR function may be influenced by other NMDAR subunits.

We hypothesized that the NMDAR subunits involved in the developmental regulation of preNMDARs would have properties distinct from their postsynaptic counterparts. Surprisingly, and despite the characteristic voltage-dependence of most NMDARs, neocortical preNMDARs are tonically active in the absence of depolarization (Bender et al., 2006; Berretta & Jones, 1996; Brasier & Feldman, 2008; Corlew et al., 2007; Sjostrom et al., 2003; J. Yang, Woodhall, & Jones, 2006). Because inclusion of the GluN2C/D or GluN3A/B subunits dramatically decreases the receptor's Mg^{2+} sensitivity (Cull-Candy & Leszkiewicz, 2004; Henson, Roberts, Perez-Otano, & Philpot, 2010), we wondered whether this could explain the tonic activity of preNMDARs. To determine which subunits have a developmental profile matching that of functional preNMDARs, we quantified protein expression of candidate NMDAR subunits during V1 development (**Fig. 2.1g-k** and **Fig. 2.6**). Similar to the obligatory GluN1 subunit (**Fig. 2.1g**), protein levels of GluN2A and GluN2B subunits increase with age in V1 (**Fig. 2.1h-i**). Temporal and regional expression of GluN2C (Karavanova, Vasudevan, Cheng, & Buonanno, 2007) and GluN3B (Sasaki et al., 2002)

suggest that they do not contribute to preNMDAR functions in the visual cortex. GluN2D expression levels are extremely low in V1 compared to the brainstem (**Fig. 2.6**), and there was no main effect of age on GluN2D expression (ANOVA, $P = 0.15$), despite a trend suggesting that GluN2D expression levels peak at P16 and become lower in adulthood (**Fig. 2.1j**). In contrast, the expression of GluN3A is high early in development and declines dramatically after the third postnatal week (ANOVA group effect, $P < 0.001$, **Fig. 2.1k**), consistent with previous observations (Henson et al., 2010; Roberts et al., 2009; Wong et al., 2002). Thus, the developmental decreases in GluN3A expression parallels the loss of preNMDAR function observed by the third postnatal week (Corlew et al., 2007). These findings raised the possibility that GluN3A- or perhaps GluN2D-containing NMDARs might underlie the tonic activity of preNMDARs.

2.2.2 GluN2B is required for tonic preNMDAR activity

Next, we used genetic and pharmacological approaches to determine which subunits are required for preNMDAR function. To detect the tonic activity of preNMDARs, we examined the effect of the NMDAR antagonist D-AP5 (50 μM) on the frequency and amplitude of miniature excitatory postsynaptic currents (mEPSCs) while postsynaptic NMDARs were blocked by both hyperpolarization and the inclusion of the NMDAR antagonist MK-801 in the recording pipette (Bender et al., 2006; Berretta & Jones, 1996; Brasier & Feldman, 2008; Corlew et al., 2007; Rodriguez-Moreno & Paulsen, 2008). In L2/3 pyramidal neurons from V1 of P13–18 (juvenile) mice, D-AP5 decreased the frequency but not the amplitude of AMPA receptor (AMPAR)-mediated mEPSCs in wildtype mice (**Fig.**

2.2a-d and **Fig. 2.7**), indicating that preNMDARs are tonically active at this age. We first examined the involvement of GluN2 subunits in tonic preNMDAR function. Compared to GluN3 subunits, GluN2 subunits have a high affinity for glutamate (Laurie & Seeburg, 1994) and therefore are presumably involved in the response of preNMDARs to NMDA or AP5 application (Brasier & Feldman, 2008; Laube, Hirai, Sturgess, Betz, & Kuhse, 1997). In *GluN2A*$^{-/-}$ mice, D-AP5 decreased mEPSC frequency but not amplitude (**Fig. 2.2c-d** and **Fig. 2.7**), demonstrating that GluN2A does not significantly contribute to tonic preNMDAR activity in juvenile V1.

To investigate the potential involvement of GluN2D in preNMDAR tonic activity, we measured changes in mEPSCs in response to application of the moderately subunit-selective GluN2C/D antagonist UBP141 (3 μM) (Costa et al., 2009). Unexpectedly, UBP141 decreased the amplitude of spontaneous and evoked AMPAR-currents (**Fig. 2.8**), suggesting that that UBP141 modulates postsynaptic AMPAR-mediated responses. The effect of UBP141 on AMPAR currents may be direct, but might instead be indirect, since UBP141 has previously been shown to inhibit AMPA receptors only moderately at high concentrations (100 μM) (Costa et al., 2009). This effect of UBP141 on AMPAR mEPSC amplitude precluded us from interpreting its effects on mEPSC frequency. As an alternative and more direct approach, we measured the effects of D-AP5 on mEPSC frequency and amplitude in *GluN2D*$^{-/-}$ mice to assay this subunit's contribution to preNMDAR function. Similar to the effect in *GluN2A*$^{-/-}$ mice, D-AP5 reduced mEPSC frequency, but not amplitude, in mice lacking

GluN2D, suggesting that this subunit is not required for tonic preNMDAR activity (**Fig. 2.2** and **Fig 2.8**). Because previous studies have localized GluN2B to presynaptic terminals in the mature cortex (Charton, Herkert, Becker, & Schroder, 1999; DeBiasi, Minelli, Melone, & Conti, 1996), we next investigated the role of GluN2B subunits in tonic preNMDAR activity. The activity-dependent GluN2B-selective antagonist Ro 25-6981 (0.5 μM) mimicked the effects of D-AP5 by decreasing mEPSC frequency without affecting amplitude (**Fig. 2.2** and **Fig. 2.9**). Another GluN2B-selective antagonist, ifenprodil (3 μM), also decreased mEPSC frequency, but not amplitude, in a manner similar to Ro 25-6981 (**Fig. 2.10**). Consistent with previous observations (Brasier & Feldman, 2008 ; Li, Wang, & Zhang, 2009; J. Yang et al., 2006), our findings indicate that tonically-active preNMDARs contain GluN2B.

2.2.3 Mg^{2+}-insensitive GluN3A promotes spontaneous release

The involvement of GluN2B in preNMDAR activity explains how these receptors can be activated by low concentrations of glutamate (Corlew et al., 2008; Laube et al., 1997), since GluN2B has a high affinity for glutamate (Laurie & Seeburg, 1994), but it does not explain the developmental regulation of preNMDARs, nor their tonic activity in the absence of depolarization. We therefore determined the effect of D-AP5 application on mEPSC frequency in mice lacking GluN3A. Remarkably, the effect of D-AP5 on mEPSC frequency observed in wildtype controls was completely abolished in L2/3 pyramidal neurons from *GluN3A*$^{-/-}$ mice, without affecting mEPSC amplitude (**Fig. 2.3a-b**

and **Fig. 2.11**). This finding indicates GluN3A is required for tonic function of preNMDARs in the juvenile visual cortex.

Since developmental changes in GluN3A expression correlate with changes in tonic preNMDAR functionality (**Fig. 2.1**), we hypothesized that a developmental switch in subunit composition, from GluN3A-containing to GluN3A-lacking, might block the tonic function of preNMDARs in more mature neocortex. We therefore tested whether maintaining GluN3A expression later in development (Roberts et al., 2009; Wong et al., 2002) – at an age when preNMDARs have little spontaneous activity (Corlew et al., 2007) – enhances tonic preNMDAR activity. To extend the time course of GluN3A expression, we crossed mice expressing GluN3A tagged with EGFP (GFPGluN3A) under the control of the tetO promoter to mice expressing the tetracycline-controlled transactivator (tTA) under the CaMKIIα promoter (Mayford et al., 1996; Roberts et al., 2009). This system allows overexpression of GluN3A specifically in excitatory neurons in double-transgenic, but not single-transgenic, progeny (Mayford et al., 1996; Roberts et al., 2009). In double-transgenic (OE) mice, we first observed GluN3A overexpression in excitatory V1 neurons starting at ~P20, when the loss of tonic preNMDAR activity begins (Corlew et al., 2007) (**Fig. 2.12**). In recordings from L2/3 pyramidal cells, we found that the decrease in mEPSC frequency with D-AP5 application was much larger in older (P26–P30) double-transgenic mice overexpressing GluN3A, compared to their single transgenic (STg, *tTA* or *GFPGluN3A* only) controls (**Fig. 2.1b** and **Supplementary Fig. 2.12**). Moreover, the overexpression of GluN3A increased

the baseline mEPSC frequency prior to D-AP5 application in GluN3A overexpressing mice as compared to STg mice, though this effect did not reach statistical significance ($P < 0.07$, **Fig. 2.12**). Thus, genetically increasing GluN3A expression is sufficient to enhance tonic preNMDAR activity in the mature visual cortex.

The developmental removal of GluN3A might limit preNMDAR functions by causing the receptor to gain Mg^{2+} sensitivity. To test whether Mg^{2+} normally blocks tonic preNMDAR activity in L2/3 pyramidal neurons from juvenile (P13–18) *GluN3A*$^{-/-}$ mice, or in older (P25–P28) wildtype mice, we recorded the effect of D-AP5 on mEPSC frequency in ACSF containing only trace amounts of Mg^{2+}. These low Mg^{2+} conditions revealed functional preNMDARs that were previously masked, as D-AP5 reduced mEPSC frequency in both juvenile *GluN3A*$^{-/-}$ mice and older wildtype mice (**Fig. 2.3d** and **Figs. 2.13-2.14**), without altering mEPSC amplitude (**Fig. 2.3c**). We found that tonically-active preNMDARs in older wildtype mice contained GluN2B subunits, as Ro 25-6981 mimicked D-AP5 in reducing the mEPSC frequency in the absence of Mg^{2+} (**Fig. 2.3d**). These findings demonstrate that, despite the developmental loss of GluN3A-containing NMDARs in wildtype mice, Mg^{2+}-sensitive GluN2B-containing preNMDARs can continue to influence neurotransmission under certain circumstances. Therefore, preNMDARs in the mature cortex may require simultaneous depolarization-induced removal of Mg^{2+} and glutamate binding to modulate glutamate release.

A parsimonious explanation for how preNMDARs modulate glutamate release is that GluN3A-containing NMDARs are localized near the presynaptic

release machinery. To determine whether GluN3A is expressed at excitatory presynaptic terminals, we performed electron microscopy for GluN3A in juvenile (P16) V1. Postembedding methods provide optimal quantitative data, but are rather insensitive and potentially noisy; to optimize signal detection, we therefore performed pre-embedding immunoperoxidase electron microscopy. While the majority of GluN3A labeling was postsynaptic (**Fig. 2.3g-h**), we also observed labeling of GluN3A near presynaptic active zones, where GluN3A would be well-positioned to affect neurotransmitter release early in V1 development (**Fig. 2.3e-f**). This signal was specific for GluN3A, because accumulations of reaction product were not detected in comparable material from *GluN3A*$^{-/-}$ mice. Coupled with previous findings suggesting that GluN3A labeling is absent from presynaptic terminals in the adult rodent brain (Perez-Otano et al., 2006; Wong et al., 2002), our findings suggest that GluN3A-containing preNMDARs are selectively expressed only early in the juvenile visual cortex, where they promote tonic preNMDAR functionality.

2.2.4 GluN3A-containing preNMDARs modulate evoked release

In addition to their role in tonic transmitter release, preNMDARs enhance evoked neurotransmitter release early in development (Brasier & Feldman, 2008; Sjostrom et al., 2003). Synaptic responses evoked by L4 stimulation and recorded in L2/3 undergo a developmental shift, from paired-pulse depression in the juvenile visual cortex to paired-pulse facilitation, at a time when GluN3A is downregulated and preNMDARs are no longer tonically active (>P28) (Cheetham & Fox, 2010). To test for a role of GluN3A in evoked transmitter release, we

analyzed the paired-pulse ratio (PPR) in V1 L2/3 synapses before and after D-AP5 application in *GluN3A*$^{-/-}$ mice and their wildtype controls (P13–18). Postsynaptic NMDARs were blocked by loading the NMDAR antagonist MK-801 in the postsynaptic recording pipette, and paired-pulse stimuli were delivered to L4 while recording EPSPs in L2/3 pyramidal neurons. In wildtype mice, D-AP5 application increased the PPR from depressing to facilitating responses and decreased the amplitude of the first EPSP (**Fig. 2.4a-c**), suggesting that preNMDARs enhance evoked transmitter release. In contrast, *GluN3A*$^{-/-}$ mice had facilitating baseline responses, and D-AP5 had no effect on either the PPR or EPSP amplitude (**Fig. 2.4a-c**). Thus, GluN3A-containing NMDARs enhance evoked neurotransmitter release early in V1 development.

2.2.5 tLTD requires GluN2B- and GluN3A-containing preNMDARs

Spike timing-dependent LTD (tLTD), a plausible mechanism for cortical map refinement (Larsen, Rao, Manis, & Philpot, 2010), is associated with presynaptic changes in neurotransmitter release that rely on the activation of preNMDARs during early (Banerjee et al., 2009; Bender et al., 2006; Rodriguez-Moreno & Paulsen, 2008; Sjostrom et al., 2003) —but not later— cortical development (Banerjee et al., 2009; Corlew et al., 2008; Corlew et al., 2007; Rodríguez-Moreno et al., 2010). We thus tested whether GluN2B- and GluN3A-containing NMDARs participate in tLTD induction, as they do in tonic preNMDAR functions. To induce tLTD at L2/3 V1 synapses, we monitored L2/3 EPSPs evoked in L4 before and after inducing tLTD with a L4 post-before-presynaptic induction protocol (tLTD pathway). In some experiments, we simultaneously

monitored EPSPs evoked in L2/3 which did not receive the tLTD induction protocol (control pathway). In all experiments, postsynaptic NMDARs were blocked by including MK-801 in the recording pipette. In wildtype mice, post-before-pre pairing induced robust tLTD (**Fig. 2.5a**). The reduction in EPSP slope was specific to synapses undergoing EPSP–AP pairings, as there was no change in EPSP slope in control pathways which did not undergo EPSP–AP pairings (**Fig. 2.5b**). To test for a role of GluN2B-containing receptors in tLTD induction, we examined tLTD induction when the GluN2B-selective antagonist Ro 25-6981 (0.5 μM) was included in the extracellular recording solution. Similar to previous findings in V1 (Sjostrom et al., 2003), blockade of GluN2B-containing receptors abolished tLTD in wildtype mice without significantly affecting EPSPs evoked in the control L2/3 pathway (**Fig. 2.5a-b**). In contrast, GluN2D was not required for tLTD, since *GluN2D*$^{-/-}$ mice lacking this subunit demonstrated significant synaptic depression following EPSP–AP pairings (**Supplemental Fig. 2.15**). Therefore, tLTD induced in V1 L2/3 pyramidal neurons by L4 activation requires GluN2B-containing, but not GluN2D-containing, preNMDARs.

Because the developmental switch in the properties of tLTD correlates with the down-regulation of GluN3A and the loss of tonic preNMDAR functions (**Fig. 2.1** and (Corlew et al., 2007; Wong et al., 2002)), we tested whether GluN3A is required to induce tLTD at the L4–2/3 synapse in juvenile V1. As expected, wildtype littermate mice demonstrated robust tLTD (**Fig. 2.5c-d**) with a magnitude similar to that observed in previous studies where postsynaptic NMDARs were blocked (Bender et al., 2006; Corlew et al., 2007). This tLTD

required preNMDAR activation, since including D-AP5 in the bath abolished tLTD in wildtype mice (**Fig. 2.5d**). Additionally, tLTD in wildtype mice was timing-dependent, because synaptic depression was not observed when the timing interval between paired action potentials and EPSPs was increased to 250 ms (**Fig. 2.5d**), consistent with previous results (Froemke et al., 2005; Larsen et al., 2010). To determine if tLTD induction requires GluN3A-containing NMDARs, we examined the effects of EPSP–AP pairings in *GluN3A*$^{-/-}$ mice and their wildtype controls. In contrast to wildtype mice, no significant tLTD was induced in *GluN3A*$^{-/-}$ mice (**Fig. 2.5c-d**). Therefore, GluN3A is required for the induction of preNMDAR-dependent tLTD in L2/3 pyramidal cells of the visual cortex.

2.3 Discussion

Our findings demonstrate a critical and previously unrecognized role for GluN3A-containing NMDARs in enhancing neurotransmitter release and mediating temporally restricted forms of synaptic plasticity in the juvenile visual cortex. We found that GluN3A- and GluN2B-containing NMDARs promote glutamate release at L2/3 synapses in the developing visual cortex. The finding that the loss and gain of GluN3A function have opposing effects on preNMDAR-mediated tonic neurotransmitter release suggests that this NMDAR subunit is critical in modulating release at L2/3 visual cortical pyramidal neurons. Interestingly, both GluN3A- and GluN2B-containing preNMDARs are also required for a timing-dependent form of LTD, which is expressed as a reduction of glutamate release from presynaptic neurons (Bender et al., 2006; Corlew et al., 2007; Rodriguez-Moreno & Paulsen, 2008; Sjostrom et al., 2003). GluN3A-

containing preNMDARs may therefore promote two functions in the developing visual cortex: to help maintain a necessary high probability of glutamate release acutely, and to weaken synaptic communication in response to uncoordinated synaptic activity (Larsen et al., 2010; McKinney, Capogna, Durr, Gahwiler, & Thompson, 1999). Our results demonstrate that GluN3A-containing preNMDARs are active in the visual cortex just following eye opening in mice (~P13), at a time that corresponds with the development of early receptive field properties *in vivo* (Smith & Trachtenberg, 2007). Therefore, GluN3A-containing preNMDARs may modulate the formation of early receptive fields by promoting timing-dependent synaptic weakening in response to early visual information.

2.3.1 Subunit composition of preNMDARs through development

What is the heteromeric subunit composition of preNMDARs? While the GluN2B-selective antagonists used in this study would be predicted to block heterotrimeric receptors less effectively than receptors containing GluN1–GluN2B alone (Hatton & Paoletti, 2005) (but see (Smothers & Woodward, 2003)), we speculate that during early development these receptors are triheteromeric NMDARs containing GluN1, GluN2B, and GluN3A. Triheteromeric GluN3A-containing NMDARs have been suggested to exist *in vivo*, as GluN3A coimmunoprecipates with both GluN2B and GluN1 in the rodent brain (Das et al., 1998; Pérez-Otaño et al., 2001). In support of the presence of triheteromeric preNMDARs, we have demonstrated that GluN3A is required for tonic preNMDAR activity in the presence of Mg^{2+}, and that the activity-dependent

GluN2B antagonists Ro 25-6981and ifenprodil block preNMDAR activity as effectively as the non-selective NMDAR antagonist D-AP5. Moreover, GluN1–GluN3A diheteromeric preNMDARs lacking GluN2 are unable to bind glutamate (Y. Yao & Mayer, 2006) and function as excitatory glycine receptors, which have been found on myelin (Piña-Créspo et al., 2010) but not on neurons (Chatterton et al., 2002; Das et al., 1998; Pérez-Otaño et al., 2001). Further evidence against a role for GluN1–GluN3A diheteromeric preNMDARs is provided by the observation that preNMDARs are activated by NMDA and blocked by AP5 (Brasier & Feldman, 2008; Corlew et al., 2007), which both act on the glutamate binding site (Laube et al., 1997). Therefore, our results raise the possibility that triheteromeric GluN1–GluN2B–GluN3A receptors function at excitatory synapses in the juvenile visual cortex, where they promote glutamate release and tLTD.

In contrast to preNMDAR roles in the juvenile neocortex, the activity of GluN3A-lacking preNMDARs in older neocortex is tightly regulated by voltage-sensitive blockade by magnesium. GluN2B-containing, GluN3A-lacking preNMDARs in the mature cortex are not tonically active, but may become active in strongly depolarizing conditions, such as during high frequency bursts, which presumably remove the magnesium block. Thus, GluN2B-containing preNMDARs expressed in the mature neocortex may promote the facilitation of repetitive stimuli, which predominate in the mature visual cortex (Cheetham & Fox, 2010).

While this study is the first to test the role of GluN3A in preNMDARs, previous studies have implicated other GluN2 subunits in preNMDAR functions.

Our finding that GluN2B is required for tonic preNMDAR activity and tLTD is in agreement with the majority of functional and anatomical studies of preNMDARs (Brasier & Feldman, 2008; Charton et al., 1999; DeBiasi et al., 1996; Herkert, Rottger, & Becker, 1998; Y. H. Li et al., 2009; McGuinness et al., 2010; Sjostrom et al., 2003; J. Yang et al., 2006) (but see (Mameli, Carta, Partridge, & Valenzuela, 2005)). However, a recent study in mouse somatosensory cortex also demonstrated a potential role for GluN2C/D-containing receptors in tLTD between L4 and L2/3 synapses (Banerjee et al., 2009), which differs from the results reported here. This apparent discrepancy may be due to regional (somatosensory versus visual cortices) and/or pathway-specific differences in the expression and function of preNMDARs. Segregation of preNMDAR subunits is supported by several findings that suggest that preNMDARs might influence neurotransmitter release differently based on the anatomical region examined (Corlew et al., 2008). For example, GluN2B-containing preNMDARs expressed at hippocampal boutons (McGuinness et al., 2010) might lack GluN3A since preNMDARs at CA1 synapses are not tonically active (Mameli et al., 2005), are Mg^{2+} sensitive (McGuinness et al., 2010), and because overexpression of GluN3A does not alter the paired pulse ratio (Roberts et al., 2009). A similar segregation of preNMDAR subunits based on anatomical region may exist between somatosensory and visual cortices. Additionally, in the somatosensory cortex, the NMDAR-subunit dependence of preNMDARs in the L4–L2/3 pathway is different from that in the L2/3–L2/3 pathway (Banerjee et al., 2009; Brasier & Feldman, 2008). With these possibilities in mind, we attempted to corroborate

the suggestion that preNMDARs contained GluN2C/D (Rodríguez-Moreno et al., 2010) using UBP141, as previously reported (Banerjee et al., 2009). We found that commonly employed concentrations of UBP141 reduced AMPAR responses in the visual cortex, suggesting that UBP141 lacks the specificity needed to assess the role of GluN2C or GluN2D in the tonic activity of preNMDARs (**Fig. 2.9**). However, by using GluN2D$^{-/-}$ mice, we found that GluN2D is not required for tLTD or tonic preNMDAR function in the visual cortex. Nevertheless, we cannot exclude the possibility that GluN2C or GluN2D contribute to the modulation of glutamate release by preNMDARs in certain pathways, regions, or developmental stages.

2.3.2 Subcellular localization of preNMDARs

GluN3A-containing NMDARs can influence neurotransmitter release and presynaptically-expressed forms of synaptic plasticity, but remains unclear where these receptors are localized. Our finding that the NMDAR subunits GluN1 and GluN3A can be found at presynaptic terminals raises the possibility that NMDARs may promote glutamate release and tLTD by direct effects at synaptic boutons. However, an important caveat of our studies, and others, is that the precise location of functionally relevant preNMDARs has not been definitively determined. Studies attempting to identify functional preNMDARs in axons have produced variable results. While studies attempting to localize preNMDARs to cerebellar stellate cells and L5 cortical neurons axons have failed to observe NMDAR-mediated axonal calcium influx or depolarization (Christie & Jahr, 2008, 2009), a study of cortical neurons observed both phenomena in presynaptic

boutons (H. Lin et al., 2010). Furthermore, activation of NMDARs at hippocampal Schaffer collateral boutons selectively enhanced large Ca^{2+} transients, which themselves underlied increases in the probability of neurotransmitter release (McGuinness et al., 2010). What might account for the apparent discrepancy between studies? One possibility is that there may be anatomical region differences in the localization of preNMDARs. Alternatively, preNMDAR activation may only contribute to a subpopulation of Ca^{2+} transients observed at axons. This is supported by the finding that preNMDARs at Schaffer collaterals contribute to only a portion of large action potential-generated calcium influxes, and only at axon boutons, not at axon collaterals (McGuinness et al., 2010). Another possibility is that the localization of GluN3A-containing NMDARs may be difficult to detect by traditional electrophysiological or calcium imaging methods. GluN3A-containing NMDARs have lower conductances (Chatterton et al., 2002), rapidly desensitize in the presence of D-serine or glycine (Piña-Créspo et al., 2010; Y. Yao & Mayer, 2006), and are 5–10 times less permeable to calcium than GluN2-containing NMDARs (Henson et al., 2010). Due to the abundance of functional studies implicating preNMDARs in modulating neurotransmitter release (Corlew et al., 2008; Rodríguez-Moreno et al., 2010), future studies that both localize active preNMDARs and simultaneously measure their effects on neurotransmitter release are warranted.

In summary, our data provide evidence for a unique role of GluN3A-containing preNMDARs in visual cortical development. Our findings also provide an explanation for how preNMDARs may be tonically active during early

development but not later in life. Finally, we suggest that the developmental downregulation of GluN3A may limit the normal ability to induce tLTD at L2/3 neocortical synapses. These findings add a new dimension to our understanding of how NMDAR-subunit composition influences cortical developmental processes that occur in response to visual activity.

2.4 Materials and Methods

2.4.1 Animals

Under the animal care guidelines for University of North Carolina at Chapel Hill, male and female mice were maintained on a 12h:12h light:dark cycle and fed *ad libitum*. *GluN2A*$^{-/-}$ mice were generously supplied by S. Nakanishi (Kyoto, Japan), and re-derived on the C57BL/6 background by Charles River Laboratories. Mice lacking functional GluN2D were generated on a C57BL/6 as previously described (Ikeda et al., 1995). *GluN3A*$^{-/-}$ mice were generated on the 129 background as previously described and backcrossed to C57BL/6 several generations (Das et al., 1998). GluN3A double-transgenic (overexpressing) and single-transgenic (non-overexpressing) mice were used as previously described (Mayford et al., 1996; Roberts et al., 2009). All other wild-type mice were on the C57BL/6 strain (Charles River laboratories).

2.4.2 Biochemistry

Biochemical fractionation: Tissue from the visual cortex or brainstem of 2–4 mice was rapidly dissected and stored at -80°C until use. Biochemical fractions were prepared essentially as previously described (Roberts et al., 2009). Briefly, samples were dounce-homogenized in HEPES-buffered sucrose (4 mM HEPES,

0.32 M sucrose, pH 7.4), and spun twice at 1000 x *g* for 10 min to eliminate nuclei. The postnuclear supernatant fraction was then centrifuged at 10,000 x *g* for 20 min to isolate crude synaptosomal pellets (P2 fraction, intact synaptosomes), and resuspended in buffer.

Quantitative immunoblotting: Increasing amounts (5 -15 µg) of total protein from each sample were loaded on 8% tris-glycine NuPage gels (Invitrogen), resolved by SDS-PAGE, and transferred to nitrocellulose membranes. Blotting (Bio-Rad) and Odyssey system imaging and quantification (LI-COR) were carried out following manufacturers' protocols. The following antibodies were used: rabbit anti-GluN3A (07-356, Millipore), rabbit anti-GluN2A (AB1555 and 04-901, Millipore), goat anti-GluN2D (sc-1471, Santa Cruz Biotechnology), goat anti-GluN2B (sc-1469, Santa Cruz Biotechnology), goat anti-GluN1 (sc-1467, Santa Cruz Biotechnology), rabbit anti-GluN2D (35448, Abcam and sc-1471, Santa Cruz), mouse anti-β-actin (A5316, Sigma-Aldrich), Alexa Fluor 680-labeled anti-goat IgG (A21084, Invitrogen), Alexa Fluor 680-labeled anti-mouse IgG (A21058, Invitrogen), and IRDye 800-labeled anti-rabbit IgG (611-732-127, Rockland Immunochemicals). Two antibodies against GluN2A and GluN2D were used, and each produced similar results against its respective antigen. Calculations of signal intensity per microgram protein were determined for each antibody and averaged across multiple gels.

Immunohistochemistry: Mice were perfused using 4% PFA in PBS, cut in a cryostat or sliding microtome at 15-20 µm, and stained using anti-GFP antibody after TX100 permeabilization, similar to previously described (Roberts et al., 2009).

2.4.3 Electrophysiology

Cortical slice preparation: Mice were anesthetized with pentobarbital sodium and decapitated after disappearance of corneal reflexes. Brains were rapidly removed and cut at 350 µm using a vibrating microtome (Leica VT1000S or VT1200S) in ice-cold dissection buffer containing (in mM), 87 NaCl, 2.5 KCl, 1.25 NaH_2PO_4, 25 $NaHCO_3$, 75 sucrose, 10 D-(+)-glucose, 1.3 ascorbic acid, 7 $MgCl_2$, and 0.5 $CaCl_2$, bubbled with 95% O_2 and 5% CO_2. Slices recovered for 20 min at 35°C in ACSF containing: (in mM) 124 NaCl, 3 KCl, 1.25 Na_2PO_4, 26 $NaHCO_3$, 1 $MgCl_2$, 2 $CaCl_2$, and 20 D-(+)-glucose, saturated with 95% O_2, 5% CO_2 and kept at room temperature for at least 40 min. Recordings were made in a submersion chamber at 30-32°C in the same ACSF except in low Mg^{2+} conditions where 1 mM $MgCl_2$ was excluded or when drugs were added as noted. Ifenprodil, MK-801, and picrotoxin were purchased from Sigma (St. Louis, MO). All other pharmacological agents were purchased from Ascent Scientific (Weston-Super-Mare, UK).

Whole-cell recordings: L2/3 pyramidal cells were visually identified with IR-DIC optics and pyramidal morphology was confirmed in the majority of neurons by filling them with Alexa 488 (0.01% wt/vol). Patch pipettes were pulled from thick-

walled borosilicate glass with open tip resistances of 2-7 MΩ when filled with internal solution containing: (in mM) 20 KCl, 100 (K)Gluconate, 10 HEPES, 4 (Mg)ATP, 0.3 (Na)GTP, 10 (Na)Phosphocreatine with pH adjusted to 7.25 and osmolarity adjusted to ~295 mOsm with sucrose. In all experiments, the internal solution contained the NMDAR antagonist MK-801 (1 mM) to block postsynaptic NMDARs, including GluN3A-containing (Das et al., 1998), and to ensure isolation of AMPAR-mediated responses (Berretta & Jones, 1996; Corlew et al., 2007; Rodriguez-Moreno & Paulsen, 2008). Cells were recorded in either voltage- or current-clamp configuration with a patch clamp amplifier (Multiclamp 700A; Molecular Devices), and data were acquired and analyzed using pCLAMP 9.2 or 10 software (Molecular Devices). Series and input resistances were monitored throughout experiments by measuring the response to a -5 mV step at the beginning of each sweep. Series resistance was calculated using the capacitive transient at the onset of the step and input resistance was calculated from the steady-state current during the step. No series resistance compensation was applied.

mEPSC recordings: Similar to previously described (Corlew et al., 2007), AMPA receptor-mediated mEPSCs were recorded in the presence of tetrodotoxin (200 nM) and picrotoxin (50 μM) at negative holding potentials (-80 mV) to facilitate block of postsynaptic NMDARs. Minimal glycine (1 μM) was also added to bind the preNMDAR co-agonist binding site without saturating postsynaptic NMDARs (Li & Han, 2007). We measured mEPSC amplitude and frequency during a

baseline period at the beginning of the experiment and during bath application of an NMDAR antagonist. D-AP5 (50 μM) and ifenprodil (3 μM) were bath applied for 10 minutes and all other pharmacological agents were applied for 15 minutes. Events with a rapid (<3 ms) rise time and exponential decay were identified using an automatic detection template. Quantification of mEPSCs was calculated from the percentage change in frequency or amplitude of the last 5 minutes of NMDAR antagonist application normalized to the last 5 minutes of baseline. Cells were only included for analysis if (1) there was < 30% change in R_{input} and R_{series}, (2) there was < 100 pA change for $I_{holding}$, and (3) R_{series} was < 30 MΩ.

Evoked glutamate release: Recording solutions for these experiments and tLTD experiments were the same as in mEPSC recordings except for the omission of tetrodotoxin, picrotoxin, and glycine from the ACSF. For all evoked and tLTD experiments, L2/3 pyramidal cells were recorded in voltage- or current-clamp while L4 axons were stimulated extracellularly every 15 seconds with a two-conductor cluster electrode with 75 μm tip separation (FHC Inc., Bowdoin, ME). To analyze the effect of UBP141 on non-NMDAR currents, the effect of 15 minute application of UBP141 on single AMPAR EPSCs was determined in high divalent ACSF (4mM Ca^{2+} and 4mM Mg^{2+}) containing 50 μM picrotoxin and 100 μM D,L-AP5.

For current-clamp experiments measuring evoked glutamate release or tLTD, current was injected to maintain a -70 mV resting potential if necessary; cells were excluded from analysis if input resistance changed more than 30% or

if >200 pA of current was required to maintain a -70 mV resting potential. To measure the effect of D-AP5 on evoked glutamate release, the amplitude and paired pulse ratio (PPR; second EPSP/first EPSP) of two EPSPs evoked at 30Hz were measured. After a 10 minute baseline during which monophasic and fixed latency EPSPs maintained no change in slope or amplitude, D-AP5 (50 μM) was applied for 10 minutes. Change in the amplitudes of the first and second EPSPs was quantified as a percentage of baseline (the last 5 minutes of D-AP5 / the last 5 minutes of baseline). In a single instance, D-AP5 application in a wildtype animal reduced both EPSPs to noise levels and was excluded from analysis because it was not possible to properly assess release probability via PPR.

tLTD induction: To demonstrate that tLTD in wildtype mice was homosynaptic, EPSPs were alternately generated by one of two bipolar stimulating electrodes placed in L4 and L2/3 of V1 except in tLTD experiments in *GluN2D*$^{-/-}$ mice and in a subset of experiments comparing tLTD in wildtype and *GluN3A*$^{-/-}$ mice. A steady baseline was recorded for 10 minutes during which monophasic and fixed latency response EPSPs were maintained with no change in amplitude or slope. The tLTD induction period consisted of 100 action potentials (APs) at 0.2 Hz each followed within 15-20 ms by an EPSP generated selectively by L4 stimulation. Postsynaptic APs were produced by a brief (< 5 ms) depolarization of the postsynaptic L2/3 cell and EPSPs generated in L4 were produced in an identical manner as the baseline period. Change in EPSP slope was calculated

as the percentage decrease in slope from the last 10 minutes post-LTD normalized to the last 5 minutes of baseline.

2.4.4 Electron microscopy

Mice were given an overdose of pentobarbital sodium and perfused transcardially with 0.9% saline solution for 1 min followed by a mixture of 2% paraformaldehyde (depolymerized in 0.1 M phosphate buffer at pH 7.4) and 2% glutaraldehyde (Electron Microscopy Science, Hatfield, PA) for 15 min. After perfusion, brains were postfixed at 4ºC for 48 hours in the same fixative. A vibrating microtome was used to cut 200 µm coronal visual cortical sections. Sections were pre-treated in 0.1% calcium chloride in 0.1M sodium acetate, rinsed, then cryoprotected in a graded series to 30% glycerol in 0.1M sodium acetate. Pieces were then isolated from slices containing L2/3 of V1. These L2/3 V1 pieces were quick frozen in CO_2-chilled isopentane. Freeze substitution in 4% uranyl acetate in methanol was carried out in a Leica Electron Microscopy Automatic Freeze Substitution System; pieces were embedded in Lowicryl HM-20 and polymerized with UV.

Sections were cut at ~70-90 nm with an ultramicrotome and collected on nickel grids, coated with Coat-Quick. Postembedding immunocytochemistry was performed as previously described. Grids were pre-treated using 4% *p*-phenylenediamine dihydrochloride in Tris-buffered saline with 0.005% Tergitol NP-10, blocked in 1% BSA, then incubated overnight at room temperature in the rabbit monoclonal primary antibody GluN1 (1:100) (AB9864, Millipore). Grids were rinsed, blocked in 1% normal goat serum, and incubated in goat anti-rabbit

IgG F(ab')2 conjugated to 10-nm gold particles (Ted Pella, 1:15) for 2 hours, rinsed, then counterstained with 1% with uranyl acetate followed by Sato's lead.

Electron microscopy data collection and quantitative analysis of postembedding material were performed with a Philips Tecnai electron microscope (Hillsboro, OR) at 80 kV with a magnification at 10,000X–40,000X; images were acquired with a Gatan 12-bit 1024 x 1024 CCD camera (Pleasanton, CA). Random grid squares were chosen and online scoring and image acquisition was done with observer blind to animal age. Synapses were analyzed if they were asymmetric, had well defined membranes, postsynaptic densities and presynaptic terminals with synaptic vesicles. To analyze the developmental decrease in preNMDAR expression, synapses were scored for presynaptic labeling, postsynaptic labeling, or no labeling. Synapses were counted if they could be identified as excitatory synapses, having clear presynaptic terminals, postsynaptic spines, and an obvious cleft. Synapses were considered labeled if a gold particle lay < 20 nm from either the pre- or postsynaptic membrane; and only particles that lay within the PSD or active zone were considered for this analysis.

Preembedding immunocytochemistry for identification of GluN3A-positive synapses was performed on material fixed with a mixture of 4% depolymerized paraformaldehyde and 0.1% glutaraldehyde according to standard methods as described in (A. L. Jacob, Jordan, & Weinberg, 2010). Briefly, 50 µm sections were incubated in 1% sodium borohydride, 3% hydrogen peroxide, and 10% normal serum prior to incubation with GluN3A primary antibody (diluted 1:100 or

1:200) (Watanabe, unpublished); some sections were pre-treated with 50% ethanol to improve antibody penetration. After overnight incubation on a shaker at room temperature, sections were rinsed, incubated with biotinylated anti-rabbit secondary antibody (5 µg/ml, Jackson ImmunoResearch) and ExtrAvidin-peroxidase (0.5 µg/ml, Sigma), and processed with nickel-diaminobenzidine. Immunoreacted sections were postfixed in 1% osmium tetroxide, 1% uranyl acetate, dehydrated, embedded in epoxy resin, and heat-polymerized between two sheets of Aclar plastic. Relevant chips of visual cortex were glued to plastic blocks; 80-100 nm sections were cut on an ultramicrotome, collected on copper mesh grids, and post-stained with uranyl acetate and Sato's lead.

2.4.5 Statistics

Statistical evaluations were performed for multiple comparisons using a one-way ANOVA with Tukey-Kramer post-hoc analysis. Paired *t*-tests were performed on raw data comparing baseline to post drug/tLTD periods within a group and unpaired *t*-tests were performed on normalized means comparing $^{-/-}$ and wildtype protein expression levels. To compare the effect of an NMDAR antagonist between groups, data were normalized to the baseline period prior to application of the NMDAR antagonist and unpaired *t*-tests were performed between groups comparing percent changes. Significance level was set at $P < 0.05$. * $P < 0.05$, ** $P < 0.01$, and *** $P < 0.001$.

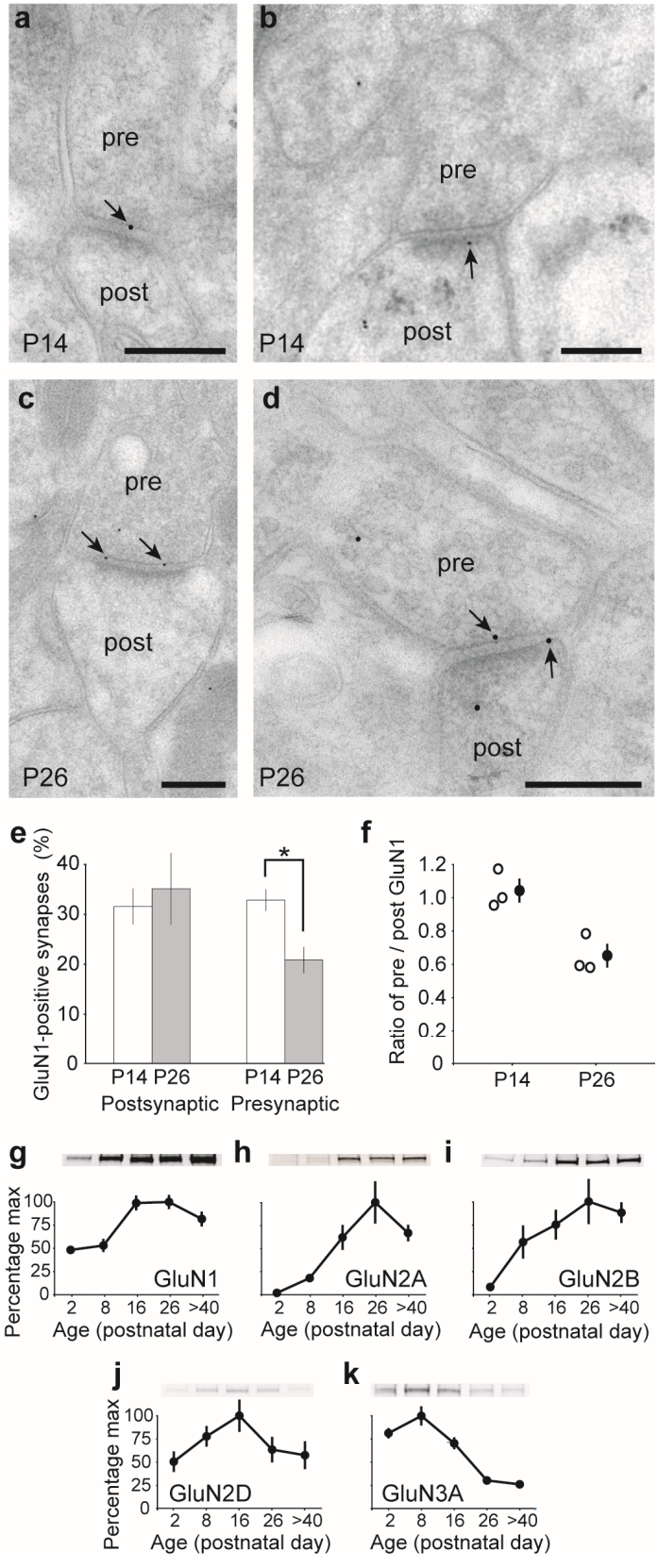
a
pre
post
P14
b
pre
post
P14
c
pre
post
P26
d
pre
post
P26
e
GluN1-positive synapses (%)
40
30
20
10
0
*
P14 P26
Postsynaptic
P14 P26
Presynaptic
f
Ratio of pre / post GluN1
1.2
1.0
0.8
0.6
0.4
0.2
0
P14
P26
g
h
i
Percentage max
100
75
50
25
0
GluN1
GluN2A
GluN2B
2 8 16 26 >40
Age (postnatal day)
j
k
GluN2D
GluN3A

Figure 2.1: Both the presynaptic localization of GluN1 and the biochemical expression of Mg^{2+}-insensitive NMDAR subunits decrease during early visual cortex development. Electron micrographs demonstrating immunogold localization of GluN1 at both presynaptic (pre) and postsynaptic (post) sites in L2/3 of mouse primary visual cortex (V1) at P14 (**a,b**) and at P26 (**c,d**). Scale bars indicate 200 nm. (**e**) While the percentage of synapses containing GluN1 immunogold label within the postsynaptic density (PSD) did not change with development (P14: 31 ± 3.6%, *n* = 3 mice; P26: 35 ± 7.1%, *n* = 3 mice; >70 synapses/animal were analyzed; $P < 0.68$), the percentage of synapses positive for GluN1 within the presynaptic active zone decreased significantly (P14: 33 ± 2.1% *n* = 3; P26: 21 ± 2.6%, *n* = 3, $P < 0.03$). Despite the reduction, presynaptic GluN1 labeling persisted at P26. (**f**) Open circles represent the ratio of pre- to postsynaptic GluN1 labeling per animal; closed circles represent the average of three animals at P14 and P26. (**g-k**) Quantification and representative immunoblots for NMDAR subunits in synaptosomal fractions from the developing visual cortex. Levels of GluN2D and GluN3A, which confer magnesium insensitivity to NMDARs, decrease during development. Protein levels were normalized to β-actin and presented as percent of maximum expression. Sample sizes were 2–5 for each data point. Each visual cortex sample was pooled from 2–4 mice. For larger blot areas see **Supplementary Figure 1**. Error bars represent s.e.m. * $P < 0.05$.

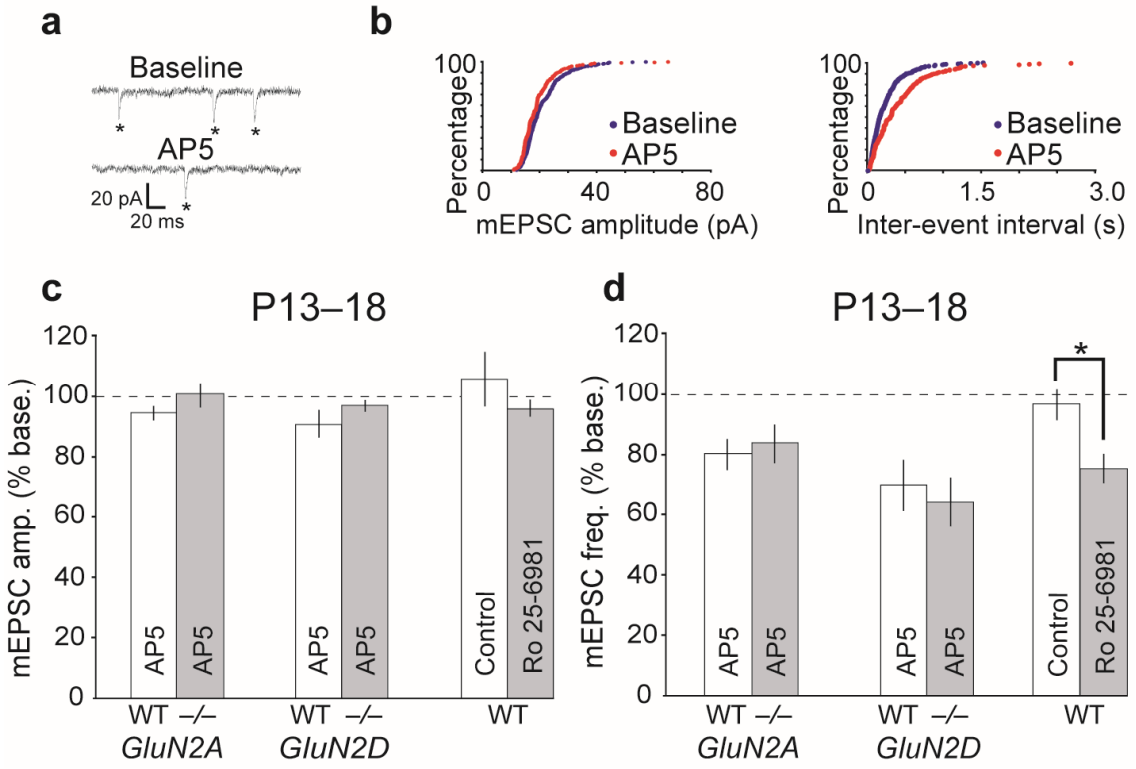

Figure 2.2: Glutamate-sensitive preNMDARs containing GluN2B, but not GluN2A or GluN2D, enhance spontaneous neurotransmitter release onto juvenile L2/3 pyramidal neurons. (**a**) Sample traces showing AMPAR-mediated mEPSCs. Recordings were made during blockade of postsynaptic NMDARs in a L2/3 pyramidal neuron in V1 of a P14 wildtype (WT) mouse before and after bath-applied D-AP5. (**b**) Cumulative probability histograms from the cell in **a** show a decrease in mEPSC frequency, but not amplitude, with D-AP5 application. (**c**) Neither D-AP5 nor the GluN2B-selective antagonist Ro 25-6981 significantly altered mEPSC amplitude in V1 mEPSCs recordings. (**d**) L2/3 pyramidal cells exhibited a significant reduction in mEPSC frequency in response to D-AP5 application in both *GluN2A*$^{-/-}$ mice and their wildtype controls (*GluN2A*$^{-}$

$^{-/-}$, n = 7, P < 0.04; WT, n = 7, P < 0.03). Similarly, D-AP5 reduced the frequency, but not amplitude, in both *GluN2D*$^{-/-}$ mice and their wildtype controls (WT, n = 5, P < 0.05; *GluN2D*$^{-/-}$, n = 6, P < 0.007). Ro 25-6981 (0.5 μM) significantly reduced mEPSC frequency in wildtype mice compared to vehicle controls (controls n = 6, Ro 25-6981 n = 7; P < 0.02). Individual data points are normalized to their respective baseline mEPSC frequencies to allow for the comparison of the effect of D-AP5 across genotypes and conditions. Error bars represent s.e.m. * P < 0.05

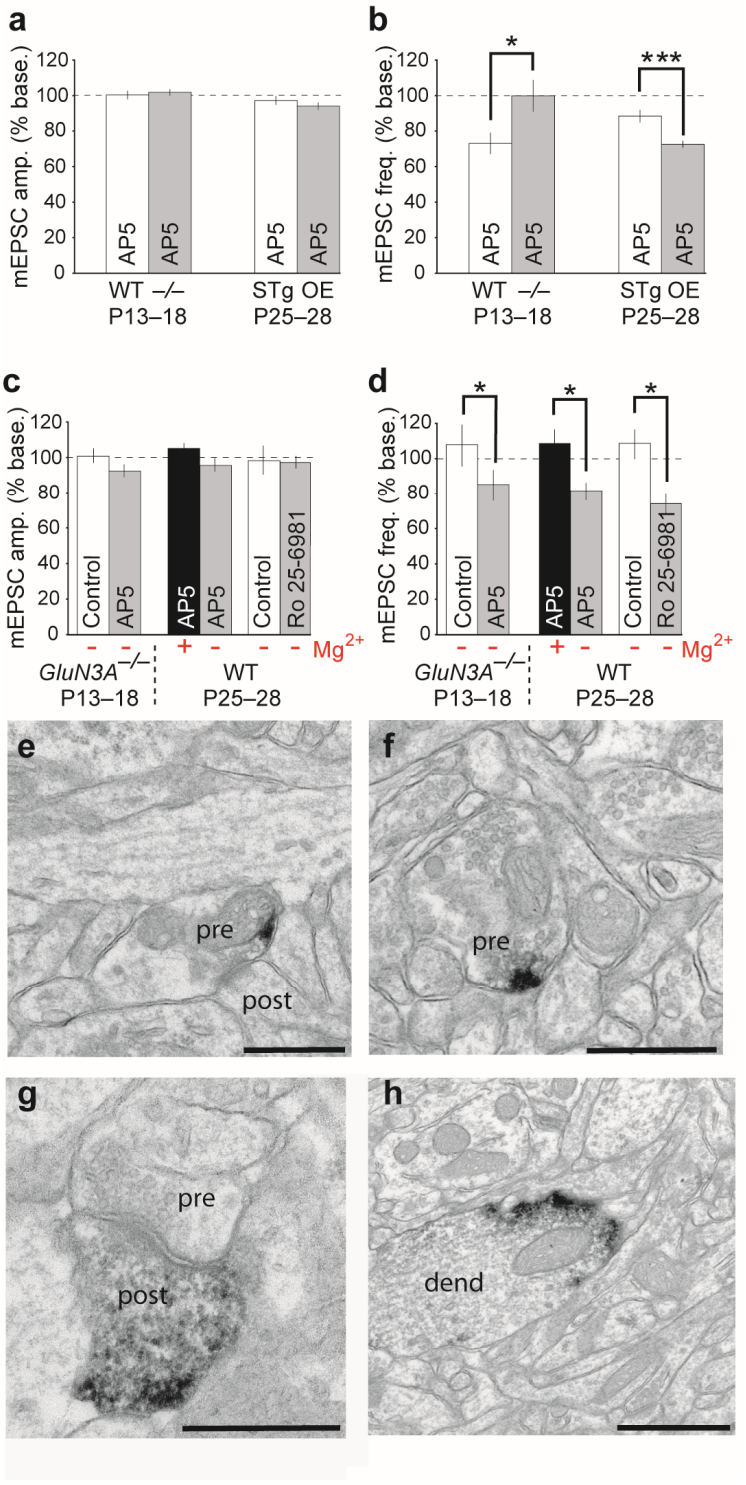
a
mEPSC amp. (% base.)
120
100
80
60
40
20
0
AP5
AP5
AP5
AP5
WT –/–
P13–18
STg OE
P25–28
b
mEPSC freq. (% base.)
*
***
c
mEPSC amp. (% base.)
Control
AP5
AP5
AP5
Control
Ro 25-6981
- - + - - - Mg2+
GluN3A–/–
P13–18
WT
P25–28
d
mEPSC freq. (% base.)
*
*
*
e
pre
post
f
pre
g
pre
post
h
dend

Figure 2.3: The reduced Mg^{2+}-sensitivity of GluN3A-containing preNMDARs promotes spontaneous neurotransmitter release in juvenile V1. (**a**) Normalized and averaged mEPSC amplitudes confirm that D-AP5 did not affect postsynaptic AMPAR-mediated responses in L2/3 pyramidal neurons from juvenile (P13–P18) wildtype and *GluN3A*$^{-/-}$ mice. D-AP5 application also did not affect mEPSC amplitude in older (P25–P28) double-transgenic mice that overexpress (OE) GluN3A nor in single-transgenic (STg) control mice expressing only one of the two transgenes necessary for GluN3A overexpression (*tet-O-GFPGluN3A* or *CaMKII-tTA* transgenes). (**b**) Normalized mEPSC frequency showing effects of D-AP5 in P13–P18 *GluN3A*$^{-/-}$ mice (WT $n = 8$, *GluN3A*$^{-/-}$ n = 10; $P < 0.03$), P25-28 OE mice (STg $n = 7$, OE $n = 10$; $P < 0.0009$), and their appropriate littermate controls. (**c**) Neither D-AP5 nor Ro 25-6981 significantly altered mEPSC amplitude recorded in low Mg^{2+} solutions in either young (P13–18) *GluN3A*$^{-/-}$ mice or in older (P25–28) wildtype mice. (**d**) In low Mg^{2+} solutions, D-AP5 reduced mEPSC frequency in both young (P13–18) *GluN3A*$^{-/-}$ mice ($n = 12$, $P < 0.05$) and in older (P25–28) wildtype mice, compared to vehicle controls ($n = 9$, $P < 0.05$). Similar to D-AP5, 0.5 μM Ro 25-6981 reduced the mEPSC frequency in older mice in low Mg^{2+} conditions as compared to vehicle controls (controls, $n = 6$, Ro 25-6981, $n = 7$; $P < 0.03$). (**e-h**) Electron micrographs demonstrating immunoperoxidase labeling of GluN3A over presynaptic (**e-f**), postsynaptic (**g**), and putative dendritic (dend) (**h**) profiles in the primary visual cortex at P16. Scale bars indicate 0.5 μm in (e-g) and 1 μm in (h). Error bars represent s.e.m. * $P < 0.05$ and *** $P < 0.001$.

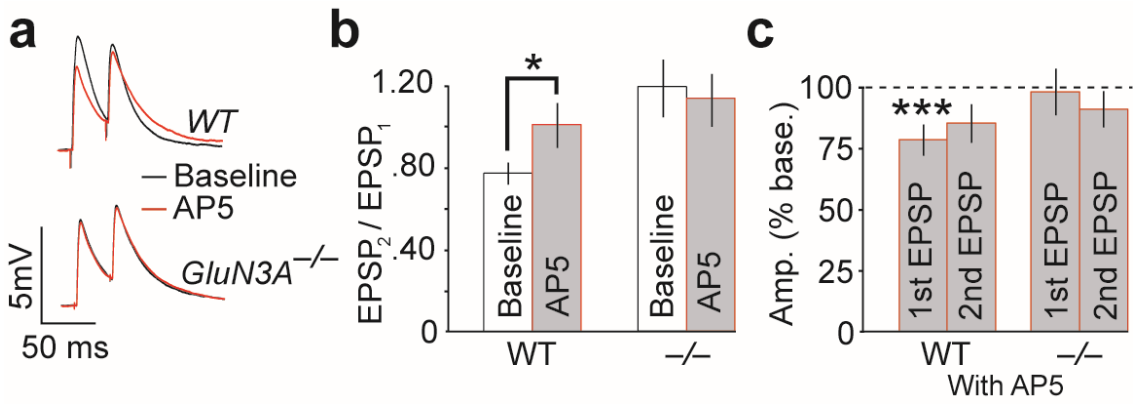

Figure 2.4: GluN3A-containing preNMDARs enhance evoked neurotransmitter release at L2/3 visual cortical synapses. (**a**) Representative traces of EPSPs evoked by a 30-Hz pair of stimuli in L4 before and after D-AP5 application from wildtype and *GluN3A*$^{-/-}$ mice. (**b**) Paired-pulse ratio (PPR) of EPSPs increased after D-AP5 application in the wildtype but not *GluN3A*$^{-/-}$ mice (WT n = 14, *GluN3A*$^{-/-}$ n = 12; $P < 0.05$). (**c**) The change in PPR was primarily due to a decrease in the amplitude of the first EPSP in the pair in wildtype mice ($P < 0.001$). Error bars represent s.e.m. * $P < 0.05$ and *** $P < 0.001$.

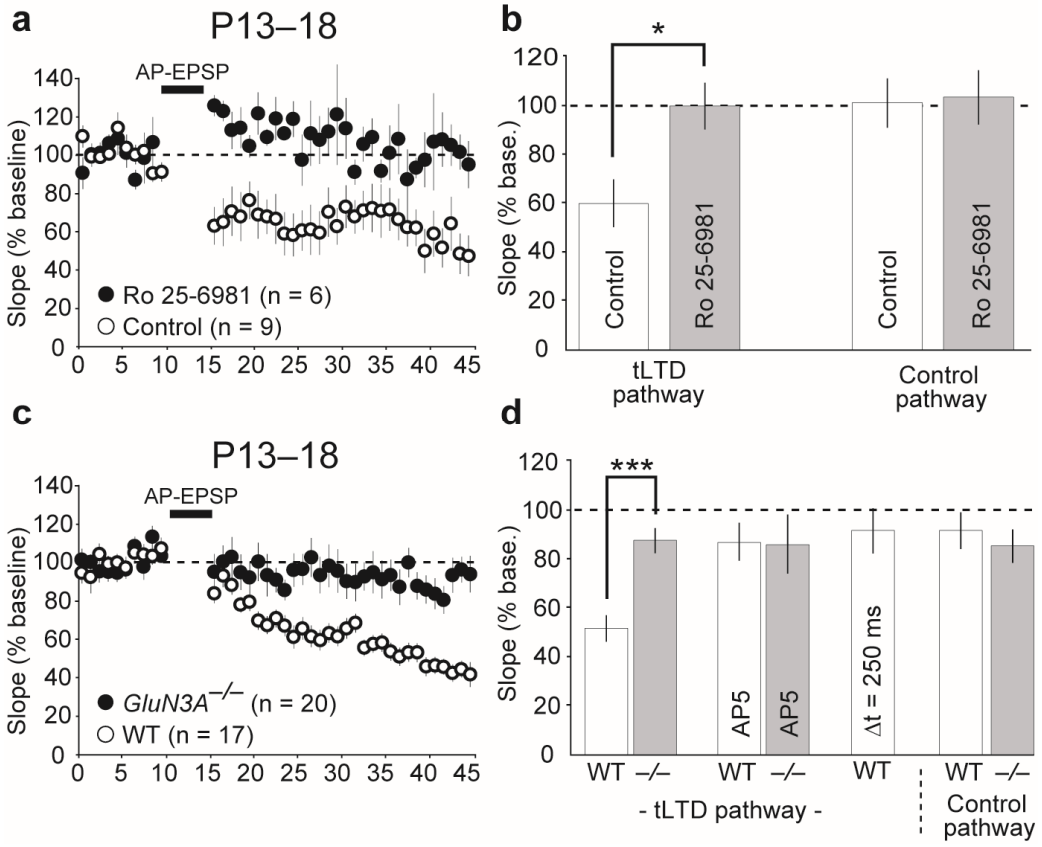

Figure 2.5: GluN2B- and GluN3A-containing preNMDARs promote spike timing-dependent long-term depression (tLTD) in juvenile V1. **(a)** tLTD was induced in L2/3 V1 synapses in response to action potentials (APs) paired with L4-generated EPSPs in wildtype mice (*n* = 9), but not when the GluN2B-selective antagonist Ro 25-6981 (0.5 μM) was included in the bath (*n* = 6; *P* < 0.02). (**b**) Quantification of the last 10 minutes of the averages shown in **a**. Quantified data are also shown from a control pathway not receiving AP–EPSP pairings, performed in a subset of experiments, to demonstrate the synapse specificity of tLTD (control, *n* = 9; Ro 25-6981, *n* = 6). (**c**) Robust tLTD was induced in L2/3 synapses of juvenile V1 in wildtype (*n* = 20), but not *GluN3A*$^{-/-}$ mice (*n* = 17), with

AP-EPSP pairing. (**d**) Quantification of the last 10 minutes in **c** demonstrating *GluN3A*$^{-/-}$ mice have significantly reduced tLTD magnitude, compared to wildtype mice ($P < 0.001$). Control AP-EPSP pairing experiments in which either D-AP5 was present throughout the recording session (WT, $n = 5$; *GluN3A*$^{-/-}$, $n = 5$) or the time between AP–EPSP pairing was increased to 250 ms ($n = 7$). These control experiments demonstrate tLTD observed in wildtype mice was dependent on NMDARs and the temporal precision of AP–EPSP pairings. Moreover, control pathways not receiving the AP–EPSP pairing also failed to exhibit significant depression (WT, $n = 8$; *GluN3A*$^{-/-}$, $n = 9$). Error bars represent s.e.m. * $P < 0.05$ and *** $P < 0.001$.

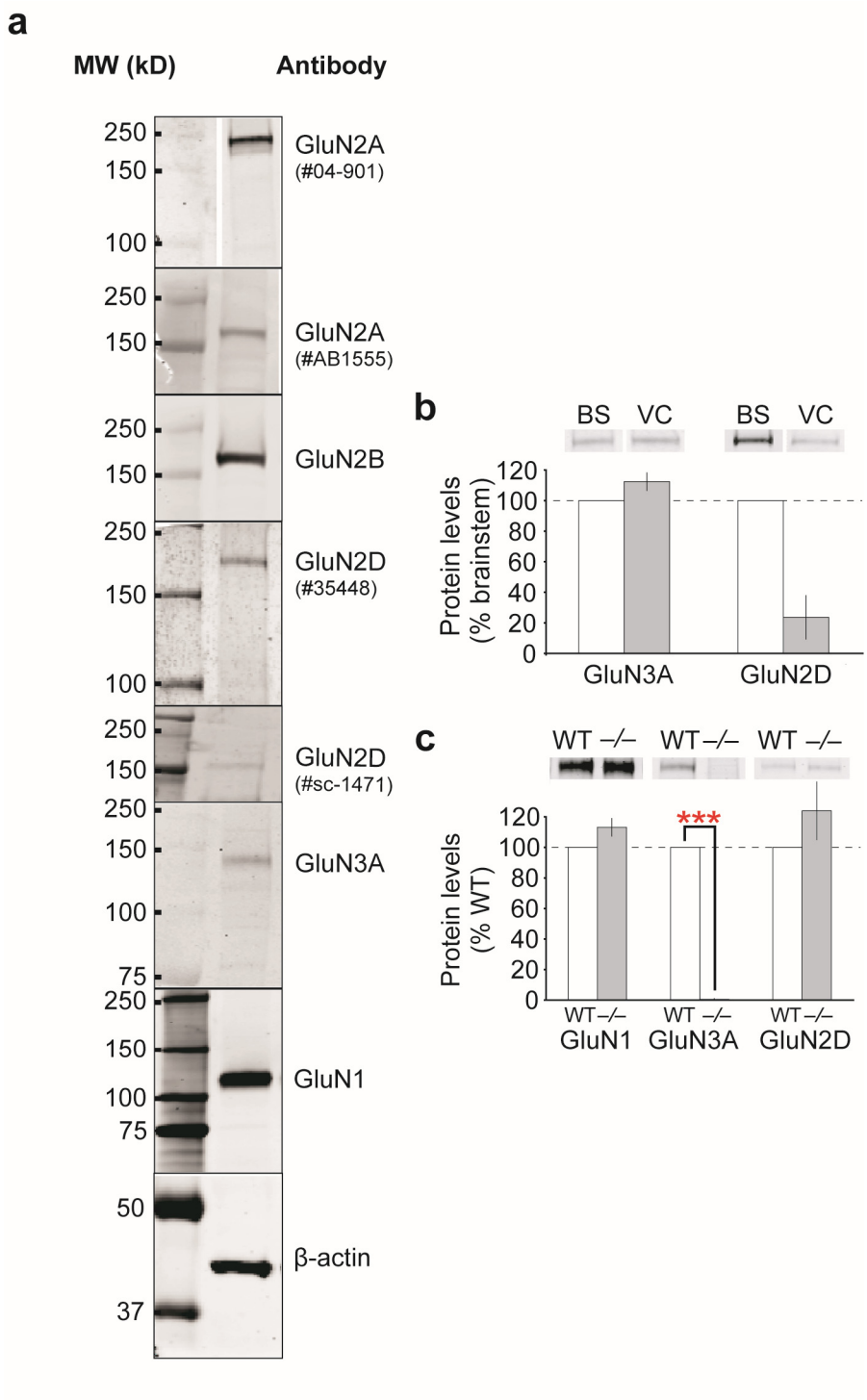
a
MW (kD)
Antibody
250
150
100
GluN2A
(#04-901)
250
150
GluN2A
(#AB1555)
250
150
GluN2B
250
150
100
GluN2D
(#35448)
250
150
GluN2D
(#sc-1471)
250
150
100
75
GluN3A
250
150
100
75
GluN1
50
37
β-actin
b
BS
VC
BS
VC
Protein levels
(% brainstem)
120
100
80
60
40
20
0
GluN3A
GluN2D
c
WT
–/–
WT
–/–
WT
–/–
***
Protein levels
(% WT)
120
100
80
60
40
20
0
WT
–/–
WT
–/–
WT
–/–
GluN1
GluN3A
GluN2D

Figure 2.6: GluN2D levels are comparatively low in visual cortex (VC), and these levels are unchanged in GluN3A–/– mice. (a) Larger representative blots show antibody specificity for the target antigens with molecular weight markers. (b) Representative blots and quantified protein levels of GluN3A and GluN2D in P8–P10 V1 (n = 2) and brainstem (BS) (n = 2). GluN3A levels were comparable in brainstem and visual cortex, but GluN2D levels were minimal in visual cortex compared to brainstem. Protein levels were standardized to an actin loading control and normalized to brainstem values. (c) Representative blots and quantification of GluN1 (n = 4 per genotype), GluN3A (n = 3 per genotype), and GluN2D (n = 3 per genotype) protein levels in visual cortex. GluN1 and GluN2D levels were unchanged in P8 GluN3A–/– mice compared to WT controls ($P = 0.8$ and $P = 0.6$, respectively) while GluN3A was not detected in GluN3A–/– mice ($P << 0.00001$). Protein levels in GluN3A–/– and WT animals were standardized to a β-actin loading control and expressed as a percentage of WT levels. Error bars represent s.e.m. *** $P < 0.001$.

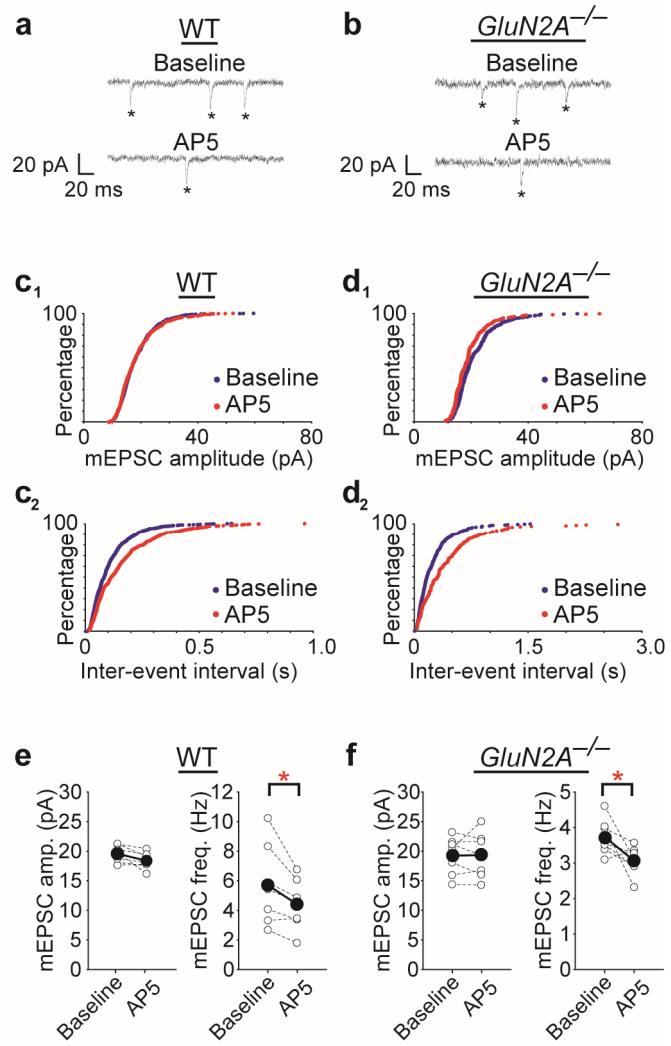

Figure 2.7: The GluN2A subunit does not significantly contribute to the ability of preNMDARs to enhance spontaneous neurotransmitter release onto L2/3 pyramidal neurons in juvenile V1. (a,b) Sample voltage-clamp recordings of AMPAR-mediated mEPSCs from L2/3 pyramidal cells during baseline and D-AP5 application periods in (a) WT and (b) GluN2A–/– mice. mEPSCs are indicated by "*". (c1,d1) Amplitude and (c2,d2) inter-event interval cumulative probability histograms from the same cells shown in a and b during baseline and D-AP5 (50 μm) application reveal a change in mEPSC frequency, but not amplitude, for both

(c2) WT control and (d2) GluN2A–/– mice. (e,f) Scatter plots of amplitude and frequency, before and after D-AP5 application, in (e) WT and (f) GluN2A–/– mice. L2/3 pyramidal cells exhibited a significant reduction in mEPSC frequency by D-AP5 in both WT ($n = 7$, $P < 0.03$) and GluN2A–/– mice ($n = 7$, $P < 0.04$), but no changes in amplitude. The D-AP5 effect on mEPSC frequency was similar between WT and GluN2A–/– mice. * $P < 0.05$.

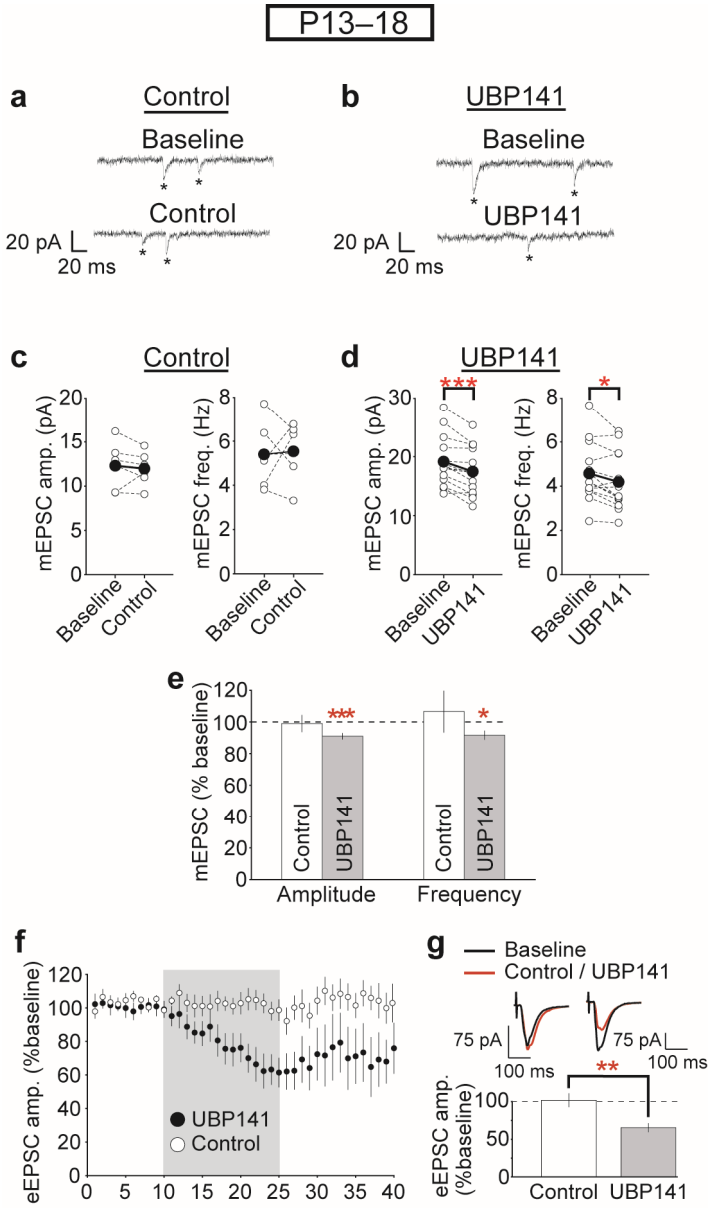

Figure 2.8: The NMDAR antagonist UBP141 affects the amplitude of AMPAR-mediated currents when all NMDARs are blocked, suggesting that this drug lacks specificity. (a,b) Sample voltage-clamp recordings of AMPAR-mediated mEPSCs from L2/3 pyramidal cells from P13–P18 WT mice during (a) vehicle

(ACSF) control or (b) UBP141 (3 μM) application. mEPSC events are indicated by "*". (c,d) Scatter plots of mEPSC amplitude and frequency before and after (c) vehicle control or (d) UBP141 application. UBP141 significantly decreased both amplitude ($n = 14$, $P < 0.0003$) and frequency ($P < 0.01$) of AMPAR-mediated mEPSCs, while there were no changes in amplitude and frequency in vehicle control experiments ($n = 5$). Because postsynaptic NMDARs were blocked, this decrease in amplitude suggests that UBP141 might affect AMPAR-mediated currents by an NMDAR-independent pathway. (e) mEPSC amplitude after vehicle ACSF vehicle control or UBP141 application, averaged and normalized to baseline controls (bar graph of data presented in c and d). (f) UBP141 application decreased the amplitude of evoked AMPAR currents in L4–2/3 synapses recorded in voltage-clamp from P14–P18 WT mice ($n = 15$), while there were no changes with vehicle control ($n = 14$). All NMDARs were blocked during this experiment by D,L-AP5 (100 μM) in the external recording solution. (g) Quantification and sample traces from data taken from the last five minutes of drug treatment in f, demonstrating that UBP141 significantly reduced AMPAR EPSC amplitudes compared to vehicle controls ($P < 0.001$). Because UBP141 affected our postsynaptic readout of glutamate release (AMPAR currents), we were unable to use this drug to assess the role of UBP141-targeted preNMDAR subunits on neurotransmitter release. Error bars represent s.e.m. * $P < 0.05$, ** $P < 0.01$, *** $P < 0.001$.

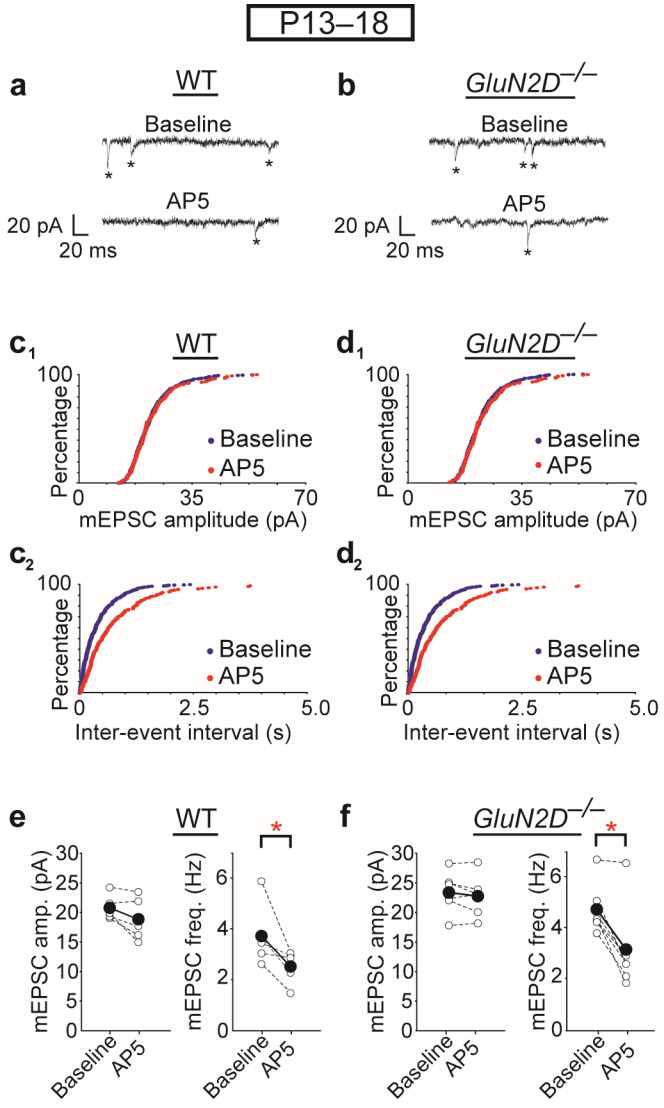

Figure 2.9: The GluN2D subunit is not required for preNMDARs to enhance spontaneous neurotransmitter release onto L2/3 pyramidal neurons in juvenile V1. (a,b) Sample voltage-clamp recordings of AMPAR-mediated mEPSCs from L2/3 pyramidal cells during baseline and D-AP5 application periods in (a) WT and (b) GluN2D–/– mice. mEPSCs are indicated by "*". (c1,d1) Amplitude and (c2,d2) inter-event interval cumulative probability histograms from the same cells shown in a and b during baseline and D-AP5 application reveal a change in

mEPSC frequency but not amplitude for both (c2) WT control and (d2) GluN2D–/– mice. (e,f) Scatter plots of amplitude and frequency, before and after D-AP5 application, in (e) WT and (f) GluN2D–/– mice. L2/3 pyramidal cells exhibited a significant reduction in mEPSC frequency by D-AP5 in both WT ($n = 5$, $P = 0.05$) and GluN2D–/– mice ($n = 6$, $P < 0.007$), but no changes in amplitude. The AP5 effect on mEPSC frequency was similar between WT and GluN2D–/– mice. * $P < 0.05$.

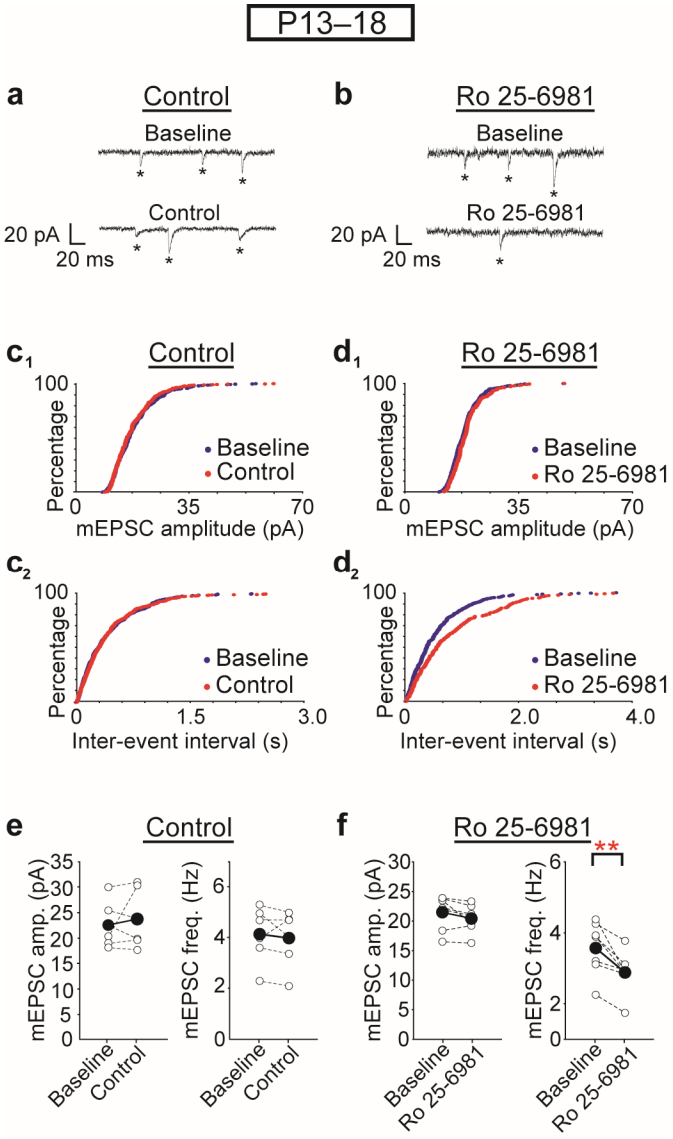

Figure 2.10: GluN2B-containing preNMDARs enhance spontaneous neurotransmitter release onto L2/3 pyramidal neurons in juvenile V1. (a-b) Sample voltage-clamp recordings of AMPAR-mediated mEPSCs from WT L2/3 pyramidal cells in (a) control experiments with vehicle (ACSF) application or (b) with 0.5 μM Ro 25-6981 application. mEPSCs are indicated by "*". (c1,d1) Amplitude and (c2,d2) inter-event interval cumulative probability histograms from

the same cells shown in a and b during baseline and (c) vehicle control or (d) Ro 25-6981 application. There was no change in either mEPSC amplitude or frequency in the control experiment with vehicle application, while Ro 25-6981 application decreased mEPSC frequency without changing amplitude. (e,f) Scatter plots of amplitude and frequency before and after (e) vehicle (ACSF) control or (f) Ro 25-6981 application. There were no significant changes in amplitude or frequency in control experiments (n = 6). Ro 25-6981 caused a significant reduction in mEPSC frequency (n = 7, $P < 0.007$), but did not alter mEPSC amplitude. ** $P < 0.01$.

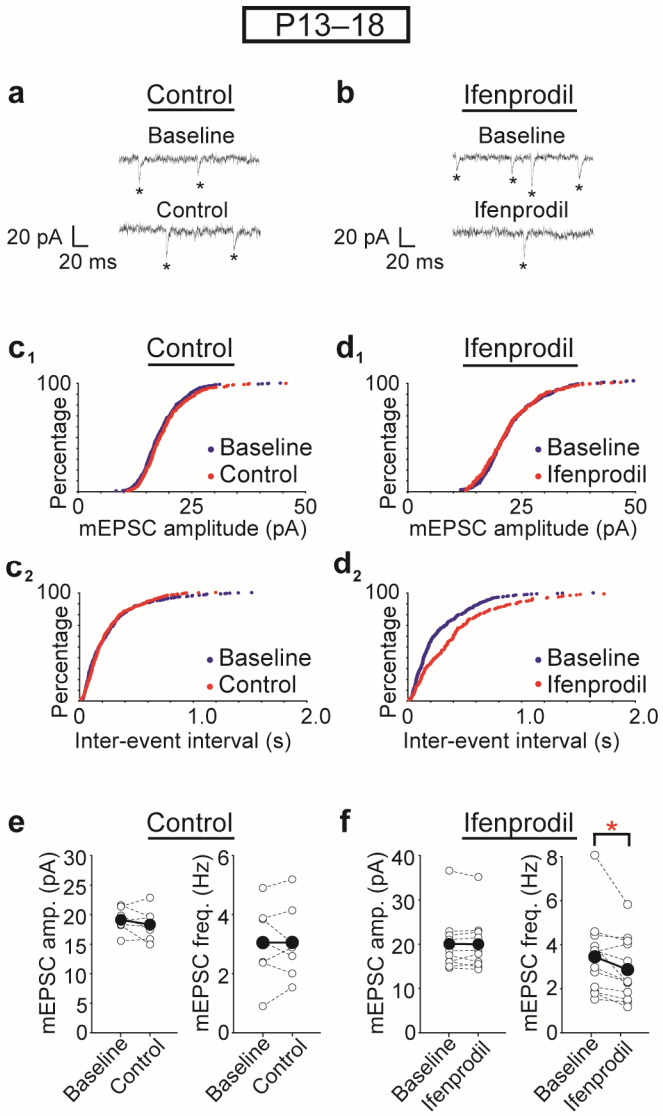

Figure 2.11: Blockade of GluN2B-containing preNMDARs by ifenprodil reduces spontaneous neurotransmitter release onto L2/3 pyramidal neurons. (a-b) Sample voltage-clamp recordings of AMPAR-mediated mEPSCs from WT L2/3 pyramidal cells in (a) control experiments with vehicle (ACSF) application or (b) with 3 μM ifenprodil application. mEPSCs are indicated by "*". (c1,d1) Amplitude and (c2,d2) inter-event interval cumulative probability histograms from

the same cells shown in a and b during baseline and (c) vehicle control or (d) ifenprodil application. (e,f) Scatter plots of amplitude and frequency before and after (e) vehicle (ACSF) control or (f) ifenprodil application. There were no significant changes in amplitude or frequency in control experiments (n = 7). Ifenprodil caused a significant reduction in mEPSC frequency (n = 12, P < 0.02), but did not alter mEPSC amplitude. * P < 0.05.

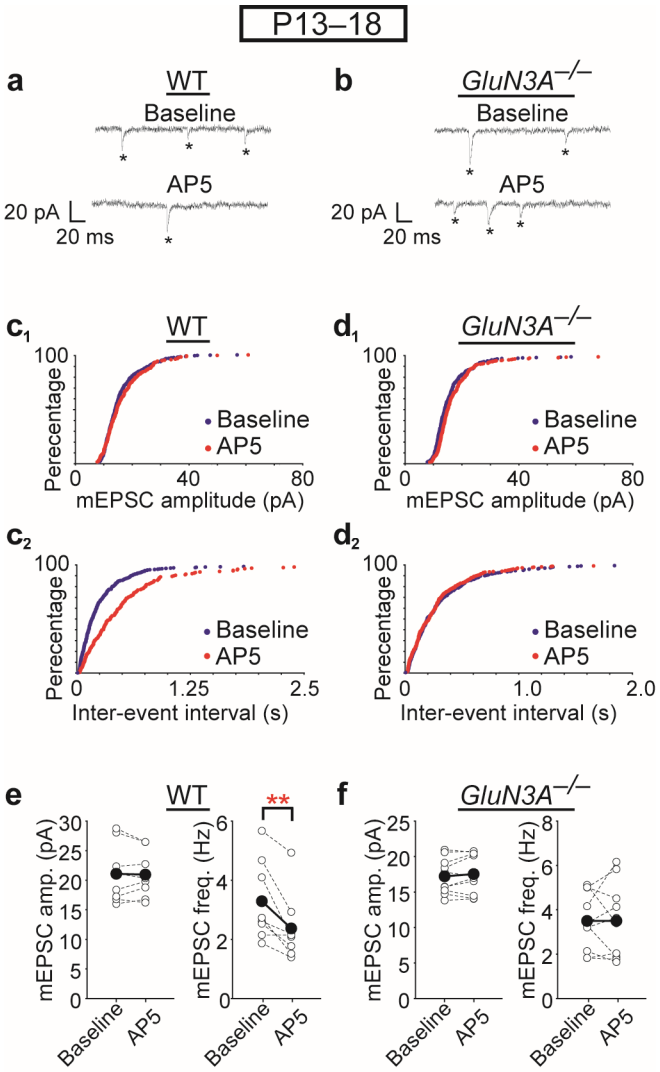

Figure 2.12: The GluN3A subunit is required for the ability of preNMDARs to enhance spontaneous neurotransmitter release in juvenile V1. (a,b) Sample voltage-clamp recordings of AMPAR-mediated mEPSCs from L2/3 pyramidal cells during baseline and D-AP5 application periods in (a) WT and (b) GluN3A–/– mice. mEPSCs are indicated by "*". (c1,d1) Amplitude and (c2,d2) inter-event interval cumulative probability histograms from the same cells shown in a and b. D-AP5 decreased mEPSC frequency but not amplitude in L2/3 neurons in WT mice, while there was no change in either amplitude or frequency in GluN3A–/– mice. (e,f) Scatter plots of amplitude and frequency before and after D-AP5 application in (e) WT and (f) GluN3A–/– mice. mEPSC frequency ($n = 8$, $P < 0.007$), but not amplitude, was significantly reduced in L2/3 pyramidal neurons from WT mice. There were no changes in mEPSC frequency and amplitude observed in L2/3 pyramidal neurons from GluN3A–/– mice ($n = 10$). ** $P < 0.01$.

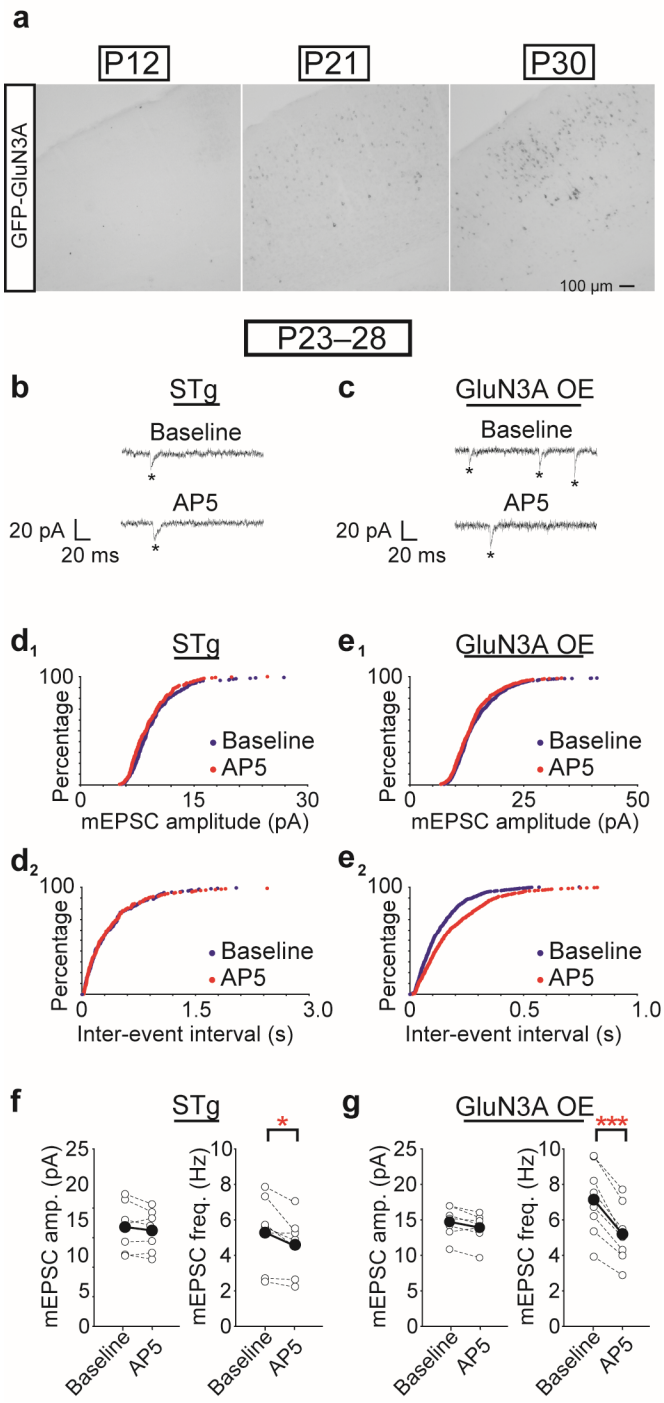

Figure 2.13: Overexpression of the GluN3A subunit in excitatory neurons endows preNMDARs with a greater ability to enhance spontaneous

neurotransmitter release in L2/3 pyramidal cells of more mature V1. (a) Developmental timecourse of GFP-GluN3A overexpression in V1 demonstrating minimal expression of the transgene before P21. (b,c) Sample voltage-clamp recordings of AMPAR-mediated mEPSCs from L2/3 pyramidal cells during baseline and D-AP5 application periods in (b) single-transgenic (STg) mice and (c) double-transgenic mice overexpressing (OE) GluN3A. mEPSCs are indicated by "*". (d1,e1) Amplitude and (d2,e2) inter-event interval cumulative probability histograms from the same cells shown in b and c during baseline and D-AP5 application. (f,g) Scatter plots of amplitude and frequncy before and after D-AP5 application in (f) STg and (g) GluN3A OE mice. There was no change in amplitude with D-AP5 application in either STg or GluN3A OE mice. The decrease in mEPSC frequency with D-AP5 application was much larger in OE mice ($n = 8$, $P < 0.001$) compared to their STg littermates ($n = 7$, $P < 0.03$). Baseline frequency prior to D-AP5 was also higher in OE mice as compared to STg mice, although this effect did not reach statistical significance (OE = 7.1 Hz, STg = 5.3 Hz, $P < 0.07$). * $P < 0.05$ and *** $P < 0.001$.

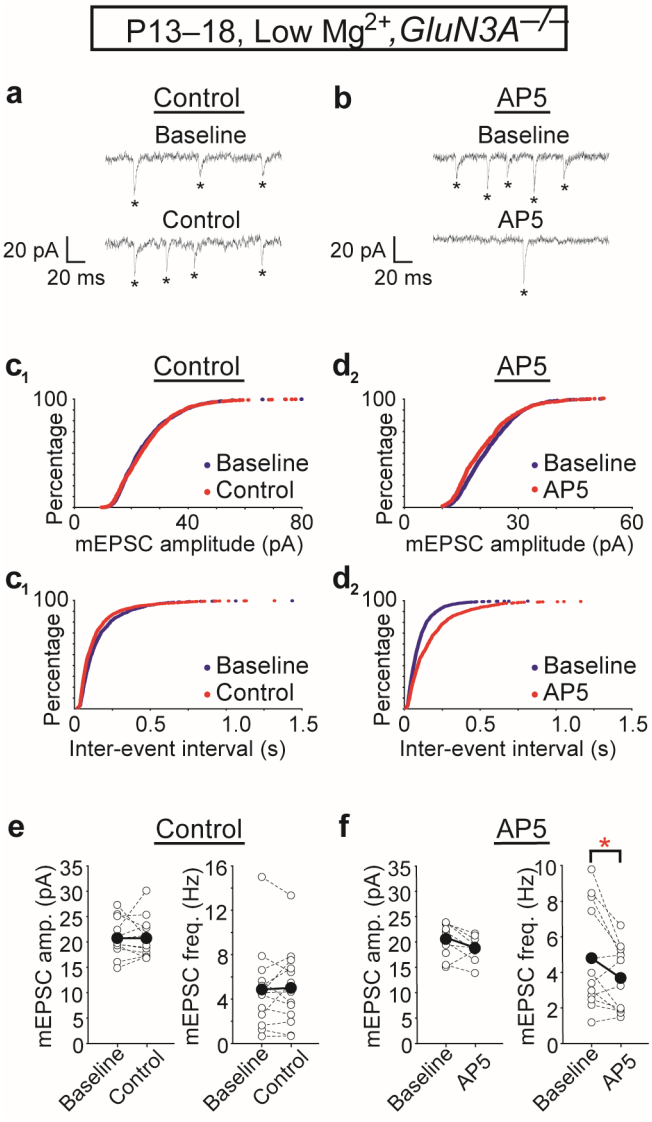

Figure 2.14: In low Mg2+ conditions, preNMDARs lacking GluN3A are able to enhance spontaneous neurotransmitter release in juvenile V1. (a,b) Sample voltage-clamp recordings in low Mg2+ ACSF from L2/3 pyramidal cells in GluN3A–/– mice before or after (a) vehicle (ACSF) or (b) D-AP5 application. mEPSCs are indicated by "*". (c1,d1) Amplitude and (c2,d2) inter-event interval cumulative probability histograms from cells shown in a and b during baseline

and D-AP5 application periods. Note that D-AP5 reduced mEPSC frequency. (e,f) Scatter plots of amplitude and frequency before and after (e) vehicle or (f) D-AP5 application in GluN3A–/– mice. In low Mg2+ ACSF, mEPSC amplitude and frequency were constant in control experiments (n = 13), but D-AP5 application reduced mEPSC frequency (n = 12, P < 0.04) without affecting amplitude. * P < 0.05.

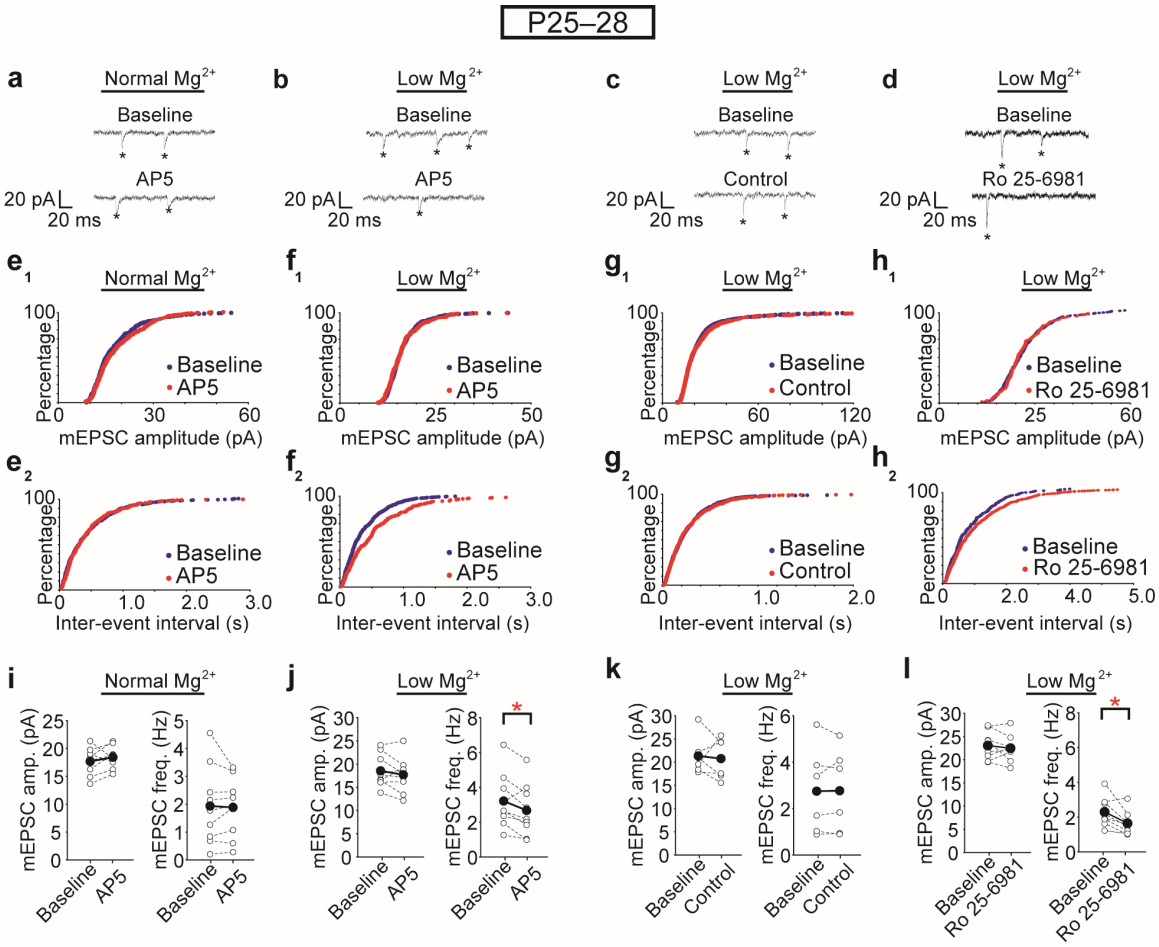

Figure 2.15: In low Mg2+, GluN2B-containing preNMDARs enhance neurotransmitter release in P25–28 WT mice. (a) Sample voltage-clamp recording in normal Mg2+ (1 mM) ACSF from L2/3 pyramidal cells in a P26 mouse during baseline and D-AP5 application periods. (b,c,d) Recordings in low Mg2+ ACSF from WT L2/3 pyramidal cells in P25–28 mice during (b) vehicle (ACSF) control, (c) D-AP5, or (d) Ro 25-6981 application periods. mEPSCs are indicated by "*". (e-h) Amplitude and inter-event interval cumulative probability histograms from the same cells shown in a-d. There is no change in mEPSC amplitude in any condition, but mEPSC frequency decreased with D-AP5 or Ro 25-6981 application in the low Mg2+ condition. (i-l) Scatter plots of mEPSC amplitude and frequency demonstrating responses to control or NMDAR antagonist application when recordings were made in (i) normal Mg2+ (n = 9), or (j,k,l) low Mg2+ (n = 6 for control experiments, n = 9 for AP5 experiments, n = 7 for Ro 25-6981 experiments). A significant reduction in mEPSC frequency was observed only in the low magnesium condition with D-AP5 application ($P < 0.02$) or with Ro 25-6981 application ($P < 0.02$). * $P < 0.05$.

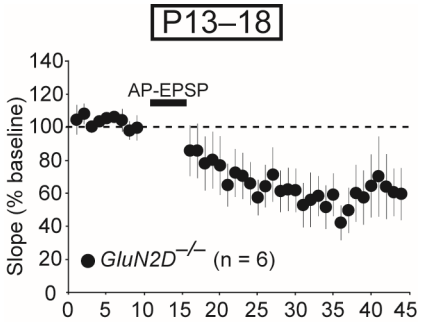

Figure 2.16: GluN2D-containing NMDARs are not required for spike timing-dependent long-term depression (tLTD) in juvenile V1. tLTD was induced in L2/3 V1 synapses in response to action potentials paired with L4-generated EPSPs while postsynaptic NMDARs were blocked in P13–P18 GluN2D–/– mice (n = 6, quantification of the last 10 minutes = 51 ± 16% of baseline EPSP slope, $P < 0.04$).

Chapter 3: Sensory experience regulates glutamate release and timing-dependent plasticity in a presynaptic NMDA receptor-dependent manner.

3.1 Introduction

Fundamental to understanding the brain is knowing how sensory stimuli modify neuronal circuits to allow for adaptive behavior. Manipulations of the sensory environment have long been known to influence the development of emergent circuit properties within sensory cortices (Wiesel & Hubel, 1963). Such manipulations in the sensory environment are believed to alter the expression of synaptic proteins, which subsequently modify properties of synaptic plasticity and transmission to sculpt overall circuit output (Espinosa & Stryker, 2012; Hensch, 2005b; Tropea et al., 2006).

One of the varied mechanisms by which sensory experience may modify cortical circuitry occurs via alterations in the expression of Hebbian plasticity. Classically, Hebbian plasticity is studied by changing presynaptic neurons' firing rates: high frequency stimulation results in LTP and low frequencies result in LTD (Malenka & Bear, 2004). In the visual cortex, sensory deprivation shifts this frequency-dependent threshold, allowing LTP to occur at lower frequencies, in agreement with the Bienenstock, Cooper, and Munro (BCM) theory of synaptic modification (Bienenstock, Cooper, & Munro, 1982; Kirkwood, Rioult, & Bear, 1996). However, in the visual cortex, Hebbian plasticity can be also be induced

by spike timing-dependent plasticity (STDP) (Dan & Poo, 2006). The substrates of STDP produce changes in synaptic efficacy based the relative timing of presynaptic and postsynaptic firing, rather than only the rate of presynaptic firing. The BCM theory can be modified to account for these spike-timing interactions (Izhikevich & Desai, 2003), but how sensory experience modifies STDP induction is just beginning to be understood (Cooper & Bear, 2012).

The cellular mechanisms which distinguish STDP from frequency-based plasticity suggest that these two forms of plasticity may be differentially altered by sensory experience. While timing- and rate-based forms plasticity often activate the same synaptic proteins, such as postsynaptic NMDARs, STDP in sensory cortices can involve the activation of a unique array of synaptic proteins (Feldman, 2012). Perhaps most notably, spike timing-dependent long-term depression (tLTD) in sensory cortices can be expressed presynaptically, and involves astrocytic endocannibinoid signaling (Min & Nevian, 2012), magnesium-insensitive presynaptic NMDARs (Larsen et al., 2011), and metabatropic glutamate receptor activation (Bender et al., 2006). This form of timing-dependent plasticity is also developmentally down-regulated following early sensory milestones such as eye-opening (Corlew et al., 2007), suggesting the synaptic proteins involved in its induction may be modified by early sensory experience (Larsen et al., 2010).

We sought to determine how sensory experience modified the induction of STDP. Remarkably, we find that visual deprivation completely reverses the developmental loss in the ability to induce presynaptically-expressed tLTD. This

restoration of tLTD is accompanied by increases in the function of presynaptic NMDARs, demonstrating that these receptors developmentally-gate this form of plasticity in a sensory experience-dependent manner. Our results demonstrate a previously unappreciated mechanism by which sensory experience can modify visual cortical circuitry via changes in NMDARs uniquely expressed at presynaptic L4 neurons.

3.2 Results

3.2.1 Visual experience bidirectionally modifies the ability to induce tLTD

To determine how sensory experience modifies the induction of spike timing-dependent plasticity, we performed whole cell recordings from visual cortical (V1) L2/3 neurons during the period of heightened synaptic plasticity known as the critical period (P26-30) (Espinosa & Stryker, 2012). To induce spike timing-dependent plasticity, we monitored two EPSPs evoked in L4 before and after pairing EPSPs with action potentials (APs) initiated in postsynaptic L2/3 neurons. To influence the polarity of plasticity, we varied whether the EPSP preceded or followed the action potential by ten milliseconds. In developing sensory cortices (<P20), this canonical spike-timing protocol results in potentiation (tLTP) when the EPSP precedes the AP and depression (tLTD) when the EPSP follows it (Feldman, 2000; Sjostrom et al., 2001). However in agreement with previous studies (Corlew et al., 2007; Seol et al., 2007), when we attempted to induce either tLTP or tLTD during the visual critical period in normally-reared mice (NR), we observed no net change in synaptic strength (**Fig.**

3.1). This suggests that spike timing-dependent plasticity in the visual cortex is tightly regulated by synaptic changes that occur through development.

To determine if sensory experience influenced this developmental loss in the ability to induce spike timing-dependent plasticity, we raised separate cohorts of mice in the dark from near birth and again attempted to induce plasticity with the same induction parameters. Similar to their normally-reared controls, dark-reared (DR) mice, showed no potentiation when EPSPs preceded APs to induce tLTP (**Fig. 3.1A**). Remarkably however, DR mice showed a complete restoration in the ability to induce tLTD (**Fig. 3.1B**). Intriguingly, dark-rearing also reduced the baseline paired-pulse ratio (PPR) evoked at 30 Hz regardless of plasticity outcome, and following tLTD, this ratio increased, consistent with tLTD resulting from a decrease in presynaptic glutamate release (Zucker & Regehr, 2002). These results suggest that visual experience regulates the ability to induce tLTD, but not tLTP, and that this may be accompanied by changes in presynaptic release.

At L2/3 synapses within developing sensory cortices, two forms of tLTD are expressed: one which depends on calcium influx through postsynaptic NMDARs, and a presynaptically-expressed form which depends on endocannabinoid signaling and presynaptic NMDARs (Feldman, 2012). To determine whether tLTD induced following visual deprivation required postsynaptic NMDARs, we repeated experiments in normally- and dark-reared mice and included the NMDAR antagonist MK-801 in recording pipette to selectively block postsynaptic NMDARs (Corlew et al., 2008). With postsynaptic

NMDARs blocked, DR mice still showed substantial tLTD that was accompanied by increases in the PPR at 30 Hz (**Fig. 3.2A**). We next sought to determine if tLTD in DR mice required any NMDAR signaling at all by attempting to induce tLTD in the presence of the NMDAR antagonist D-AP5 (50 μM). In the presence of D-AP5, tLTD and accompanying changes in the PPR in DR mice were completely blocked (**Fig. 3.2B-D**). This suggests that tLTD in DR mice occurs independently of postsynaptic NMDARs, but requires NMDARs elsewhere, likely those expressed presynaptically (Corlew et al., 2008).

Visual deprivation during the critical period is known to induce forms of plasticity which are highly dependent on changes in GABAergic signaling (Hensch, 2005b). To determine if GABA(A) signaling acutely influences the ability to induce presynaptically-expressed tLTD during the critical period, we developed an approach to focally block GABA(A)-mediated synaptic transmission by applying 50 μM gabazine (SR95531) near the postsynaptic recording pipette (**Fig 3.3**). With GABA(A) signaling blocked, NR mice still lacked presynaptically-expressed tLTD which was present in DR mice, suggesting this form of plasticity was not acutely gated by fast inhibitory neurotransmission (**Fig 3.2B**). We next wondered whether the restoration in the ability to induce tLTD observed in DR mice could be reversed by placing these mice in a normal visual environment. In recording from mice which had been dark-reared and then returned to normal visual environment for ten days, we could no longer induce tLTD, similar to their age-matched normally-reared controls (**Fig 3.2C**). Our findings indicate that visual experience can bidirectionally modify the ability to induce spike timing-

dependent plasticity in a manner independent of acute GABA(A) activation or classical postsynaptic NMDAR signaling.

3.2.2 Visual Experience alters the contribution of presynaptic NMDARs to glutamate release

We sought to determine the mechanism by which sensory experience acted to modify the ability to induce tLTD within the visual cortex. Since tLTD observed following visual deprivation appeared to be expressed presynaptically, we hypothesized visual deprivation acted to restore a developmental-regulated form of tLTD observed at L2/3 synapses that is dependent on presynaptic, but not postsynaptic, NMDARs (Corlew et al., 2007). In addition to being required for some forms of tLTD in the developing visual cortex, presynaptic NMDARs enhance evoked and spontaneous glutamate release at L2/3 synapses during a restricted developmental window (<P20) (Corlew et al., 2007; Larsen et al., 2011). If sensory experience restored tLTD which was dependent on presynaptic NMDARs, we hypothesized it would also restore the contribution of presynaptic NMDARs to glutamate release at L2/3 synapses.

To determine if sensory deprivation reversed the developmental loss in the contribution of presynaptic NMDARs to glutamate release, we analyzed short-term plasticity at L2/3 synapses by repetitively evoking glutamate release at variable frequencies (5-30 Hz) before and after D-AP5 application (50 μM, **Fig. 3.4A**). In all experiments, we included MK-801 and BAPTA in the postsynaptic recording pipette while maintaining the neuron at hyperpolarized potentials (near -75 mV) to minimize contributions of postsynaptic NMDARs. At 30 Hz, trains of

six EPSPs evoked by L4 stimulation in DR mice showed more synaptic depression and had a lower paired pulse ratio compared to their NR controls, consistent with a higher initial release probability (**Fig. 3.4B-C**). Additionally, D-AP5 increased the paired-pulse ratio at 30 Hz in DR mice via a reduction in the first EPSP in the train, but did not change the paired pulse ratio in NR mice. These effects of visual deprivation on glutamate release evoked at 30 Hz could be reversed by placing DR mice in normal visual environment for ten days (**Fig 3.4C**).

Both the initial paired-pulse ratio and whether it increased following D-AP5 was highly dependent on stimulation frequency in DR mice: the initial paired-pulse ratio at 5 Hz was not different from NR controls but was substantially lower at higher stimulation frequencies (**Fig. 3.4E**). In correlation with this frequency dependence, application of D-AP5 only increased the paired-pulse ratio in DR mice at frequencies above 5 Hz. Interestingly, in the presence of D-AP5 paired-pulse ratios at all frequencies were the same in recordings from NR and DR mice (**Fig. 3.4F**). This demonstrates that visual deprivation bidirectionally alters presynaptic glutamate release at L2/3 synapses in a frequency- and presynaptic NMDAR-dependent manner.

Given the enhancement of evoked glutamate release at higher frequencies following visual deprivation, we wondered if visual deprivation was accompanied by a change in contribution of presynaptic NMDARs to spontaneous glutamate release at L2/3 visual cortical synapses. To assay this, we examined the effect D-AP5 on the frequency and amplitude of miniature

excitatory postsynaptic currents (mEPSCs) in DR or NR mice while postsynaptic NMDARs were blocked by both hyperpolarization and the inclusion of MK-801 in the recording pipette. In agreement with previous results demonstrating that visual deprivation results in postsynaptic synaptic scaling of AMPAR responses (Desai, Cudmore, Nelson, & Turrigiano, 2002; Goel et al., 2006), mEPSC amplitudes were significantly larger in recording from DR mice, but were not affected by D-AP5 application (**Fig. 3.5C**). Additionally, while dark-rearing did not alter the baseline mEPSC frequency, D-AP5 reduced the frequency in recordings from DR mice, without affecting the frequency in NR mice (**Fig. 3.5D**). This suggests that dark-rearing increases the contribution of presynaptic NMDARs to spontaneous release. However, since we did not observe a change in the baseline mEPSC frequency following dark-rearing, this indicates that presynaptic NMDARs may only contribute to spontaneous release at a portion of L2/3 synapses or that their contribution is masked by known reductions in synapse number which occur following dark-rearing (Valverde, 1971; Wallace & Bear, 2004).

Visual deprivation beginning near birth and extending until the critical period may alter synaptic properties through the mechanisms restricted to this developmental period or duration of deprivation. To address this, we measured short-term plasticity in mice that had been normally-reared up until adulthood (P60) and which then underwent late-onset visual deprivation (LOVD) by being kept in the dark for ten days. Similar to our previous findings (Yashiro, Corlew, & Philpot, 2005), EPSP trains evoked at 30 Hz, but not 5 Hz, in recordings from

LOVD mice had lower initial paired-pulse ratios compared to normally-reared littermates (**Fig. 3.6**). Similarly, D-AP5 increased the initially lower 30 Hz paired-pulse ratio observed in deprived mice without affecting synaptic depression in normally-reared littermates. These results suggest that even visual deprivation that occurs for relatively brief periods during adulthood is capable of reversing the developmental loss in the contribution of presynaptic NMDARs to glutamate release at L2/3 synapses.

Given these findings, we next addressed whether visual deprivation in adulthood could also reverse the developmental loss in the ability to induce tLTD. Indeed, we were able to induce tLTD in recordings from mice which had undergone LOVD, whereas we observed no significant tLTD in recordings from their aged-matched, normally-reared littermates (**Fig. 3.6**). As we observed in mice which had been visual deprived from birth until the critical period, tLTD was accompanied by increases in the paired-pulse ratio, suggesting that it resulted from a decrease in presynaptic glutamate release. Taken together with our previous findings, this suggests that sensory deprivation even in adulthood (>P60) is capable of restoring contributions by presynaptic NMDARs to glutamate release and STDP which normally become dormant through development.

3.2.3 Presynaptic Layer 4 NMDARs are required for the effects of visual deprivation on spontaneous glutamate release

If sensory experience modifies the activity of presynaptic NMDARs at a subset of V1 synapses, we hypothesized that targeted genetic deletion of presynaptic NMDARs at a subset of L2/3 afferents should occlude the effects of

visual deprivation on tLTD and glutamate release. Cortical L2/3 neurons receive predominant excitatory intracortical input from L4 and other L2/3 neurons (Lefort, Tomm, Floyd Sarria, & Petersen, 2009). However, in early development presynaptic NMDARs are selectively expressed at L4 inputs, but not at L2/3 intralaminar synapses (Brasier & Feldman, 2008; Zilberter et al., 2009). We therefore focused on genetically disrupting presynaptic NMDAR expression at L4 neurons using the *Scnn1a-Tg3:Cre* driver (Madisen et al., 2010).

As previously described, mice transgenic for *Scnn1a-Tg3:Cre* had Td-tomato fluorescence confined to L4 within the visual cortex after being crossed to stop-floxed-Tdtomato reporter mice, demonstrating the intracortical L4-specificity of this line (Ai9, **Fig. 3.7**). We next sought to determine the developmental onset of L4 Cre activity within V1 by analyzing Td-tomato fluorescence driven by *Scnn1a-Tg3:Cre* at different stages of development. While we did not observe Cre-mediated fluorescence at P10 or P15, we did see fluorescence beginning at P20 which persisted into adulthood (**Fig. 3.8**). Importantly, Cre-driven fluorescence was confined to non-GABAergic neurons in agreement with initial description *Scnn1a-Tg3:Cre* (**Fig. 3.8**). To disrupt expression of NMDARs at L4 neurons within the visual cortex, we crossed *Scnn1a-Tg3:Cre* to mice expressing a floxed version of the obligatory NMDAR subunit gene, *Grin1* (*Grin1*$^{Fl/Fl}$) (Tsien, Huerta, & Tonegawa, 1996). To identify L4 neurons which positively expressed Cre in *Scnn1a-Tg3:Cre:Grin1*$^{Fl/Fl}$ mice (hereafter referred to as *Grin1*^{L4CKO}) and which lacked NMDARs, we generated triple-transgenic *Grin1*^{L4CKO}*,* stop-floxed-Zsgreen mice (Ai6). We then recorded pharmacologically-isolated NMDAR

currents in fluorescently-labeled L4 V1 neurons in *Grin1*^{L4CKO} mice or from their *Grin1*$^{Fl/Fl}$-only littermates to verify loss of NMDARs in L4 neurons. We evoked NMDAR currents from the activation of two pathways, the white-matter or horizontally in L4, at increasing stimulation intensities to recruit increasing numbers of afferents from several synaptic sources. We observed that loss of NMDAR currents in fluorescent, Cre-positive neurons followed a slow developmental time course with maximal NMDAR currents being reduced only ~40% at P30 and ~60% at P60, as compared to their only *Grin1*$^{Fl/Fl}$-only littermates (**Fig. 3.7, 3.9**). However, at P75, mean NMDAR currents were reduced by ~80% and many neurons lacked any NMDAR currents (**Fig. 3.7**). We therefore focused on determining the effects of L4 NMDAR deletion in adult mice (>P85).

To determine how the loss of NMDARs in L4 neurons influenced synaptic transmission at postsynaptic L2/3 neurons, we recorded mEPSCs from L2/3 neurons in NR *Grin1*^{L4CKO} mice and their *Grin1*$^{Fl/Fl}$-only littermates at P85-95. Consistent with little contribution of presynaptic NMDARs to synaptic transmission in NR adult mice (Corlew et al., 2007), loss of L4 NMDARS did not significantly alter either the mEPSC frequency or amplitude at L2/3 synapses. In agreement, loss of L4 NMDARs in *Grin1*^{L4CKO} mice also did not alter presynaptic release at various stimulation frequencies as assayed by changes in PPR (**Fig. 3.10**). We next sought to determine if loss of L4 NMDARs affected the contribution of presynaptic NMDARs to glutamate release observed following visual deprivation. We therefore visually-deprived *Grin1*^{L4CKO} and their *Grin1*$^{Fl/Fl}$-

only littermates for 10-15 days using the LOVD paradigm as previously described. In recordings from LOVD, but not NR *Grin1*$^{Fl/Fl}$-only mice, D-AP5 reduced the baseline mEPSC frequency without affecting mEPSC amplitude (**Fig. 3.10**). The reduction in frequency was smaller than previously seen following dark-rearing, but suggests that LOVD in adulthood also increases the contribution of presynaptic NMDARs to spontaneous release at L2/3 synapses. In contrast, in *Grin1*^{L4CKO} mice which had undergone LOVD, D-AP5 failed to reduce the mEPSC frequency (**Fig. 3.10**). This demonstrates that presynaptic L4 NMDARs mediate changes in the contribution of presynaptic NMDARs to spontaneous release following visual deprivation.

We hypothesized that if presynaptic L4 NMDARs increased spontaneous release at L2/3 V1 synapses following LOVD that these receptors would also be required for tLTD induced in LOVD mice. To determine if this was the case, we crossed *Scnn1a-Tg3:Cre* into mice expressing stop-floxed-ChR2(H134R)-YFP (Ai32) allowing us to achieve uniform channelrhodpsin expression in L4 between mouse cohorts (Madisen et al., 2012). In these mice (referred to as ChR2^{L4}) we confirmed expression of channerhodpsin was confined to L4 neurons within V1 (**Fig. 3.11A**). To activate channelrhodpsin in ChR2^{L4} neurons, we focally stimulated them with blue-light (470 nm) using a Mosaic digital mirror device coupled to arc illumination source. In recordings from L4 channelrhodpsin-positive neurons, focal stimulation over the soma reliably resulted in single action potentials at 20 Hz with brief (2-4 ms) light pulses. Correspondingly, recordings in L2/3 neurons demonstrated that activation of channelrhodpsin over L4 somata

reliably produced EPSPs at 20 Hz which were action potential-dependent, suggesting that they did not result from direct illumination of presynaptic terminals expressing channelrhodpsin (**Fig. 3.11B**).

To address whether visual deprivation altered the ability to induce tLTD specifically at L4 to L2/3 synapses, we attempted to induce tLTD in $ChR2^{L4}$ mice which had either been NR or underwent LOVD. To accomplish this, we recorded L4 ChR2-mediated EPSPs at 20 Hz and then paired single light-mediated EPSPs with action potentials following a 10-12 ms delay. Consistent with our previous results, NR $ChR2^{L4}$ mice lacked tLTD. However, their LOVD $ChR2^{L4}$ littermates showed a complete restoration in the ability to induce tLTD (**Fig. 3.11C-D**). Additionally, LOVD $ChR2^{L4}$ mice had a lower initial 20 Hz PPR ratio compared to NR controls, which increased following tLTD, suggesting this plasticity was expressed presynaptically (**Fig. 3.11E)**.

If this change in the ability to induce tLTD following visual deprivation was mediated by presynaptic L4 NMDARs, we hypothesized loss of L4 NMDARs would occlude it in LOVD mice. We therefore generated triple transgenic mice by crossing *Grin1*^{L4CKO} mice to stop-floxed-ChR2(H134R)-YFP mice, resulting in channelrhodpsin expression selectively in neurons which lack NMDARs. In *Grin1*^{L4CKO}*:ChR2* mice which had undergone LOVD, the ability to induce tLTD was occluded (**Fig. 3.11C-D**), demonstrating that presynaptic L4 NMDARs were required for the restoration of tLTD following visual deprivation. Furthermore, loss of L4 NMDARs also occluded the initial decrease in PPR as well as its subsequent increase following tLTD induction observed in LOVD mice. Light-

mediated stimulation parameters such as area and pulse length were not different between groups, suggesting that differences in these variables did not account for the observed changes following visual deprivation. These results demonstrate that visual deprivation selectively modifies the function of presynaptic NMDARs at L4 to L2/3 synapses which increase glutamate release and allow for presynaptic tLTD induction.

3.2.4 GluN3A expression is regulated by visual experience and is required for tLTD induced following dark-rearing

Since visual deprivation is known to change the composition of postsynaptic NMDARs, we hypothesized that a similar change in presynaptic NMDAR composition might occur following dark-rearing to mediate the changes we observed in synaptic plasticity and neurotransmission. We therefore quantified changes in the synaptic expression of candidate NMDAR subunits in DR mice or their NR controls. Consistent with previous findings (Quinlan, Philpot, Huganir, & Bear, 1999; Yashiro et al., 2005), dark-rearing did not significantly alter the expression of the obligatory NMDAR subunit GluN1, but decreased the expression ratio of GluN2A to GluN2B (**Fig. 3.12a** and **3.13**). Interestingly, we also observed that dark-rearing increased the expression of the magnesium-insensitive NMDAR subunit GluN3A as compared to age-matched NR controls **(Fig. 3.12b)**. This suggests a previously unknown regulation of synaptic GluN3A expression by visual experience.

We previously demonstrated that the NMDAR subunit GluN3A is expressed at excitatory presynaptic terminals and is required for presynaptic

NMDAR function early in development at L2/3 V1 synapses (Larsen et al., 2011). Given the upregulation in the expression of this NMDAR subunit following dark-rearing, we next determined how genetic loss of GluN3A influenced the effects of dark-rearing on tLTD and presynaptic release by recording from L2/3 neurons in *Grin3A*$^{-/-}$ mice and their wild-type littermates (Das et al., 1998). In NR wild-type mice as well as their NR *Grin3A*$^{-/-}$ littermates, AP-EPSP pairings failed to induce tLTD (**Fig. 3.12c**). In contrast, DR wild-type mice showed a restoration in the ability to induce tLTD that was absent in DR Grin3A$^{-/-}$ mice, demonstrating a requirement of GluN3A in tLTD induced following visual deprivation **(Fig. 3.12d)**. Additionally, DR wild-type mice, but not *Grin3A*$^{-/-}$ littermates, had an initially reduced 30 Hz PPR which increased following tLTD. Similarly, when we tested the effect of D-AP5 on short-term plasticity, it only increased the 30 Hz PPR in DR wild-type mice, but not DR *Grin3A*$^{-/-}$ littermates **(Fig. 3.13)**. These results demonstrate that loss of GluN3A impairs changes in STDP and presynaptic glutamate release selectively following visual deprivation during the critical period, without affecting NR mice at this age.

3.3 Discussion

Our findings demonstrate that visual experience dramatically regulates the ability to induce STDP at L2/3 synapses. We found that visual deprivation either during the critical period or during adulthood is capable of reversing the developmental loss in the ability to induce presynaptically-expressed tLTD. Increases in presynaptic glutamate release at high frequencies accompanied this restoration in the ability to induce tLTD. These effects required both presynaptic

L4 NMDARs and GluN3A expression, suggesting changes in the expression of GluN3A at defined presynaptic sites may mediate changes induced by visual deprivation. As STDP has been shown sufficient to induce alterations in V1 receptive fields *in vivo* (Meliza & Dan, 2006), synapse-specific alterations in the ability to induce STDP may be involved in the expansion of receptive fields known to occur following visual deprivation (Czepita, Reid, & Daw, 1994; Fagiolini, Pizzorusso, Berardi, Domenici, & Maffei, 1994).

Our results demonstrate a novel form of experience-dependent plasticity that depends on the relative timing of pre- and postsynaptic neurons' activation. However, the substrates of timing- and rate-based plasticity likely interact to produce overall changes in synaptic strength following patterned neuronal activity (Sjöström, Turrigiano, & Nelson, 2001). Somewhat paradoxically, our results demonstrate that visual deprivation restores a form of dormant tLTD while also selectively increasing the efficacy of glutamate release at high frequencies. Since frequency-dependent LTP is induced as a result of such high frequency presynaptic firing, one additional suggestion arising from our findings is that synaptic transmission at high frequencies may become more reliable following visual deprivation due to increased contributions to release by presynaptic NMDARs. Hypothetically, this would assist in the increased ability to induce frequency-dependent LTP that has been observed following sensory deprivation (Allen, Celikel, & Feldman, 2003; Kirkwood et al., 1996). In agreement with this bidirectional contribution of presynaptic NMDARs to plasticity outcomes, presynaptic NMDARs are required for both slow-wave LTP and LTD at

intralaminar L4 visual cortical synapses (L. Wang, Fontanini, & Maffei, 2012). Therefore, our results support the conclusion that visual deprivation does not result in favored synaptic depression over potentiation, but likely expands distinct mechanisms for achieving both plasticity outcomes.

Like many forms of sensory deprivation-induced synaptic changes (Maffei & Turrigiano, 2008), the exact duration and nature of the deprivation are likely to determine how they affect STDP. In agreement with this, a previous study demonstrated that two days of visual deprivation does not result in the restoration of tLTD at L2/3 synapses, but extends the integration-window for postsynaptically-expressed tLTD induced in the presence of non-endogenous adrenergic agonists (Guo et al., 2012). Broadly, this study is agreement with our present findings that dark-rearing modifies timing-dependent synaptic properties to favor tLTD induction, but also demonstrates an additional postsynaptic mechanism for a producing a related outcome.

Similarly, previous studies have also examined the effects of various sensory deprivation paradigms on presynaptic release as assayed by alterations in PPR. The effects of visual deprivation on presynaptic release reported here were highly dependent on presynaptic input, frequency of glutamate release, and on sampling sufficient to overcome the intrinsic variability of neurotransmitter release (Ribrault, Sekimoto, & Triller, 2011). In support of our findings, we have previously observed that visual deprivation can either fail to alter PPR at L2/3 synapses, or reduce the ratio; the key difference being whether presynaptic NMDARs are blocked by the inclusion of NMDAR antagonists in the bath (Philpot

et al., 2001; Yashiro et al., 2005). Our results are broadly consistent with an experience-dependent developmental reduction in presynaptic glutamate release at L4 to L2/3 synapses which coincides with the reductions in presynaptic NMDAR function and GluN3A expression (Cheetham & Fox, 2010; Corlew et al., 2007; Larsen et al., 2011). Collectively, our results suggest sensory deprivation produces tailored alterations to presynaptic NMDAR function via changes confined to restricted numbers of synaptic sites and activation frequencies.

By selective optogenetic stimulation of presynaptic L4 neurons which lack NMDARs, we have further strengthened the already robust findings that presynaptic NMDARs can mediate tLTD at L4 to L2/3 synapses within sensory cortices (Rodriguez-Moreno et al., 2011). Additionally, while it was initially surprising that loss of L4 NMDARs did not affect synaptic transmission at L2/3 synapses from NR mice, this result is consistent with findings that presynaptic NMDARs minimally contribute to plasticity or glutamate release at L2/3 synapses in adulthood (Corlew et al., 2007). Since genetic deletion of L4 NMDARs resulted in a complete loss in the ability to modulate L2/3 spontaneous neurotransmission with D-AP5, it suggests that changes in presynaptic NMDAR expression following visual deprivation occur predominately at L4 synapses onto L2/3 neurons.

While it has long been known that visual deprivation increases NMDAR synaptic responses (Czepita et al., 1994), our results are the first to demonstrate a role for the NMDAR subunit GluN3A in experience-dependent plasticity in the visual cortex. We previously demonstrated that GluN3A is developmentally

downregulated in the visual cortex at a time that corresponds with the loss of both tLTD and the contribution of presynaptic NMDARs to glutamate release (Larsen et al., 2011). Reminiscent of the developmental upregulation of postsynaptic GluN2A which is partially reversed by dark-rearing (Quinlan, Philpot, et al., 1999), our results demonstrate that dark-rearing increases the synaptic expression of GluN3A. Since GluN3A is required for the effects of dark rearing on tLTD induction and glutamate release, it suggests that visual experience may prevent downregulation of these receptors or result a restoration of their expression. In neuronal culture systems, chronic activity blockade with tetrodotoxin prevents clathirin-mediated endocytosis of GluN3A, leading to the enhanced surface expression of GluN3A-containing NMDARs (Chowdhury et al., 2013). The alterations in neuronal activity induced by visual deprivation may engage similar mechanisms to reduce the developmental downregulation of GluN3A.

How GluN3A-containing NMDARs mediate long-term changes in glutamate release following tLTD is not yet known. However, presynaptic LTD at L4 to L2/3 synapses requires presynaptic calcineurin, which forms an activity-regulated complex with GluN3A-containing NMDARs (Chan & Sucher, 2001; Rodriguez-Moreno et al., 2013). Among other processes, presynaptic calcineurin is important for the regulation of synaptic vesicle dynamics via the dephophorylation of dephosphins (Cousin & Robinson, 2001). As such, alterations in this process may be important for tLTD induction, but remain to be explored. In combination with previous results demonstrating that GluN3A

expression regulates presynaptic glutamate release and tLTD in the juvenile cortex (Larsen et al., 2011), our present findings demonstrate a critical role for this NMDAR subunit in cortical synaptic function.

3.4 Methods

3.4.1 Animals.

NR mice were raised on a 12:12 light:dark cycle, whereas DR mice were raised in complete darkness from P2-3 until P26-30. In some instances, DR mice were returned to a 12:12 light:dark cycle for 10-12 days beginning at P30. LOVD was achieved by placing NR mice at P60-63 into complete darkness for 10-12 days. Experimental mice were raised with corn cob bedding and nestlets only and were fed *ad libitum*.

Scnn1a-tg3:Cre (009613) and *Rosa26*-stop-floxed-*Tdtomato* (Ai9, 007909), *Zsgreen* (Ai6, 007906), and *ChR2(H134R)-EYFP* (Ai32, 012569) were created by The Allen Institute for Brain Science on a C57BL/6 background (Madisen et al., 2012; Madisen et al., 2010) and were purchased from The Jackson Laboratory (JAX). *Grin1*-floxed mice were created by Dr. S. Tonegowa (Tsien et al., 1996) and were on a mixed 129S4/SvJae:C57BL/6 background (JAX, 005246). *Grin3A*$^{-/-}$ mice were generously provided by Dr. I Pérez-Otaño, Dr. N. Nakanashi, and Dr. S. Lipton and were on a mixed 129S4/SvJae:C57BL/6 background (Das et al., 1998). All other wild-type mice were on the C57BL/6 strain (Charles River Laboratories). Mice lacking NMDAR subunits were compared to either wildtype (*Grin3A*$^{+/+}$) or Floxed-only (*Grin1*$^{Fl/Fl}$) littermates and these experiments were performed with the experimenter blind to genotype.

Germline transmission of *Scnn1a-tg3:Cre* was via paternal mice. All mice were compared to interleaved, age-matched controls. Electrophysiological recordings were obtained from a minimum of three mice for each condition.

3.4.2 Biochemistry

Biochemical fractionation and immunoblotting: Tissue from the pooled visual cortex of 2 mice per replicate was rapidly dissected and stored at -80C until use. Biochemical fractions were prepared by dounce-homogenizing samples in HEPES-buffered sucrose (4 mM HEPES, 0.32 M sucrose, pH 7.4), and spinning twice at 1000 x g for 10 min to eliminate nuclei. The postnuclear supernatant fraction was then centrifuged at 10,000 x g for 20 min to isolate crude synaptosomal pellets (P2 fraction, intact synaptosomes), and resuspended in buffer. 15 µg of total protein from each sample were loaded on 8% tris-glycine NuPage gels (Invitrogen), resolved by SDS-PAGE, and transferred to nitrocellulose membranes. Blotting (Bio-Rad) and Odyssey system imaging and quantification (LI-COR) were carried out following manufacturers' protocols. The following antibodies were used: rabbit anti-GluN3A (07-356, Millipore), rabbit anti-GluN2A (AB1555 and 04-901, Millipore) goat anti-GluN2B (sc-1469, Santa Cruz Biotechnology), goat anti-GluN1 (sc-1467, Santa Cruz Biotechnology mouse anti-β-actin (A5316, Sigma-Aldrich), Alexa Fluor 680-labeled anti-goat IgG (A21084, Invitrogen), Alexa Fluor 680-labeled anti-mouse IgG (A21058, Invitrogen), and IRDye 800-labeled anti-rabbit IgG (611-732-127, Rockland Immunochemicals).

Immunohistochemistry

Mice were anesthetized with pentobarbital sodium and then perfused 4% paraformaldehyde in PBS. Samples were incubated in 10, 20, and then 30% sucrose in PBS before being cut at 40 μM using a freezing-sliding microtome. Sections were collected, rinsed and blocked with 5% normal goat serum and 0.2% Triton X-100 in PBS. Sections were then incubate in this blocking solution with primary antibody for 48 hours at 4°C. The primary antibodies used in this study were mouse anti-NeuN (1:500, MAB377, Millipore), rabbit anti-GABA (1:1500, A2052, Sigma-Aldrich), and rabbit anti-CDP (1:500, sc-13024, Santa Cruz Biotechnology). Fluorescent proteins expressed via *Cre*-mediated recombination were not further antibody enhanced (those from Ai9, Ai6, Ai32 mice). Secondary detection was performed with Alexa Fluor 488, 546, or 647 conjugated goat anti-rabbit or anti-mouse antibodies (Invitrogen). Mounted sections were imaged on a Zeiss LSM 710 Confocal Microscope using 20×/0.8 NA or 40×/1.3 NA objectives.

3.4.3 *Ex vivo* Electrophysiology.

For cortical slice preparation, mice were anesthetized with pentobarbital sodium and decapitated after disappearance of corneal reflexes. Brains were rapidly removed and cut at 350 μm using a vibrating microtome (Leica VT1200S) in ice-cold dissection buffer containing 87 mM NaCl, 2.5 mM KCl, 1.25 mM $NaH2PO_4$, 25 mM $NaHCO_3$, 75 mM sucrose, 10 mM D-(+)-glucose, 1.3 mM ascorbic acid, 7 mM $MgCl_2$ and 0.5 mM $CaCl_2$, bubbled with 95% O_2 and 5% CO_2. Mice older than P30 were first intracardially perfused with dissection buffer.

Following dissection, slices recovered for 20 min at 35 °C in artificial cerebrospinal fluid (ACSF) containing 124 mM NaCl, 3 mM KCl, 1.25 mM Na_2PO_4, 26 mM $NaHCO_3$, 1 mM $MgCl_2$, 2 mM $CaCl_2$ and 20 mM D-(+)-glucose, saturated with 95% O2, 5% CO2 and were then kept at 21–24 °C for at least 40 min. Recordings were made in a submersion chamber at 33°C +/- 1°C in the same ACSF, except where noted. All pharmacological agents were purchased from Abcam, in water-soluble salts if necessary.

L2/3 or L4 neurons were visually identified with infrared differential interference contrast optics or by fluorescence-based targeting of Cre positive neurons. Patch pipettes were pulled from thick-walled borosilicate glass with open tip resistances of 2–7 MΩ. Neurons were recorded in either voltage- or current-clamp configuration with a patch clamp amplifier (Multiclamp 700A), and data were acquired and analyzed using pCLAMP 10 software (Molecular Devices). For evoked and plasticity experiments not involving optogenetic activation of L4, neurons were recorded in voltage- or current-clamp while L4 or white matter axons were stimulated extracellularly every 15 seconds (0.2 ms) with a two-conductor cluster electrode with 75 μm tip separation (FHC Inc., Bowdoin, ME). Series and input resistances were monitored throughout the experiments by measuring the response to a −5-mV step at the beginning of each sweep. Series resistance was calculated using the capacitive transient at the onset of the step and input resistance was calculated from the steady-state current during the step. No series resistance compensation was applied.

Current Clamp Recordings

For current-clamp experiments, patch pipettes were filled with internal solution containing (in mM), 100 potassium gluconate, 20 KCl, 10 HEPES, 4 Mg-ATP, 0.3 Na-GTP, 0.035 Alexa594, and 10 sodium phosphocreatine with pH adjusted to 7.25 and osmolarity adjusted to ~295 mOsm with sucrose. In most experiments (after Fig.1), 1 mM MK-801 was included in the internal solution to block postsynaptic NMDARs. For experiments measuring the effect of D-AP5 on short-term plasticity, 5 mM tetra-potassium BAPTA was included in the above internal solution and the concentration of potassium gluconate was reduced to 80 mM. In all current clamp experiments, current was injected to maintain a −75 mV resting potential if necessary; cells were excluded from analysis if input resistance changed more than 20% or if the initial resting potential was >-60 mV. The amplitude of the first EPSP in a train was restricted to <5 mV, except when attempting to induce tLTP, where it was always >3 mV in an attempt to enhance the synaptic cooperativity necessary for this form of plasticity when induced at low pairing frequencies (Sjostrom et al., 2001). Current clamp recordings were sampled at 20 kHz and filtered at 10 kHz.

Targeted blockade of inhibition was based on previously described methods (Feldman, 2000). To focally block inhibition, SR95531 (gabazine, 50 uM dissolved in ACSF), was applied 30-50 microns from the recording pipette using borosilicate pipettes with large openings (5-8 micron opening, 0.7-1.2 megaOhm open-tip resistances). To extrude gabazine towards the recorded neuron, positive pressure was applied to the back of the pipette (0.07 - 0.2 psi).

Spike timing-dependent plasticity: A steady baseline was recorded for 10 min during which monophasic and fixed latency response EPSPs were maintained with no change in amplitude or slope. The spike timing-dependent plasticity induction period consisted of 100 single action potentials at 0.2 Hz, each preceded (tLTP), or followed (tLTD) within 10–12 ms by a single EPSP generated by L4 stimulation. Postsynaptic action potentials were produced by a brief (<5 ms) depolarization of the postsynaptic L2/3 cell and EPSPs generated in L4 were produced in an identical manner as the baseline period. EPSP slope was measured from the first 2 ms of the EPSP and amplitude was measured from a consistent initial monosynaptic EPSP plateau point. Change in EPSP slope or PPR (mean $EPSP_2$ amplitude/$EPSP_1$ amplitude) was calculated as the decrease in slope or PPR from the last 10 min post-LTD compared to the last 5 min of the baseline.

Short-term plasticity: To measure the effect of D-AP5 on evoked short-term plasticity, we measured the amplitude and PPR of six EPSPs evoked at 5, 10, 20, and 30 Hz. We evoked EPSPs alternatively at 5 Hz then 30 Hz, or 10 then 20 Hz in separate recordings, with 15 second interstimulus intervals. After a 15-min baseline during which monophasic and fixed latency EPSPs maintained no change in slope or amplitude, D-AP5 (50 μM) was applied for 10 min. Changes in the short-term plasticity and PPR were assayed via comparing mean values of the last 5 minutes of the baseline period to the last 5 minutes of the D-AP5 application period.

Optogenetic activation of L4 neurons: Focal channelrhodpsin (H134R) activation was provided through a 20×/0.8 NA objective at a single-photon excitation λ of 477 nm. Light power was not modified between experiments and was provided by a Lambda DG-4 300 W Xenon bulb (Sutter Instruments). This light source was coupled to a Mosiac microelectro-mechanical-system digital mirror device (Andor Technology). Illumination was provided using square illumination patterns over L4, YFP-positive somata (28x28 μM to 45x45 μM) using brief (1.84 - 4 ms) light pulses and was shuttered via PClamp –mediated TTL inputs to the Lambda DG-4.

Voltage Clamp Recordings

For mEPSC recordings, patch pipettes were filled with (in mM),100 $CsCH_3SO_3$, 15 CsCl, 2.5 $MgCl_2$, 5 QX-314-Cl, 5 tetra-Cs-BAPTA, 10 mM HEPES, 4 mM Mg-ATP, 0.3 mM Na-GTP, 1 mM MK-801, and 0.035 Alexa-594, with pH adjusted to 7.25 and osmolarity adjusted to ~295 mOsm with sucrose. AMPAR-mediated mEPSCs were recorded in the presence of tetrodotoxin citrate (200 nM) and SR95531/Gabazine (10 μM) at −80 mV. Events with a rapid rise time and exponential decay were identified as mEPSCs using an automatic detection template in pCLAMP 10 and were post-hoc filtered to only include events with a peak amplitude <-5 pA and a <3 ms 10-90% rise time. Quantification of mEPSCs was calculated from the percentage change in frequency or amplitude of the last 5 min of a 10 min D-AP5 (50 μM) application normalized to the last 5 min of a 15 min baseline. Cells were excluded from analysis if there was a >20% change in R_{input}, a >25% change in R_{series}, or if

R_{series} was ever >20 MΩ during the recording. Voltage-clamp recordings were sampled at 10 kHz and filtered at 2 kHz.

3.4.4 Statistics

Changes in PPR or mEPSC parameters are evaluated by comparing the experimental and control group with 2-way repeated measures ANOVAs. Significant interactions via ANOVA are used to determine if the experimental manipulation produces different PPR outcomes based on genotype or rearing. Differences in baseline values, such as before plasticity induction or AP5 addition, are evaluated via multiple comparison-adjusted post-hoc Sidak-Bonferroni tests or, in the case of three groups, Tukey's post-tests. Results of these post-hoc comparisons are reported as multiplicity adjusted p-values. Unpaired t-tests are performed on single comparisons between two groups such as when comparing normalized data. Statistical analysis was performed in Prism 6 (Graphpad).

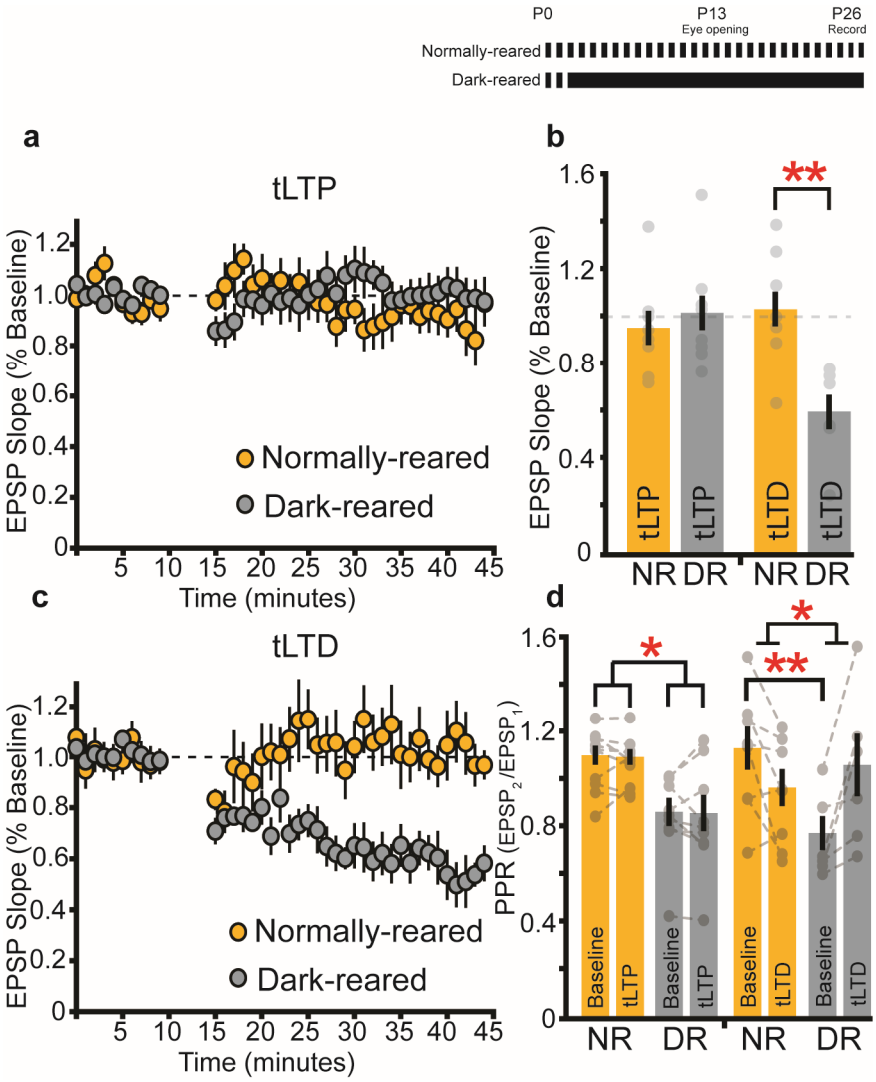

Figure 3.1: Dark-rearing restores the ability to induce tLTD, but does not change tLTP induction. (**a**) Recordings from NR mice (n = 8) lacked significant potentiation following EPSP-AP pairings and dark-rearing did not alter the lack of tLTP observed at this age (n = 9). (**b**) Quantification of the last 10 minutes in (b) and (d). The magnitude of tLTP is not different between NR and DR mice (t-test, $p = 0.57$). However, DR mice have increased tLTD magnitude compared to NR mice (t-test, $p < 0.004$). (**c**) AP-EPSP pairings fail to produce tLTD in NR mice (n

= 8), but produce robust tLTD in DR mice (n = 5). (**d**) EPSP-AP pairings to induce tLTP do not alter the PPR ratio at 30 Hz (2wRmANOVA, p = 0.74), although DR mice have a lower PPR both before (post-hoc test, p < 0.03) and after EPSP-AP pairings (post-hoc test, p < 0.02). Similarly, PPR is lower in DR mice before tLTD induction (post-hoc test, p < 0.02) and tLTD induction is accompanied by an increase in PPR in DR mice only (2wRmANOVA, p < 0.003).

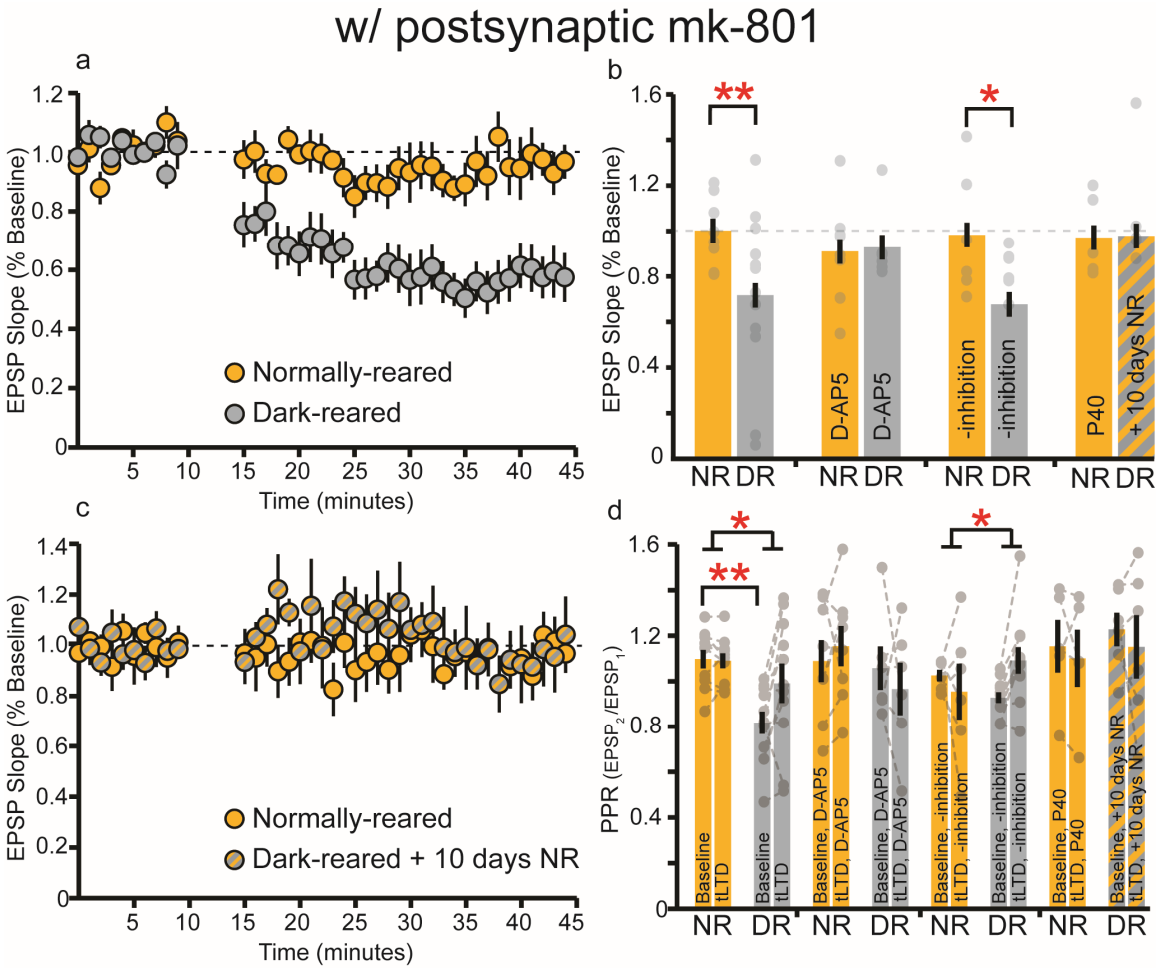

Figure 3.2: tLTD in dark-reared mice requires putatively presynaptic NMDARs and is lost following exposure to a normal visual environment. (**a**) Recordings

from DR mice (n = 11) still demonstrated substantial tLTD compared to those in NR mice (n = 10) when postsynaptic NMDARs were blocked with MK-801 (t-test, $P < 0.002$) (**b**) Quantification of the last 10 minutes in (a) and (c). Inclusion of D-AP5 in the bath blocks tLTD in DR mice (n = 6) without affecting the lack of tLTD observed in NR mice (n = 8; t-test, $P = 0.87$). When inhibition is focally blocked, recordings in DR mice (n = 9), but not NR mice (n = 6), show tLTD following AP-EPSP pairings (t-test, $P < 0.05$). (**c**) tLTD is lost when DR mice placed in a NR environment (n = 6) and is similar to that from age-matched NR controls (n = 5; t-test, $P = 0.40$). (**d**) PPR at 30 Hz is lower in recordings from DR mice compared NR controls (post-hoc test, $p < 0.04$) and following tLTD, this ratio is increased in DR mice (2wRmANOVA, $p < 0.03$). Inclusion of 50 μM D-AP5 in the bath blocks tLTD and subsequent changes in the PPR ratio (2wRmANOVA, $p = 0.31$), as does exposure to normal visual environment following dark-rearing (2wRmANOVA, $p = 0.87$). When GABA(A)-mediated transmission is blocked, tLTD is still accompanied by increases in the PPR following tLTD (2wRmANOVA, $p < 0.05$). In all experiments, 1 mM MK-801 was included in the internal solution.

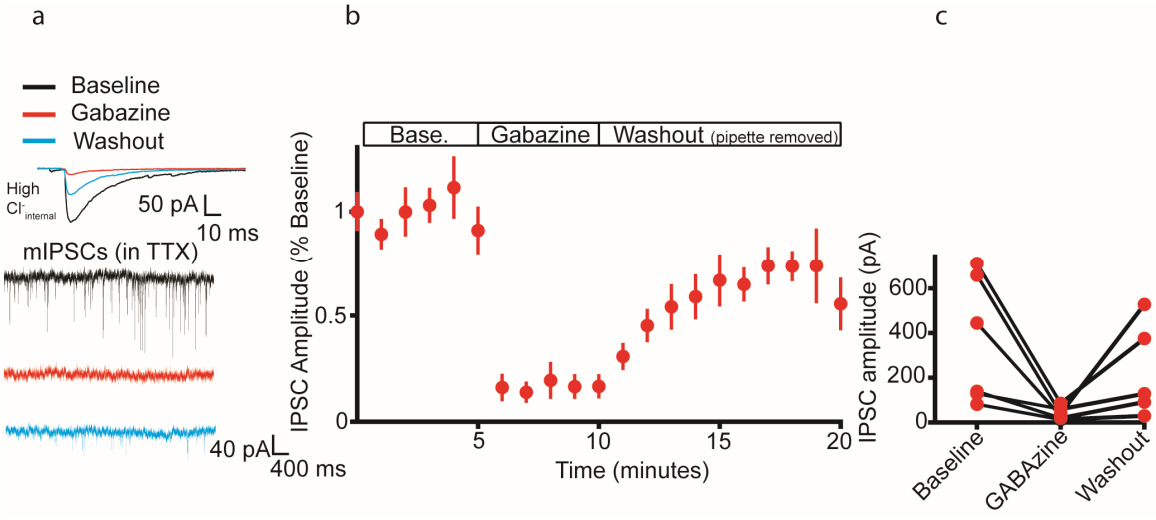

Figure 3.3: Focal gabazine application near postsynaptic L2/3 V1 neurons blocks evoked and spontaneous GABAergic transmission. (**a**) Sample traces of spontaneous and evoked inhibitory neurotransmission during baseline, gabazine application, and washout periods. (**b**) Timecourse of evoked IPSC blockade by gabazine. Evoked IPSCs were recorded in L2/3 neurons for 5 minutes (n=6), after which a pipette containing 50 μM gabazine with was lowered near the recorded cell for 5 minutes. The pipette was then removed and IPSC recovery was measured for an additional 10 minutes. (**c**) Quantified data from period described in (b) demonstrating that focal application of GABAzine reduces evoked IPSCs (paired t-test, baseline versus gabazine periods, $p < 0.04$). Recording were performed in the constant presence of 10 μM, 100 μM D,L-AP5, and 0.2 μM tetrodotoxin (for mIPSCs only). The internal solution contained (in mM), 134 KCl, 2 NaCl, 10 HEPES, 0.2 EGTA, 10 sucrose, 4 Mg-ATP, 0.3 Na-GTP, 14 Naphosphocreatine and 0.025 Alexa-488 with pH adjusted to 7.2 with KOH and osmolarity adjusted to ~300 mOsm by addition of sucrose.

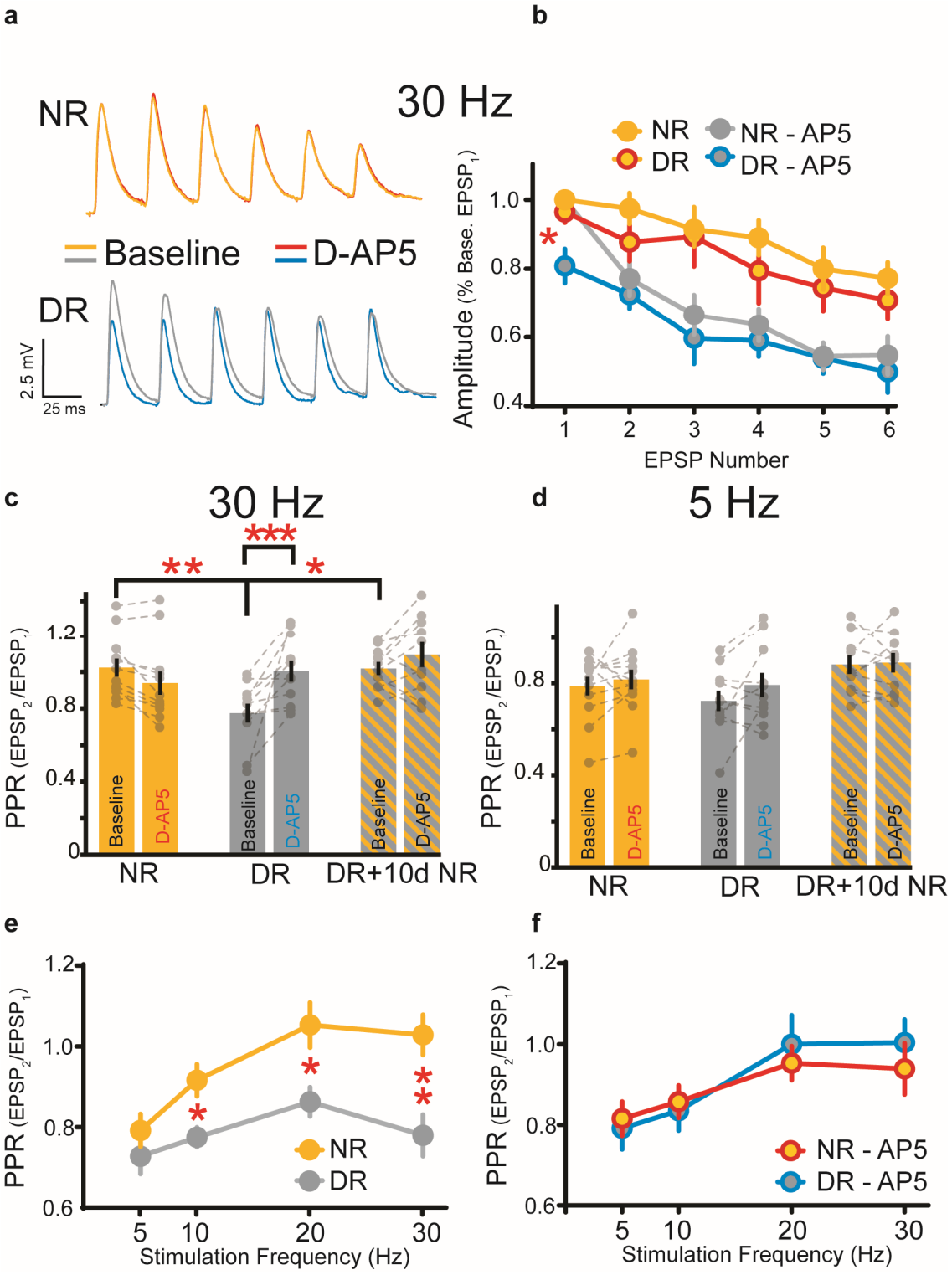
a
NR
30 Hz
Baseline
D-AP5
DR
2.5 mV
25 ms
b
NR
NR - AP5
DR
DR - AP5
Amplitude (% Base. EPSP1)
1.0
0.8
0.6
0.4
1
2
3
4
5
6
EPSP Number
c
30 Hz
***
**
*
PPR (EPSP2/EPSP1)
1.2
0.8
0.4
0
Baseline
D-AP5
NR
DR
DR+10d NR
d
5 Hz
e
1.2
1.0
0.8
0.6
5
10
20
30
Stimulation Frequency (Hz)
f

Figure 3.4: Dark-rearing increases evoked glutamate release at high frequencies (>5 Hz) in manner dependent on presynaptic NMDARs. (**a**) Representative traces of 6 EPSPs evoked by 30-Hz stimuli in L4 before and after D-AP5 application from NR and DR mice. (**b**) Normalized EPSP responses before and after D-AP5 in NR and DR mice. EPSPs within a train both before and after D-AP5 are normalized to the first baseline EPSP in NR and DR mice. In DR mice, D-AP5 reduces only the first EPSP in a train of six responses (t-test, NR-$AP5_{EPSP1}$ and DR-$AP5_{EPSP1}$, $p<0.05$). (**c**) Dark-rearing lowers the baseline 30 Hz PPR ratio (post-hoc test, $p < 0.006$) and this is reversed upon re-exposing DR mice to a normal environment for 10 days (post-hoc test, $p < 0.02$). In DR mice, D-AP5 increases the 30 Hz PPR (2wRmANOVA, rearing and AP5 interaction, $p < 0.0005$). (**d**) In contrast to PPR evoked at 30 Hz, dark-rearing does not alter either the initial PPR or the effect of D-AP5 in response to glutamate release elicited at 5 Hz (2wRmANOVA, $p = 0.26$). (**e**) Dark-rearing alters the baseline PPR ratio at 10 Hz (all post-hoc tests, $p < 0.03$), 20 Hz ($p < 0.03$), and 30 Hz ($p < 0.006$), but not at 5 Hz ($p = 0.2$). (**f**) Dark-rearing alters the effect of D-AP5 at the same frequencies which have altered initial PPR (2wRmANOVA, 5 Hz $p= 0.26$, 10 Hz $p < 0.04$, 20 Hz $p < 0.0002$, 30 hz $p < 0.006$).

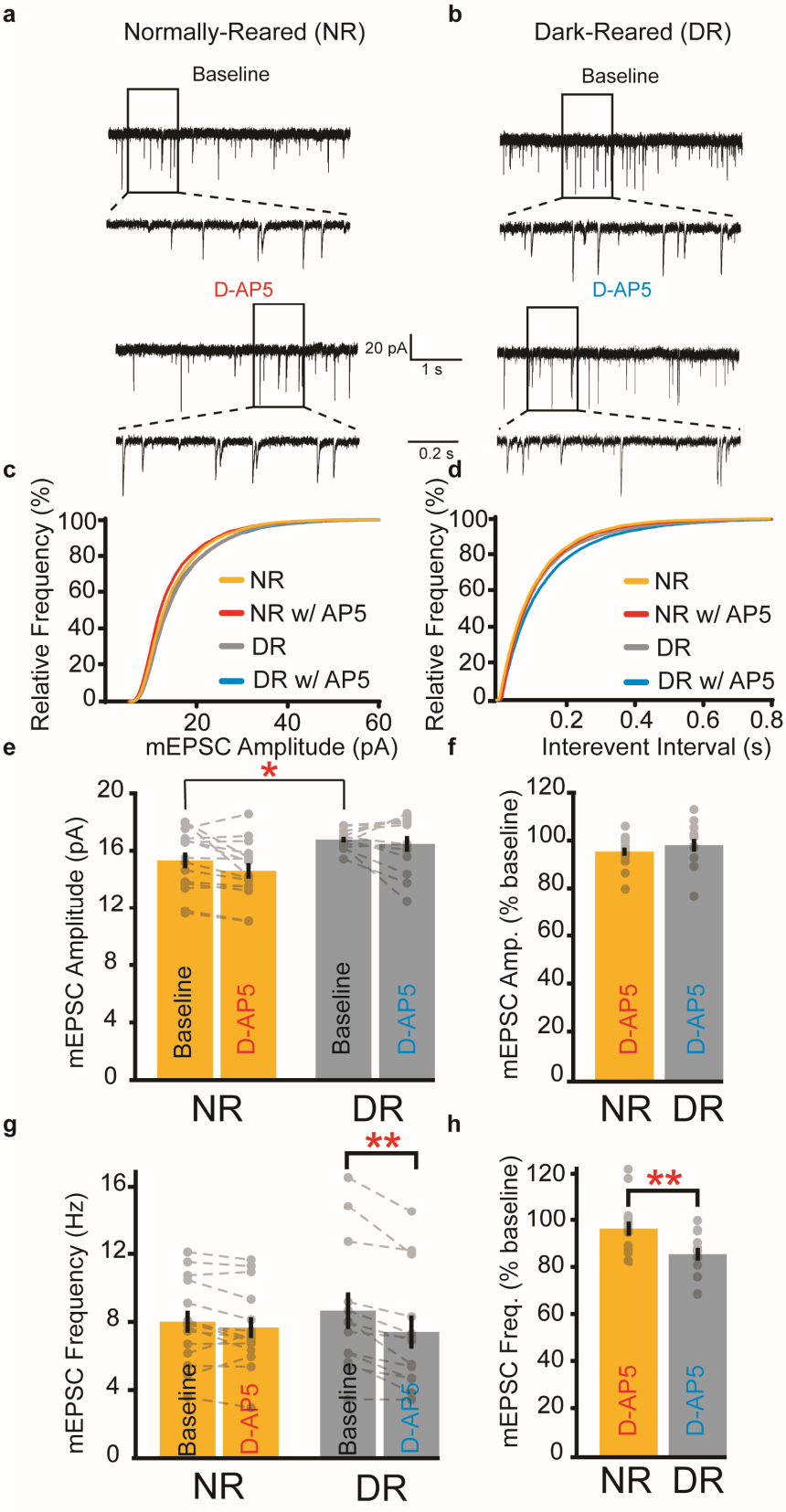
a
Normally-Reared (NR)
Baseline
D-AP5
20 pA
1 s
0.2 s
b
Dark-Reared (DR)
Baseline
D-AP5
c
Relative Frequency (%)
NR
NR w/ AP5
DR
DR w/ AP5
mEPSC Amplitude (pA)
d
Relative Frequency (%)
NR
NR w/ AP5
DR
DR w/ AP5
Interevent Interval (s)
e
mEPSC Amplitude (pA)
Baseline
D-AP5
Baseline
D-AP5
NR
DR
f
mEPSC Amp. (% baseline)
D-AP5
D-AP5
NR
DR
g
mEPSC Frequency (Hz)
Baseline
D-AP5
Baseline
D-AP5
NR
DR
h
mEPSC Freq. (% baseline)
D-AP5
D-AP5
NR
DR

Figure 3.5: Dark-rearing increases the contribution of presynaptic NMDARs to spontaneous release. (**a-b**) Sample traces showing AMPAR-mediated mEPSCs in NR (a) and DR mice (b), before and after the application of 50 μM D-AP5. (**c-d**) Average cumulative probability histograms (500 events/neuron per baseline/AP5 period) of mEPSC amplitude (c) and frequency (d) from all recordings in NR (n =15) and DR (n=13) mice (**e**) Average mEPSC amplitudes demonstrating that dark-rearing increases mEPSC amplitudes, consistent with postsynaptic AMPAR scaling (2wRmANOVA, rearing effect, $p < 0.02$). (**f**) Baseline normalized mEPSC amplitudes demonstrating that D-AP5 does not alter the mEPSC amplitude (t-test, $p= 0.4$). (**g**) Dark-rearing does not alter baseline mEPSC frequency, but alters the ability of D-AP5 to affect the frequency (2wRmANOVA, $p < 0.009$). (**h**) D-AP5 reduces the mEPSC frequency in recordings from DR, but not NR, mice (t-test, $p<0.008$).

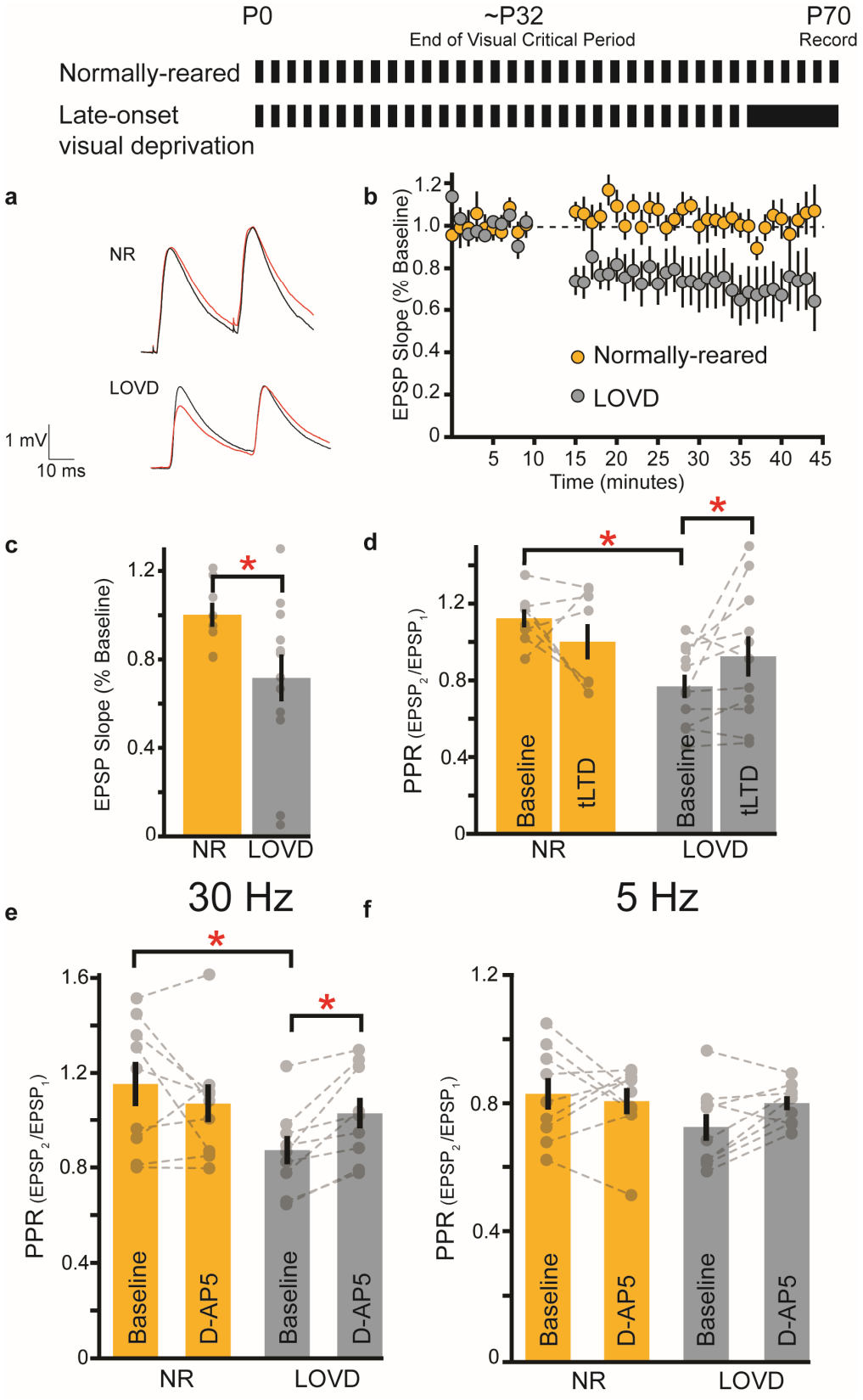
P0
~P32
End of Visual Critical Period
P70
Record
Normally-reared
Late-onset
visual deprivation
a
NR
LOVD
1 mV
10 ms
b
EPSP Slope (% Baseline)
Normally-reared
LOVD
Time (minutes)
c
EPSP Slope (% Baseline)
NR
LOVD
d
PPR (EPSP2/EPSP1)
Baseline
tLTD
NR
LOVD
30 Hz
e
PPR (EPSP2/EPSP1)
Baseline
D-AP5
NR
LOVD
5 Hz
f
PPR (EPSP2/EPSP1)
Baseline
D-AP5
NR
LOVD

Figure 3.6: Late-onset visual deprivation (LOVD) during adulthood restores the ability to induce tLTD and increases glutamate release at high frequencies in a presynaptic NMDAR-dependent manner. (**a**) Sample traces of 2 EPSPs evoked by 30-Hz stimuli in L4 before and after induction of tLTD in NR and LOVD mice. (**b**) Recordings from mice which underwent LOVD (n=11) demonstrated substantial tLTD whereas their NR littermates (n=8) showed no mean reduction in EPSP slope following AP-EPSP pairings. (**c**) Quantification of the last 10 minutes in (b) demonstrating significant differences in the magnitude of tLTD between NR and LOVD mice (t-test, $p<0.05$). (**d**) PPR at 30 Hz is lower in recordings from mice which underwent LOVD compared NR controls (post-hoc test, $p < 0.02$) and following tLTD, this ratio is increased in LOVD mice (2wRmANOVA, $p < 0.05$). (**e-f**) Similarly, in recordings in which we tested the effect D-AP5 on short-term plasticity, mice which underwent LOVD (n=9) had a lower baseline PPR at 30Hz ($p < 0.03$), but not 5 Hz ($p=0.13$), and D-AP5 increased the PPR only at 30 Hz in mice which underwent LOVD (30 Hz 2wRMANOVA, 30 Hz $p < 0.02$, 5 Hz $p =0.11$).

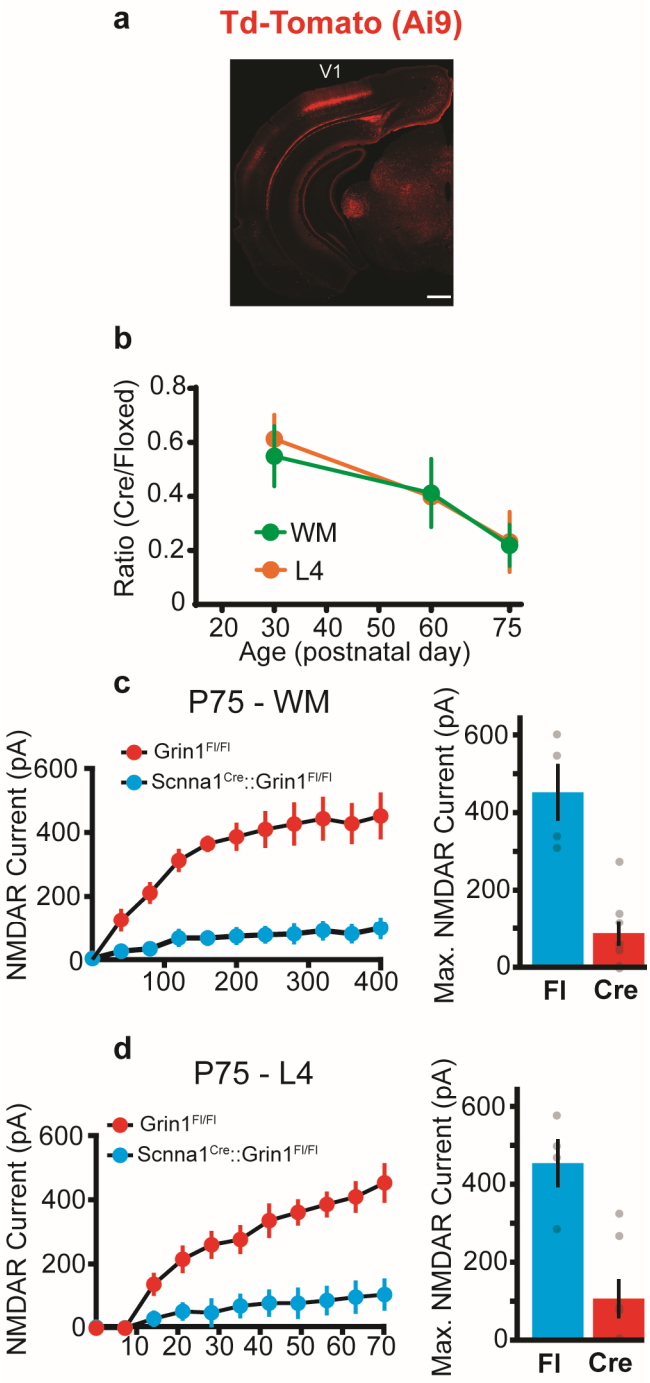

Figure 3.7: Targeted genetic disruption of L4 NMDARs in *Grin1*^{L4CKO} mice results in significant reductions L4 NMDAR currents. (**a**) At P30, *Scnn1a-tg3:cre*-mediated recombination of stop-floxed Td-tomato intracortically labels L4

neurons within the visual cortex. Scale bar represents 500 microns. (**b**) Developmental profile of the Cre-mediated loss of NMDARs demonstrating loss of gradual reductions in NMDAR currents through postnatal development. NMDAR current ratios are quantified from the maximum NMDAR currents from Fig 3.7 and Fig. 3.8 (**c)** NMDAR currents are sharply reduced at inputs activated by WM stimulation in *Grin1*^{L4CKO} mice as compared to their floxed-only littermates. (**d**) Quantification of (c) at maximal NMDAR current responses. (e) NMDAR currents are similarly reduced at inputs activated by L4 stimulation in *Grin1*^{L4CKO} mice as compared to their floxed-only littermates. (**e**) Quantification of (c) at maximal NMDAR current responses. NMDAR input-output relationships (I/Os) are recorded in AMPAR, GABA(A)R, and GABA(B)R antagonists. Following NMDAR current recordings, 50 μM D-AP5 is applied to further verify currents arise from NMDAR-type glutamate receptors.

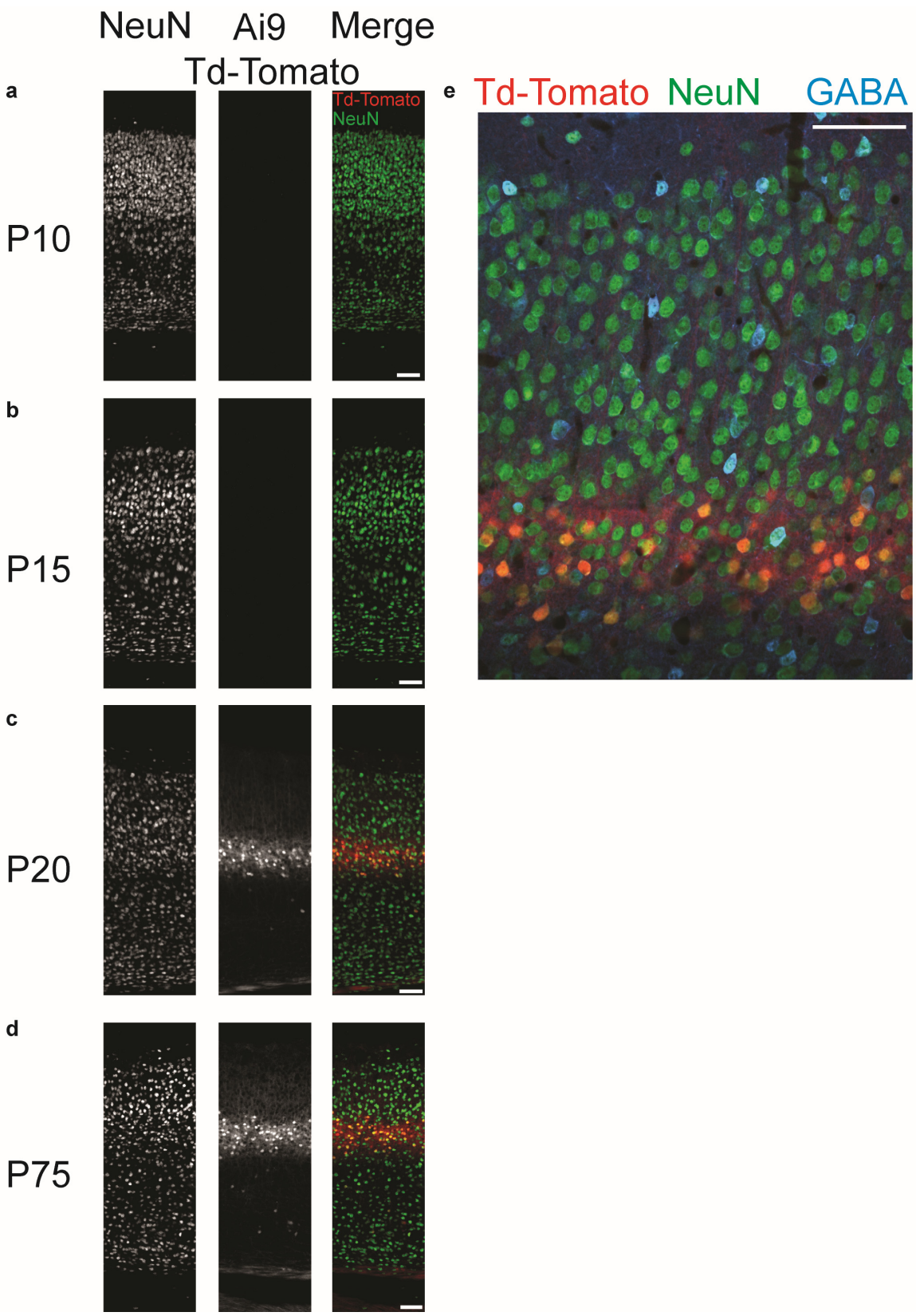
NeuN
Ai9
Td-Tomato
Merge
a
P10
Td-Tomato
NeuN
b
P15
c
P20
d
P75
e
Td-Tomato
NeuN
GABA

Figure 3.8: *Scnn1a-Tg3:Cre* mediates recombination of the stop-floxed fluorescent protein Td-tomato in non-GABAergic neurons beginning at P20. (**a-d**) Images from *Scnn1a-Tg3:Cre:Ai9* mice at various developmental timepoints (P10-P75) demonstrating Cre-mediated recombination of stop-floxed fluorescent protein in L4 V1 neurons beginning at P20, and not before. Images are co-stained with the neuronal marker NeuN. (**e**) Image from a P20 *Scnn1a-Tg3:Cre:Ai9* mouse which has also been stained with GABA to mark cortical interneurons. Note the lack of colocalization of Td-tomato-positive V1 L4 neurons with GABA. Scale bar in all instances is 50 microns.

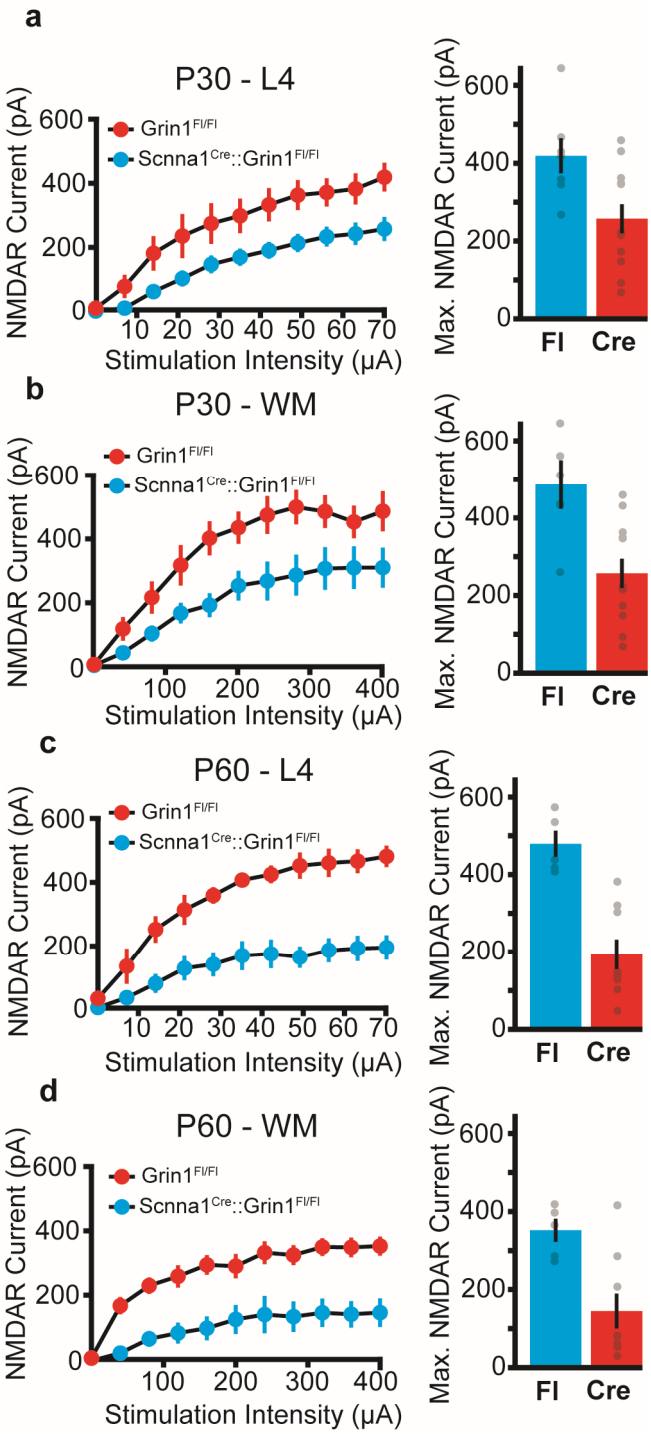

Figure 3.9: Targeted genetic disruption of L4 NMDARs in *Grin1*^{L4CKO} mice results in moderate reductions in NMDAR currents at P30 and larger reductions

at P60. (**a-b**) NMDAR currents are reduced by nearly 40% in recordings from Cre-positive, L4 V1 neurons in *Grin1*^{L4CKO} mice as compared to their floxed only controls. (**c-d**) The reduction in NMDAR current increases to nearly 60% at postnatal day 60. Note that, as illustrated in Supplemental Fig. 3, Cre-mediated recombination is first apparent at P20.

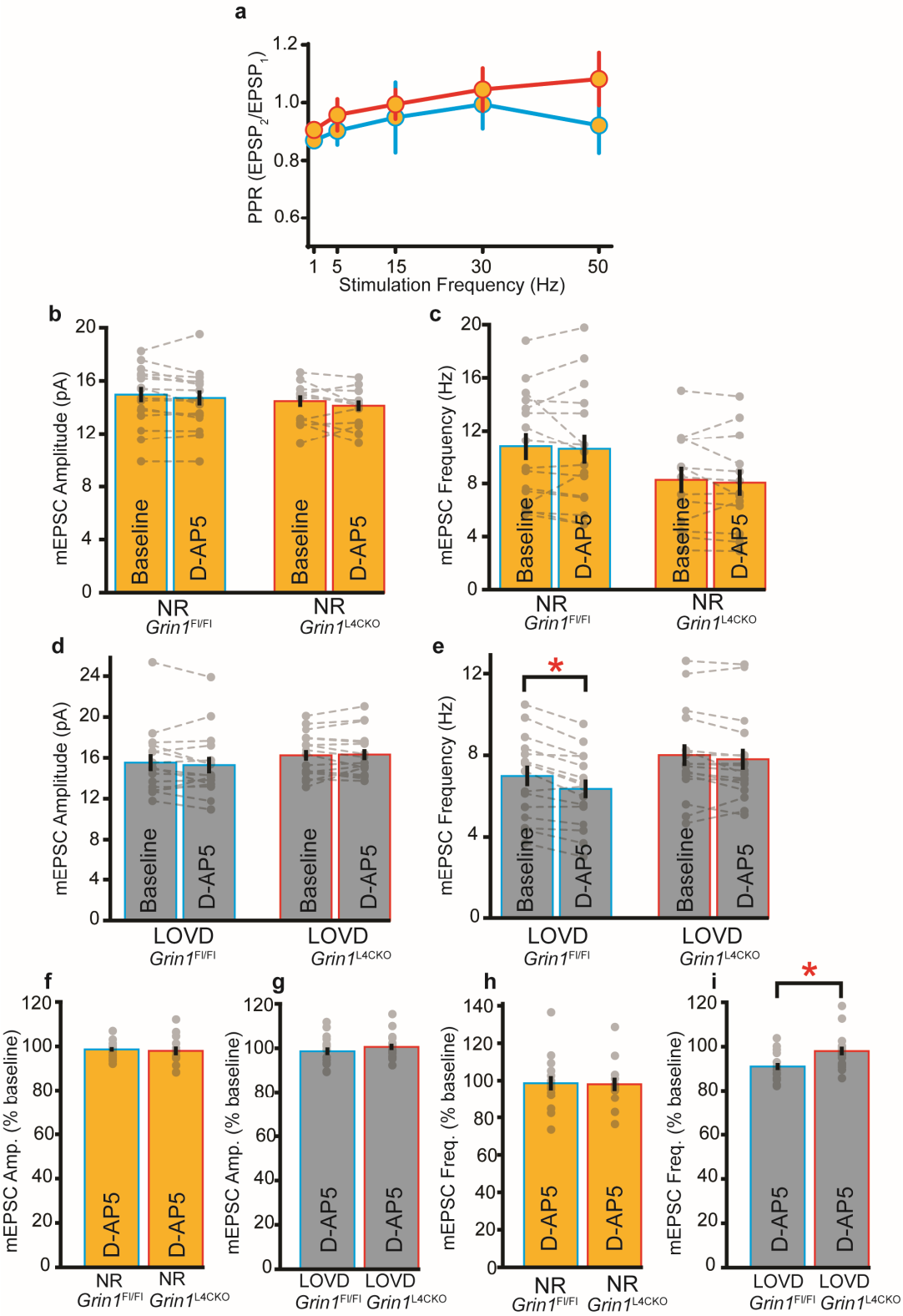
a
PPR (EPSP2/EPSP1)
1.2
1.0
0.8
0.6
1 5 15 30 50
Stimulation Frequency (Hz)
b
mEPSC Amplitude (pA)
20
16
12
8
4
0
Baseline
D-AP5
NR
Grin1FI/FI
NR
Grin1L4CKO
c
mEPSC Frequency (Hz)
d
mEPSC Amplitude (pA)
24
LOVD
Grin1FI/FI
LOVD
Grin1L4CKO
e
mEPSC Frequency (Hz)
*
f
mEPSC Amp. (% baseline)
120
100
80
60
40
20
0
g
h
mEPSC Freq. (% baseline)
140
i

Figure 3.10: Loss of NMDARs in a subset of L4 neurons does not affect spontaneous or evoked glutamate release in normally-reared mice, but occludes the increased contribution of presynaptic NMDARs to spontaneous release following LOVD. (**a**) EPSPs evoked by L4 stimulation in recordings from L2/3 neurons in NR *Grin1*^{L4CKO} mice (n=8) and their floxed-only controls (n=9) demonstrating that loss of L4 neurons does not affect short-term plasticity as assayed by PPR (2wRMANOVA, p=0.84; post-hoc tests >0.5). (**b**) Average mEPSC amplitudes from NR *Grin1*^{L4CKO} (n=13) and their floxed-only littermates demonstrating that loss of NMDARs in a subset of L4 neurons does not significantly affect mEPSC amplitude (2wRMANOVA, genotype-effect, p= 0.1). (**c**) Loss of NMDARs in a subset of L4 neurons also does not significantly affect mEPSC frequency at L2/3 synapses from NR mice (2wRMANOVA, p= 0.1). (**d**) Similarly, mEPSC amplitudes are not significantly different between *Grin1*^{L4CKO} (n=17) and their floxed-only littermates (n=16) following LOVD (2wRMANOVA, p=0.36). (**e)** In floxed-only LOVD mice, there is an enhanced reduction in mEPSC frequency following D-AP5 (2wRMANOVA, D-AP5 and genotype interaction, p<0.02). (**f-g**) Baseline normalized mEPSC amplitudes demonstrating that D-AP5 does not alter the mEPSC amplitude in NR or LOVD *Grin1*^{L4CKO} or floxed-only littermates. (**h-i**) Loss of NMDARs at a subset of L4 of neurons in LOVD *Grin1*^{L4CKO} mice occludes the reduction in mEPSC frequency following D-AP5 observed in their floxed-only littermates (t-test, p<0.02). All experiments were performed with the experimenter blind to genotype and with MK-801 in the postsynaptic, L2/3 recording pipette.

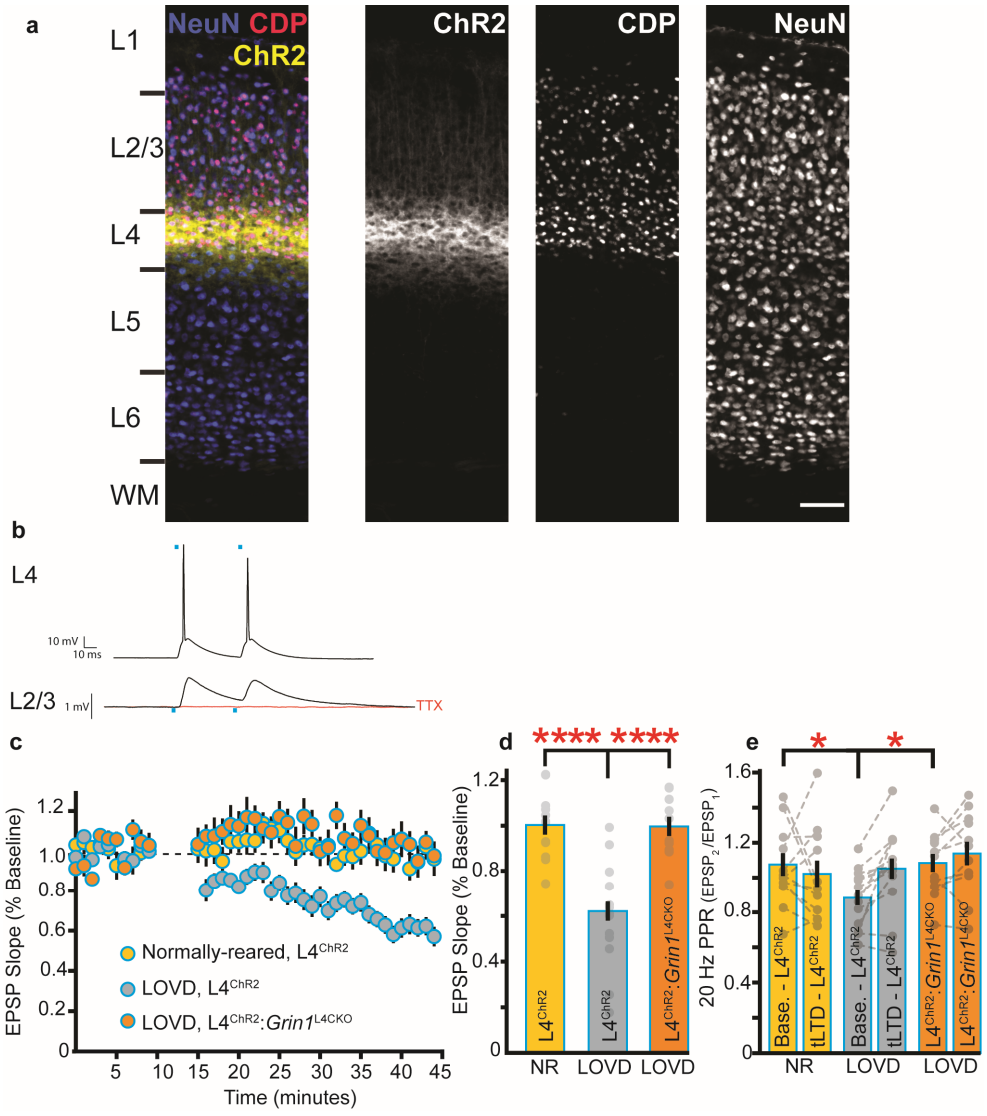

Figure 3.11: Presynaptic L4 NMDARs are required for the restoration in the ability to induce tLTD following LOVD. (**a**) Image of the visual cortex in ChR2^{L4} mouse demonstrating that ChR2-YFP expression is confined to L4 V1 neurons. Sections were also stained with the neuronal marker NeuN and the transcription factor CDP, which labels the nuclei of L2/3 and L4 cortical neurons. Scale bar represents 75 microns. (**b**) Example recordings from a L4 and a postsynaptic L2/3 neuron following activation of ChR2-expressing L4 neurons with focal light

pulses at 20 Hz. (**c**) L4 inputs to L2/3 neurons do not express tLTD in adulthood, however following LOVD, the ability to induce tLTD optogenetically is restored. However, in LOVD *Grin1*^{L4CKO}*:ChR2* mice, the ability to induce tLTD following visual deprivation is occluded. (**d**) Quantification of the last 10 minutes in (c) demonstrating significant differences in magnitude of tLTD in recordings from NR (n=12) and LOVD ChR2^{L4} mice (n=15, post-hoc test, $p < 0.0001$) and LOVD ChR2^{L4} and *Grin1*^{L4CKO}*:ChR2* mice (n=12, post-hoc test, $p < 0.0001$). (**e**) Visual deprivation decreases the baseline 20 Hz PPR in LOVD ChR2^{L4} mice as compared to NR ChR2^{L4} mice (post-hoc test, $p < 0.05$) or LOVD compared to *Grin1*^{L4CKO}*:ChR2* mice (post-hoc test, $p < 0.05$). Following tLTD, the PPR increases in recordings from LOVD ChR2^{L4} but not their NR littermates consistent with tLTD being expressed presynaptically (2wRmANOVA, $p < 0.01$).

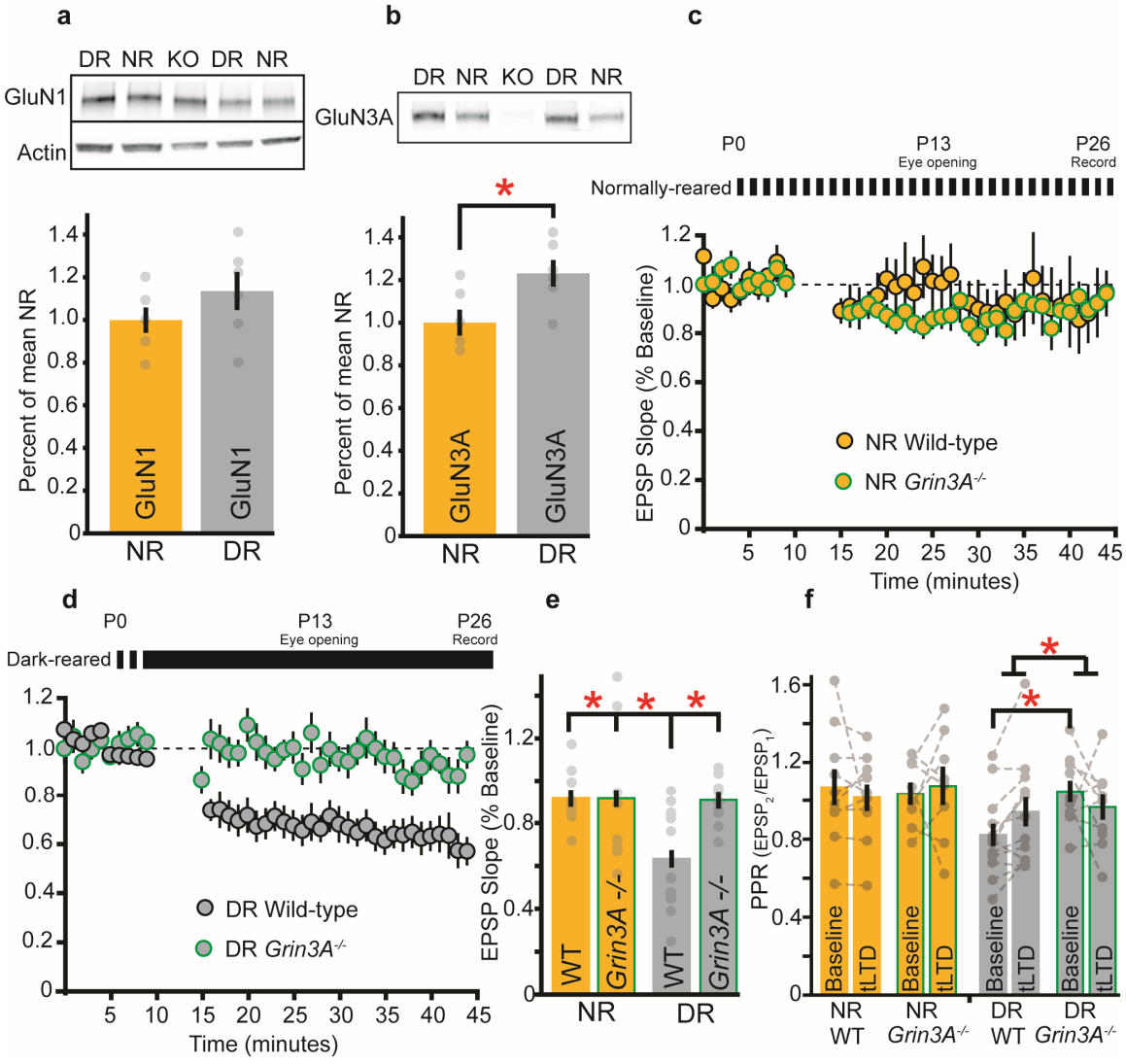

Figure 3.12: GluN3A is upregulated following dark-rearing and is required for tLTD in DR mice. (**a-b**) Quantification and representative immunoblots of GluN1 and GluN3A in synaptosomal fractions from the visual cortex (n= 6 replicates, 12 mice per group). Dark-rearing does not alter GluN1 expression, but increases the synaptic expression of GluN3A at P30 (t-test, $p < 0.05$). (**c**) NR wildtype (n=10) and *Grin3A*$^{-/-}$ (n=8) mice both lack tLTD in response to AP-EPSP at P26-30. (**d**) Following dark-rearing, wildtype mice show significant tLTD (n=13), but their

Grin3A$^{-/-}$ littermates do not (n=10). (**e**) Quantification of (c) and (d) demonstrating that the tLTD induced in DR wildtype mice is significantly different than tLTD in NR wildtype (post-hoc tests, $p<0.02$), NR *Grin3A*$^{-/-}$ ($p<0.04$), and DR *Grin3A*$^{-/-}$ ($p<0.03$) mice. (**f**) Dark-rearing decreases the baseline 30 Hz PPR in DR wildtype mice compared to DR *Grin3A*$^{-/-}$ mice (post-hoc test, $p<0.03$), and the PPR increases following tLTD in recording from DR wildtype mice (2wRmANOVA, $p < 0.02$).

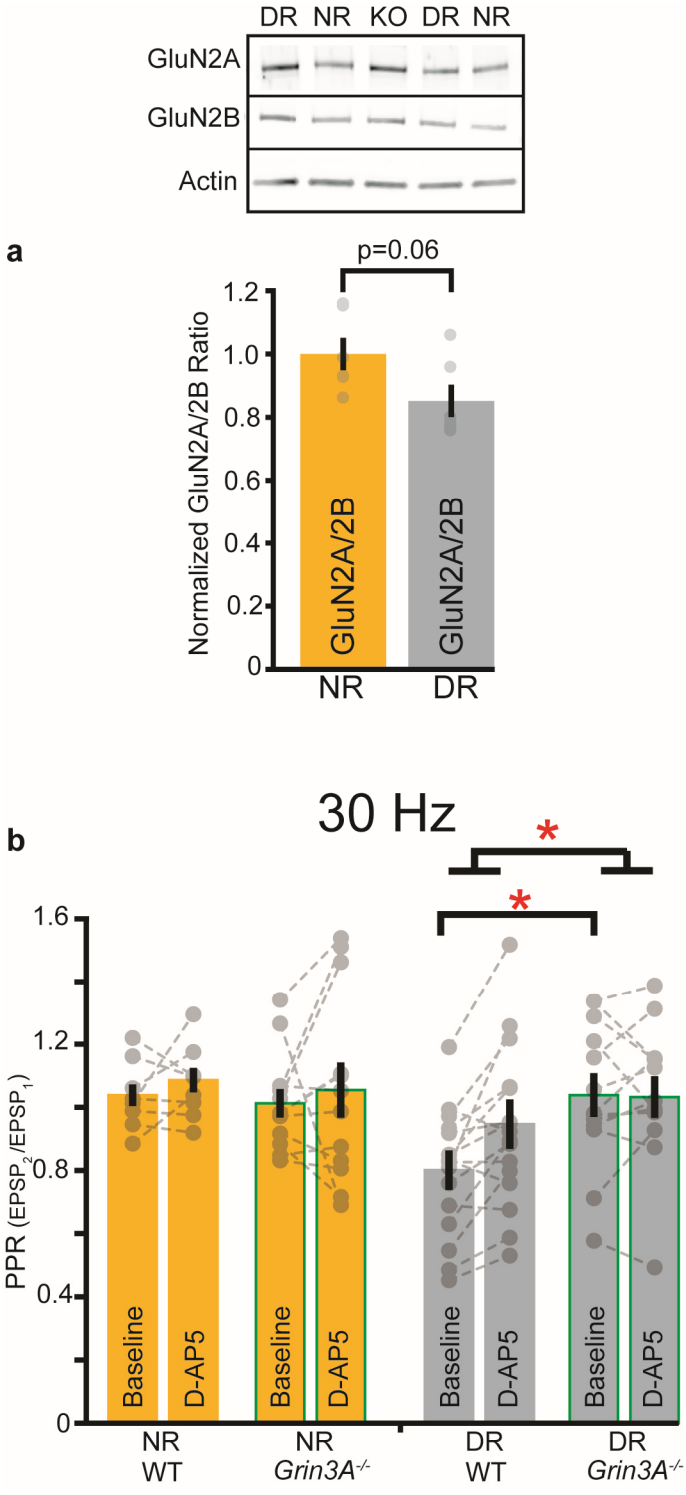
DR NR KO DR NR
GluN2A
GluN2B
Actin
a
p=0.06
Normalized GluN2A/2B Ratio
1.2
1.0
0.8
0.6
0.4
0.2
0
GluN2A/2B
GluN2A/2B
NR
DR
b
30 Hz
*
*
PPR (EPSP2/EPSP1)
1.6
1.2
0.8
0.4
0
Baseline
D-AP5
Baseline
D-AP5
Baseline
D-AP5
Baseline
D-AP5
NR
WT
NR
Grin3A-/-
DR
WT
DR
Grin3A-/-

Figure 3.13: GluN3A is required for the increased contribution of presynaptic NMDARs to evoked release following dark-rearing. (**a**) Quantification and representative immunoblots of GluN2A and GluN2B in synaptosomal fractions from the visual cortex at P30 (n= 6 replicates, 12 mice per group). Dark-rearing decreases the synaptic GluN2A to GluN2B ratio and this effect approaches statistical significance (t-test, p=0.06). (**b**) The 30 Hz PPR is decreased in DR, WT mice but this effect of dark-rearing is lost in DR *Grin3A*$^{-/-}$ mice (post-hoc test, p<0.02; NR wildtype n=9; NR *Grin3A*$^{-/-}$ n=12; DR wildtype n=16; DR *Grin3A*$^{-/-}$ n=14). Loss of GluN3A expression occludes the effects of D-AP5 on short-term plasticity in DR mice (2wRmANOVA, p < 0.03).

Chapter 4: Discussion

4.1 Roles for specific NMDAR subtypes in presynaptic NMDAR function

4.1.1 Roles for the magnesium-insensitive GluN3A NMDAR subunit

Perhaps the major finding of these studies is that the NMDAR subunit GluN3A influences presynaptic glutamate release and plasticity in the visual cortex. While unexpected given the paucity of data regarding this subunit's contribution to cortical synaptic function, the finding that GluN3A is required for presynaptic NMDAR function reconciles many of the previously unresolved questions surrounding these receptors. Most notably, as discussed below, the finding that GluN3A is required for presynaptic NMDAR function explains the developmental regulation of presynaptic NMDARs, the ability of these receptors to be tonically active in the absence of action potential-driven depolarization, and their saturation by NMDAR coagonist glycine.

The vast majority of studies implicating presynaptic NMDARs in the modulation of neurotransmitter release have been performed before the developmental age of postnatal day thirty (Corlew et al., 2008), and several of these studies have demonstrated a decline in presynaptic NMDAR function through development (Banerjee et al., 2009; Corlew et al., 2007; Mameli et al., 2005; J. Yang et al., 2006). In the case of the visual cortex, the developmental downregulation of presynaptic NMDARs is abrupt, with expression being

observed at postnatal day eighteen and not at day twenty-three (Corlew et al., 2008). Despite this sharp downregulation in presynaptic NMDAR function, the expression of the obligatory NMDAR subunit GluN1 declines only fifty percent at presynaptic sites (Corlew et al., 2007; Larsen et al., 2011). Therefore, the developmental loss in presynaptic NMDAR function likely also results from a change in subunit type, conductance, and/or downstream signaling. As demonstrated in Chapter 2, the developmental downregulation in presynaptic NMDAR function strongly correlates with downregulation of GluN3A synaptic protein in the visual cortex. Similarly, expression of GluN3A within the presynaptic terminal has only been observed early (Larsen et al., 2011), and not late in development (Pérez-Otaño et al., 2001) . Since the overexpression of GluN3A can reverse the developmental loss in presynaptic NMDAR function, these findings collectively suggest that the loss of presynaptic NMDAR function in the visual cortex is driven by the developmental downregulation of GluN3A. Changes in channel properties following loss of GluN3A may also be accompanied by significant changes that occur downstream of receptor activation and which may contribute to changes observed through development. NMDA receptors are regulated by a diverse array of signaling cascades (Husi, Ward, Choudhary, Blackstock, & Grant, 2000; Lau & Zukin, 2007; Salter & Kalia, 2004) and GluN3A is uniquely regulated by PKA, PKC, protein tyrosine kinase, calcineurin (PP2A), glycosylation, and CaMKII (Henson et al., 2010). How changes in downstream signaling cascades influence presynaptic NMDAR function or expression is presently unknown, but these changes may be another

mechanism by which developmental changes in presynaptic NMDAR function occur.

Compared to their postsynaptic counterparts, presynaptic NMDARs in several areas of the brain are active in the absence of strong depolarization. NMDARs typically are activated by the binding of glutamate and glycine/D-serine coincident with depolarization (Paoletti, Bellone, & Zhou, 2013). However, NMDAR antagonists reduce the mEPSC frequency at visual and somatosensory cortical synapses in the presence of the sodium channel blocker tetrodotoxin (Brasier & Feldman, 2008; Corlew et al., 2007), demonstrating that presynaptic NMDARs do not require action potentials to be activated. Whether any depolarization contributes to the activation of presynaptic NMDARs is less clear however. Graded, subthreshold depolarizations are known to enhance presynaptic release (Christie, Chiu, & Jahr, 2011; Shu, Hasenstaub, Duque, Yu, & McCormick, 2006) and can occur in the absence of sodium channel activation (in TTX) (Alle & Geiger, 2006; Christie & Jahr, 2008). However, subthreshold synaptic currents often only minimally depolarize the presynaptic terminal (~5 mV) (Alle & Geiger, 2006) and may not effectively propagate from dendrites to axonal boutons in pyramidal neurons of the neocortex (Christie & Jahr, 2009). Therefore, while subthreshold activity is able to influence presynaptic release independently, it may not be sufficient enough to result in significant recruitment of magnesium-sensitive presynaptic (axonal) NMDARs (Clarke & Johnson, 2006).

Assuming axonal localization of presynaptic NMDARs (discussed below) and resting potential of ~-75 mV within the presynaptic terminal (Alle & Geiger, 2006; Awatramani, Price, & Trussell, 2005), it is therefore difficult to explain the mechanism by which presynaptic NMDARs are activated. The finding that presynaptic NMDARs can express GluN3A provides a plausible mechanism for their activation of presynaptic NMDARs the absence of large depolarizations. The incorporation of GluN3A into tritheromeric (GluN1-GluN2-GluN3A) receptors results in the almost complete loss of magnesium blockade at hyperpolarized potentials (Sasaki et al., 2002). Presynaptic NMDARs expressing these triheteromeric receptors would be activated in the absence of action potentials and only in response to agonist binding. As we have shown (Chapter 2), the developmental loss or genetic deletion of GluN3A restores presynaptic NMDAR magnesium sensitivity. In combination with findings that GluN3A regulates glutamate release and tLTD require, this strongly suggests that the mechanism by which visual cortical presynaptic NMDARs are activated in the absence of depolarization is because they express GluN3A-containing NMDARs.

NMDA receptors require binding of both glutamate and glycine for channel opening (Johnson & Ascher, 1987; Kleckner & Dingledine, 1988). At L2/3 synapses within the visual cortex, application of exogenous glycine or D-serine does not alter mEPSC frequency, however application of NMDAR glycine site antagonists reduces the frequency (Li & Han, 2007; Li, Han, & Meng, 2008). This suggests that the glycine site on presynaptic NMDARs is saturated by endogenous ligands, which is not the case for postsynaptic NMDARs at this

synapse (Li & Han, 2007). The mechanisms by which presynaptic NMDAR glycine sites are saturated is unclear, but the finding that these receptors may express GluN3A supports findings that presynaptic NMDARs are saturated by glycine. Unlike GluN2 subunits, GluN3 and GluN1 subunits bind glycine or D-serine instead of glutamate (Henson et al., 2010; Hirai, Kirsch, Laube, Betz, & Kuhse, 1996). Importantly, GluN3A has a significantly higher (650 fold) affinity for glycine than GluN1 subunits despite having the same glycine binding residues (Y. Yao & Mayer, 2006). Due to this relatively high glycine affinity, receptors incorporating GluN3A have been predicted to be saturated by glycine (Henson et al., 2010). Further in support of this, extrasynaptic, GluN2B-containing NMDARs have a preference for glycine as compared to synaptic, GluN2A-containing NMDARs which have a preference for D-serine (Papouin et al., 2012). Triheteromeric, GluN1-GluN2B-GluN3A NMDARs such as those hypothesized to be expressed presynaptically in the visual cortex would therefore be likely to be saturated based on 0.5-10 micromolar extracellular glycine observed in the brain (Ferraro & Hare, 1985; Qu, Arckens, Vandenbussche, Geeraerts, & Vandesande, 1998; Y. Yao & Mayer, 2006). Therefore, saturation of the glycine binding site of presynaptic NMDARs in the visual cortex may result from presynaptic expression of GluN3A.

While our findings are consistent with GluN3A-containing NMDARs being localized to the presynaptic terminal where they may directly influence presynaptic release machinery, this has not been definitively demonstrated via the simultaneous measurement of presynaptic NMDAR function and localization.

An additional potential cofound of my findings is that they are based on data acquired from genetic models in which GluN3A is lost throughout the brain beginning in early development (GluN3A$^{-/-}$) or involves the overexpression of non-endogenous GluN3A in CaMKII-expressing (putatively glutamatergic in the neocortex) neurons for several weeks (GluN3A-OE). Indeed, these genetic models are known to produce significant changes in dendritic spine number (Das et al., 1998; Roberts et al., 2009), synaptic proteins such as AMPARs and CaMKII (Henson et al., 2012; Mohamad, Song, Wei, & Yu, 2013), postsynaptically-expressed synaptic plasticity (Mohamad et al., 2013; Roberts et al., 2009), and a variety of behaviors (Brody, Nakanishi, Tu, Lipton, & Geyer, 2005; Mohamad et al., 2013; Roberts et al., 2009) . This raises the possibility that the long-term loss or overexpression of GluN3A may influence presynaptic release and plasticity indirectly, through more global changes in synaptic structure.

Several lines of correlational evidence also argue in favor of the activation of presynaptic GluN3A-containing NMDARs modulating presynaptic release directly. First, genetic deletion of GluN3A appears to only reduce glutamate release early in development when presynaptic NMDARs are functional and not later in development when presynaptic NMDARs do not influence presynaptic release or plasticity (Chapter 3, above). Secondly, genetic deletion of GluN3A does not result in the complete loss of presynaptic NMDARs in early development, but instead restores their magnesium sensitivity while removing their tonic activity such that these receptors become functionally similar to those

expressed later in development. Third, ultrastructural localization of GluN3A has demonstrated expression of GluN3A at cortical presynaptic terminals early (Larsen et al., 2011) and not later in development (Pérez-Otaño et al., 2001; Wong et al., 2002), a time course which closely matches the developmental profile of presynaptic NMDARs (Corlew et al., 2007). Future studies are warranted however since this evidence primarily relies on correlations between presynaptic NMDAR function and GluN3A expression. Given the recent development of GluN3A-selective antagonists (Kvist, Greenwood, Hansen, Traynelis, & Brauner-Osborne, 2013), one way to implicate the direct involvement of GluN3A in presynaptic release may be to focally apply these antagonists while imaging NMDA-evoked calcium transients in axon terminals, as has been previously performed (Buchanan et al., 2012).

4.1.2 Roles for glutamate-binding GluN2 subunits in presynaptic NMDAR function

In addition to GluN3A, our results suggest that GluN2B-containing presynaptic NMDARs are also expressed at L2/3 visual cortical synapses and that a portion of these receptors persist after the downregulation of GluN3A. This finding is broadly consistent with many functional studies implicating cortical GluN2B-containing NMDARs in tLTD (Bender et al., 2006; Sjostrom et al., 2003) and in the modulation of glutamate release (Brasier & Feldman, 2008; Y. H. Li et al., 2009). In further agreement, GluN2B has been localized presynaptically in the cortex, even in the mature animals (Charton et al., 1999; DeBiasi et al., 1996), in support of the sustained expression of presynaptic GluN2B.

GluN2B-containing NMDARs have longer decay kinetics (Vicini et al., 1998), increased calcium influx per unit charge (Sobczyk, Scheuss, & Svoboda, 2005), and bind glutamate with higher affinity than GluN2A subunits (Paoletti et al., 2013). The relatively high calcium influx per unit charge and longer decay kinetics of GluN2B-containing NMDARs help explain how low numbers of presynaptic axonal NMDARs may influence presynaptic release in a manner that seems disproportionate to their expression level (Larsen et al., 2011). Indeed, due to the longer NMDAR open and decay times, NMDARs are believed to flux an order of magnitude more calcium per opening than voltage-gated calcium channels, despite their lower calcium conductance (Nimchinsky, Yasuda, Oertner, & Svoboda, 2004; Sabatini & Svoboda, 2000). Therefore, even the low number of NMDARs expressed at presynaptic terminals, such as 30% of those postsynaptic (Larsen et al., 2011), may have a large influence on presynaptic release. The inclusion of GluN2B into triheteromeric GluN3A-containing presynaptic NMDARs may also help reduce the relative decrease in calcium permeability that is observed when GluN3A is coexpressed with GluN1 and GluN2 subunits (Das et al., 1998), although these triheteromeric receptors also have increased open times that may somewhat compensate for the reduction in calcium permeability (Pérez-Otaño et al., 2001).

As noted above, presynaptic NMDARs are active in the absence of action potentials, meaning they cannot always function purely as precisely action potential-timed autoreceptors, and likely can rely on ambient sources of glutamate for their activation. The ambient glutamate concentration has been

estimated to be 0.5-10 micromolar (Featherstone & Shippy, 2008), although controversially, there is some suggestion that this concentration is significantly lower at synaptic sites (25 nanomolar) due to tight regulation by glutamate transporters (Herman & Jahr, 2007). GluN2B-containing NMDARs bind glutamate with an EC_{50} near 2 micromolar, half that of GluN2A-containing NMDARs (Paoletti et al., 2013). This suggests that the incorporation of GluN2B into presynaptic NMDARs assists in their ability to bind ambient glutamate which likely predominately mediates their activation in the absence of action potentials.

In contrast to the involvement of GluN2B in presynaptic NMDAR function, genetic deletion of GluN2A does not appear to affect presynaptic NMDAR-influenced spontaneous release (Larsen et al., 2011) and GluN2A-preferring antagonists do not block presynaptic NMDAR-dependent tLTD in the somatosensory cortex (Banerjee et al., 2009). These findings suggest that the glutamate-binding subunit which is incorporated into presynaptic NMDARs during early development is likely GluN2B, or GluN2C/D in the somatosensory cortex (Banerjee et al., 2009). However, this does not exclude a role for GluN2A in presynaptic NMDAR function. Indeed, within the adult cortex, acute in vivo blockade of NMDARs with AP5 increases presynaptic GluN2A expression, suggesting presynaptic receptors of this subtype may be trafficked in response to activity changes (Aoki et al., 2009). In many areas of the CNS (Hestrin, 1992), including the visual cortex (Chen, Cooper, & Mower, 2000; de Marchena et al., 2008; Larsen et al., 2011; Quinlan, Olstein, & Bear, 1999), GluN2A is drastically upregulated through postnatal development. Since the majority of studies of

implicating the incorporation of GluN2B in presynaptic NMDARs have been performed in early postnatal development (<P25) when presynaptic NMDAR function is most apparent (Banerjee et al., 2009; Corlew et al., 2007), a role for presynaptic GluN2A has not been thoroughly evaluated at a development time at which its expression is highest.

We briefly sought to address whether developmental decline in GluN3A in the visual cortex was accompanied by a replacement of GluN2B-containing presynaptic NMDARs with GluN2A-containing presynaptic NMDARs. However, GluN2B-selective antagonists were still capable of reducing the mEPSC frequency in mature (P26-30) mice when magnesium was excluded from the extracellular solutions. This suggests that even in later development when GluN3A and presynaptic NMDAR function are developmentally downregulated (Corlew et al., 2007), a significant portion of the remaining presynaptic NMDARs still express GluN2B. However, this does not exclude the possibility of a cortical GluN2A-containing presynaptic NMDAR population later in development which may be coexpressed with a GluN2B population. Additionally, triheteromeric (GluN2A-GluN2B-GluN1) receptors may also be expressed presynaptically given that they are believed to be more highly expressed in the adult forebrain (Gray et al., 2011; Rauner & Kohr, 2011; Tovar, McGinley, & Westbrook, 2013; Tovar & Westbrook, 1999). Importantly, these triheteromeric receptors would also be predicted to have significantly reduced sensitivity to GluN2B- or GluN2A-selective antagonists (Hatton & Paoletti, 2005). Due to the relatively shorter decay time (Erreger, Dravid, Banke, Wyllie, & Traynelis, 2005) and reduced

glutamate affinity (Laurie & Seeburg, 1994) of GluN2A-containing NMDARs compared to GluN2B-containing receptors, one prediction of the incorporation of GluN2A into mature (GluN3A-lacking) presynaptic NMDARs is that these receptors would function as non-tonically active autoreceptors whose activation has a very high frequency dependence due to their shorter decay times. Indeed, at the cerebellar parallel fiber to purkinje cell synapse which expresses presynaptic GluN2A receptors, LTD mediated by these receptors is most effectively induced by repetitive doublets of presynaptic stimulation at a high frequency (66-1000 Hz), a frequency-dependence which can be modeled based on the residence of bound glutamate on GluN2A receptors (Bidoret, Ayon, Barbour, & Casado, 2009).

One major unaddressed question arising from our studies is whether GluN3A forms functional triheteromeric presynaptic NMDA receptors with GluN2 and GluN1. Our results support the idea that these receptors are triheteromeric based on the finding that the glutamate site competitive antagonist AP5 blocks the contribution of presynaptic NMDARs to glutamate release and tLTD in a GluN3A-dependent manner (Larsen et al., 2011). However, triheteromeric (2GluN1-GluN2A-GluN2B) receptors typically have reduced sensitivity to subunit selective antagonists as a result of the loss of a subunit which binds these antagonists (Hatton & Paoletti, 2005). We did not observe this reduction in subunit-selective antagonist sensitivity when we applied GluN2B-selective antagonists however; they reduced the mEPSC frequency as effectively as non-subtype selective antagonist AP5. While not initially emphasized, we did observe

that these GluN2B-selective antagonists needed to be applied for fifteen minutes to observe significant changes in mEPSC frequency, whereas AP5 needed to only be applied for ten. Speculatively, the reduced sensitivity of a triheteromeric GluN3A-containing presynaptic NMDAR population may be responsible for this.

The stoichiometry of NMDAR subunits in a triheteromeric GluN3A-containing NMDARs has not been thoroughly investigated in non-heterologous systems. *In vivo*, it may be that tritheteromeric presynaptic receptors are composed of GluN1-GluN3A-2GluN2 subunits, instead of the predicted 2GluN1-GluN3A-GluN2 stoichiometry (Traynelis et al., 2010). If this were the case, it would explain why we did not observe a reduction in the efficacy of GluN2B-selective antagonists when assaying their effect on mEPSC frequency, since there would still be two GluN2B subunits for these antagonists to act upon. Both GluN3A and GluN2 subunits can independently bind GluN1 or each other (McIlhinney, Molnar, Atack, & Whiting, 1996; Pérez-Otaño et al., 2001). Additionally, expression of NMDAR subunits in heterologous systems produces functional glycine-gated GluN1-GluN3A NMDARs, but does not produce triheteromeric GluN3A-GluN2-GluN1 receptors at high numbers (Pérez-Otaño et al., 2001; Ulbrich & Isacoff, 2008). Since triheteromeric receptors have been observed in neurons (Roberts et al., 2009; Sasaki et al., 2002), these findings provide insights into which stoichiometries are possible in certain systems, but they do not provide insight to the numbers of each NMDAR subtype which exist in neurons expressing triheteromeric, GluN3A-containing NMDARs. In support of GluN1-GluN3A-2GluN2B NMDARs, coexpression of these three subunits does

not result in decreases in the ability GluN2B-selective antagonists to reduce NMDAR currents in some mammalian expression systems (Smothers & Woodward, 2003). Future studies are warranted to determine the exact subunit stoichiometry of NMDARs subunits expressed presynaptically in the visual cortex.

4.1.3 Regional Specificity of presynaptic NMDAR subunit expression

In contrast to the requirement for GluN3A-containining NMDARs for the induction of tLTD in the visual cortex, there is some evidence that tLTD at L4 to L2/3 somatosensory cortex synapses requires either GluN2C or GluN2D, and not GluN2A/B (Banerjee et al., 2009), but see (Bender et al., 2006). While GluN2C and GluN2D have unique properties as glutamate binding subunits, some properties of these receptor subunits are similar to those of GluN3A, making them compelling candidates for the incorporation into presynaptic NMDARs. Most notably, these subunits confer a reduced sensitivity to magnesium and reduced calcium influx compared to GluN2A/B subunits (Burnashev, Zhou, Neher, & Sakmann, 1995; Clarke & Johnson, 2006; Kuner & Schoepfer, 1996). This may allow these receptors to be active in the absence of depolarization, as has been reported in the somatosensory cortex (Brasier & Feldman, 2008). Additionally, the GluN2D is developmentally regulated in a manner similar to GluN3A, with expression peaking near P7 and decreasing thereafter (Larsen et al., 2011; Monyer, Burnashev, Laurie, Sakmann, & Seeburg, 1994). This is not the case for the GluN2C receptor whose expression peaks in adulthood (Monyer et al., 1994). However, GluN2C has been suggested to be expressed at L4

stellate cells in the somatosensory cortex (Binshtok, Fleidervish, Sprengel, & Gutnick, 2006) and since these neurons are known to heavily project to L2/3 neurons (Lubke, Egger, Sakmann, & Feldmeyer, 2000), they are an ideal site for presynaptic NMDAR to be expressed.

The tentative conclusion that tLTD within the somatosensory cortex requires GluN2C/GluN2D was largely based on the finding that two GluN2C/GluN2D preferring antagonists, PPDA and UBP141, block this form of plasticity, whereas other subunit preferring antagonists do not (Banerjee et al., 2009). In response to those findings, we sought to determine whether GluN2C or GluN2D might be required for the enhancement of glutamate release by presynaptic NMDARs in the visual cortex. We observed that genetic loss of GluN2D did not appear to reduce the contribution of presynaptic NMDARs to spontaneous glutamate release or tLTD. Additionally, we observed that the GluN2C/GluN2D antagonist UBP141 significantly reduced AMPAR responses in a manner independent of NMDAR activation (Chapter 2). UBP141 (100 micromolar) is known to reduce [^{3}H]AMPA radiolabeling by <20%, making it unclear if UBP141 is capable of strongly reducing AMPAR responses directly (Morley et al., 2005). Since both PPDA and UBP141 are not highly selective over other NMDAR subunits (less than 10 fold), future studies should couple the use of these antagonists with genetic models that specifically manipulate either GluN2C or GluN2D expression in order be certain of their specificity (Paoletti & Neyton, 2007). CIQ, an allosteric potentiator of GluN2C/D receptors which has high NMDAR subunit selectivity without affecting AMPA or kainate receptors, has

been also been recently described and may be a more ideal candidate compound for testing the involvement of GluN2C/D in presynaptic NMDAR function (Mullasseril et al., 2010).

Whether GluN3A is required for presynaptic NMDAR function in other areas outside the visual cortex is unknown. However, based on the large diversity of NMDARs subunit arrangements that have been observed to exist postsynaptically (Paoletti et al., 2013), one might predict that the exact subunit composition expressed presynaptically might similarly depend on the larger function of the circuit in which they are expressed. Furthermore at some synapses, such as those in the nucleus accumbens (Huang et al., 2011), functional presynaptic NMDARs may not be expressed at all. As discussed in Chapter 2, an illustrative example of presynaptic NMDAR subunit diversity comes from CA1 synapses. Compelling evidence suggests that at the hippocampal Schaffer collateral-CA1 synapse, presynaptic NMDARs are likely composed of GluN2B or GluN2D subunits and do not express GluN3A. This conclusion is based on the finding that GluN2B-selective antagonists, 10 mM Mg^{2+} , and the inhibition of neurotransmitter release block action potential-mediated large CA3 axonal calcium influxes that are believed to result from presynaptic NMDAR activation (McGuinness et al., 2010). This suggests that these receptors function as Mg^{2+}-sensitive GluN2B-containing autoreceptors, which lack the tonic presynaptic NMDAR activity observed at L2/3 visual cortical synapses which express GluN3A. In agreement with this lack of tonic presynaptic NMDAR activity in the hippocampus, bath application of the NMDAR antagonists does not alter

the mEPSC frequency when recording from CA1 pyramidal neurons early in development (P3-P20) (RS Larsen, unpublished observation), consistent with previous findings (Mameli et al., 2005; Nimchinsky et al., 2004). While the hippocampal CA1 synapses likely do not express GluN3A presynaptically, these synapses may undergo a similar developmental change in presynaptic subunit composition. Before postnatal day five, presynaptic NMDARs at CA1 synapse transiently express GluN2D and not GluN2B (Mameli et al., 2005), mirroring the visual cortical developmental change from a relatively magnesium-insensitive subunit (GluN2D) to one with increased magnesium sensitivity (GluN2B).

This difference in presynaptic subunit expression between the visual cortex and hippocampus appears to result in significant differences in the frequency dependence of presynaptic NMDAR activation. In sensory cortices, presynaptic NMDARs appear tuned to most effectively enhance presynaptic glutamate release at frequencies near 30 Hz or above (Brasier & Feldman, 2008; Larsen et al., 2011; Sjöström, Turrigiano, & Nelson, 2003) and, at least following visual deprivation (Chapter 3), they do not promote glutamate release at frequencies below 10 Hz. In contrast, presynaptic NMDARs at Schaffer collateral-CA1 synapses promote neurotransmitter release most effectively at ~5 Hz (theta) and very little at 20 Hz (McGuinness et al., 2010). Since theta-burst stimulation results in LTP at CA1 synapses (Hoffman, Sprengel, & Sakmann, 2002), this suggests that presynaptic NMDARs may be more effective at promoting LTP, rather than LTD, in the hippocampus. Theta rhythm is also a defining feature of the hippocampus (Csicsvari, Hirase, Czurko, Mamiya, &

Buzsaki, 1999) which can be produced in isolated hippocampal preparations (Goutagny, Jackson, & Williams, 2009). The finding that presynaptic NMDARs selectively enhance release at theta frequency in the hippocampus, but not in sensory cortices, further supports the idea that presynaptic NMDARs might be tuned to the function of the circuit they reside, and that this tuning may be accomplished via changes in subunit expression.

4.2 Mechanisms by which presynaptic NMDARs modulate glutamate release

In the visual and somatosensory cortices, presynaptic NMDARs modulate glutamate release in two opposing manners: by increasing glutamate release via their direct activation by glutamate and through their involvement in spike timing dependent long term depression, which results in the reduction of glutamate release chronically (Corlew et al., 2008). What allows for these receptors to be activated in these two opposing manners is just beginning to be understood. The subunit composition, intracellular localization, and how they interact with presynaptic cannabinoid signaling are all likely to be important factors by which presynaptic NMDARs produce changes in glutamate release.

In several cortical areas, presynaptic NMDARs increase spontaneous, evoked, and asynchronous glutamate release following their binding to glutamate (Berretta & Jones, 1996; Corlew et al., 2008). The exact mechanism for how this occurs regarding in each case is unclear, however in most instances evidence suggests that presynaptic NMDARs alter presynaptic terminal calcium levels either on a rapid time scale or gradually over repeated bursts of activity. In

contrast to spontaneous release which can occur at low levels in the absence of calcium (Fatt & Katz, 1952; M. D. Glitsch, 2008), evoked release is considerably more sensitive to extracellular calcium concentrations and does not occur in its absence (Xu, Pang, Shin, & Sudhof, 2009). In accordance with this dependence of evoked release on calcium, blockade of calcium influx through voltage-gated calcium channels and NMDARs with cobalt blocks the effects of NMDAR agonists on presynaptic release (Woodhall, Evans, Cunningham, & Jones, 2001). In agreement, axonal application of NMDAR agonists results in calcium influxes at axon terminals (Buchanan et al., 2012; Cochilla & Alford, 1999; H. Lin et al., 2010; McGuinness et al., 2010; Rossi et al., 2012), but see (Christie & Jahr, 2008, 2009). Additionally, since NMDARs are permeable to both calcium and strontium (Mayer & Westbrook, 1987), the finding that strontium replacement of calcium ions does not alter the ability of presynaptic NMDARs to alter (asynchronous) release indirectly suggests that they normally influence evoked release via calcium influx via their pore (Berretta & Jones, 1996). In summary, evidence strongly suggests that presynaptic NMDARs act to modify calcium influx at presynaptic terminals leading to increase rates of glutamate exocytosis.

While presynaptic NMDARs may influence evoked release via alterations presynaptic calcium, in many instances they appear to do so in manner that doesn't linearly correlate with the rate of presynaptic action potential firing. One of the first demonstrations that presynaptic NMDARs are activated in a frequency-dependent manner came from the finding that NMDAR antagonists reduce presynaptic release at 30 Hz, but not at 0.1 Hz, at L5 visual cortical

synapses (Sjöström et al., 2003). Following dark-rearing, presynaptic NMDARs at L2/3 synapses also seemed tuned to promote glutamate release higher frequencies (above 5 Hz, see Chapter 3). Similar results in the cerebellum have led to the conclusion that in many instances, presynaptic NMDARs act as high-pass frequency filters (Bidoret et al., 2009). How presynaptic NMDARs enhance release specifically at both high frequencies while also contributing to spontaneous release is unknown. However, changes in terminal calcium levels may promote release through mechanisms other by directly causing vesicle exocytosis. Residual calcium following release is critical for recovery from synaptic depression (Dittman & Regehr, 1998). Therefore, another possible mechanism by which presynaptic NMDARs may promote glutamate release is by enhancing the residual calcium accumulates after repetitive firing to allow for recovery from synaptic depression (Sjöström et al., 2003).

Unlike evoked release, presynaptic NMDARs can promote spontaneous glutamate release in the absence of extracellular calcium at L2/3 visual cortical synapses (Kunz, Roberts, & Philpot, 2013). However, there is not evidence that presynaptic NMDARs typically promote glutamate release in a calcium-independent manner, only that they may do so in the absence of calcium. Additionally, since the rate of spontaneous release in the absence of calcium is low –near 0.5 Hz (Kunz et al., 2013)-, contributions of presynaptic NMDARs to calcium-independent release processes are likely to be considerably smaller than their contribution to calcium-dependent processes. Therefore, presynaptic NMDARs may typically influence spontaneous release via similar changes in

residual terminal calcium levels. Since the cellular mechanisms underlying calcium-independent release are not well understood (M. D. Glitsch, 2008), it is not clear how presynaptic NMDAR enhance this form of spontaneous release, although it may involve the recruitment of intracellular signaling cascades such as PKC (Kunz et al., 2013).

Within sensory cortices, there is considerable evidence that presynaptic NMDAR expression is confined to certain synapses. In layer five of the visual cortex, presynaptic NMDARs are expressed at synapses between pyramidal neurons and at synapses from pyramidal cells onto Martinotti cells (Buchanan et al., 2012). However, they do not influence glutamate release from layer five pyramidal cells onto GABAergic basket cells. Additionally, it appears that presynaptic NMDARs are preferentially expressed at L4 inputs to L2/3 neurons and not at L2/3 to L2/3 intralaminar connections (Brasier & Feldman, 2008). In accordance with this, at L2/3 synapses it seems that forms of tLTD that are induced from L2/3 or unknown inputs is dependent on postsynaptic NMDARs, and not presynaptic NMDARs (Froemke & Dan, 2002; Zilberter et al., 2009). This suggests that sensory experience-induced changes in presynaptic NMDAR function may be confined to L4 inputs (Chapter 3). Additionally, the synapse specificity of presynaptic NMDAR expression may help explain why, in some instances, it has been difficult to detect these receptors at axons (discussed below).

4.2.1 Mechanisms for long-term changes in presynaptic glutamate release following tLTD

There is considerable evidence that endocannibinoid signaling coupled with presynaptic NMDAR activation is a prerequisite for the induction of tLTD (Bender et al., 2006; Min & Nevian, 2012; Sjostrom, Turrigiano, & Nelson, 2004; Sjöström et al., 2003), but see (Banerjee et al., 2009). Recently, it was demonstrated in the somatosensory cortex that the relevant endocannibinoid receptors (CB1) may be localized to astrocytes (Min & Nevian, 2012). To produce tLTD, it was proposed that repetitive postsynaptic action potential firing led to the retrograde release of endocannibinoids from postsynaptic neurons, which bound to astrocyte CB1Rs, resulting in the astrocytic release of glutamate onto presynaptic NMDARs. This proposed mechanism suggests that perhaps the sole mediator of the reduction in presynaptic release at excitatory axon terminals is presynaptic NMDARs. Additionally, the authors proposed that the involvement of astrocytes explains why many action potential-EPSP pairings must be performed to induce tLTD: repetitive AP-EPSP pairings allow for calcium to accumulate in astrocytes in a manner compared to acting as a time-buffer (Min & Nevian, 2012). Hypothetically, this scenario would require magnesium-insensitive presynaptic NMDAR expression, such as GluN3A, because the presynaptic terminal depolarization from the EPSP would not be coincident with the release of glutamate from an astrocytic source. While a generally similar signaling mechanism has been demonstrated in the hippocampus (Navarrete & Araque, 2010), the direct release of neurotransmitter by astrocytes is controversial

(Agulhon, Fiacco, & McCarthy, 2010; Fiacco et al., 2007). Further work is warranted to determine the exact role of astrocytes in mediating tLTD.

The intracellular signaling underlying the reduction in the presynaptic release that occurs following tLTD is just beginning to be understood. However, based on studies of endocannibinoid-mediated synaptic plasticity in the hippocampus, there are several proteins which may be involved (Heifets & Castillo, 2009). These include RIM1α, Rab3B, protein kinase A, and calcineurin (Min & Nevian, 2012). Recently, it was demonstrated that presynaptic calcineurin is indeed required for the induction of LTD mediated by presynaptic NMDARs at L4-L2/3 somatosensory cortex synapses (Rodriguez-Moreno et al., 2013). Importantly, GluN3A-containing NMDARs are known to form a signaling complex with calcineurin (PP2A) (Chan & Sucher, 2001; Ma & Sucher, 2004), suggesting that one mechanism by which GluN3A-containing NMDARs produce a result a reduction in glutamate release via this signaling cascade. The activation of GluN3A-containing NMDARs reduces PP2A activity (Chan & Sucher, 2001). Such an alteration in presynaptic calcineurin activity may reduce the dephosphorylation of the dephosphins, dynamin, synaptojanin, AP180, EPSIN, or AMPHYSIN1/2 (Cousin & Robinson, 2001). The dephosphorylation of these proteins is required for the endocytosis of synaptic vesicles following repetitive stimulation, suggesting that the tLTD could hypothetically result from reduction in dephosphin activity. However, this has not been tested, and further work is required to figure out the exact presynaptic proteins involved in tLTD.

Interestingly, with specific patterns of presynaptic firing, long-term depression can be induced at L4-L2/3 somatosensory cortical synapses independent of any postsynaptic depolarization or signaling (Rodriguez-Moreno et al., 2013). This “self-depression” (p-LTD) also requires presynaptic NMDARS and is occluded by previous tLTD induction. This form of plasticity is also independent of astroglial signaling, suggesting that the glutamate release from presynaptic activity itself can sufficiently activate presynaptic NMDARs enough to cause long-term reductions in glutamate release.

4.2.2 Axonal versus dendritic localization

Perhaps the largest current controversy regarding presynaptic NMDARs is where they are localized on the presynaptic neuron (Duguid, 2013). Whether presynaptic NMDARs are localized axonally, somatically, or dendritically is likely to inform exactly how these receptors modulate glutamate release. A large number ultrastructural studies have found that the presynaptic NMDAR subunits GluN2B, GluN2A, and GluN3A can be localized to axon terminals (Aoki et al., 2003; Aoki et al., 2009; Aoki, Venkatesan, Go, Mong, & Dawson, 1994; Charton et al., 1999; Corlew et al., 2007; DeBiasi et al., 1996; Farb, Aoki, & Ledoux, 1995; Jourdain et al., 2007; Larsen et al., 2011; McGuinness et al., 2010; Siegel et al., 1994). In some instances, genetic strategies to selectively delete NMDARs from presynaptic but not postsynaptic sites has allowed for the demonstration that immunolabeling of NMDAR subunits at axonal sites is not spurious postsynaptic labeling (McGuinness et al., 2010). However, it is unclear whether receptors at axon terminals are functionally relevant and these studies have been

critiqued because in some instances, axonal GluN1 labeling appears diffuse and not associated with the membrane (Christie & Jahr, 2009).

To address this, there have been several attempts to directly image calcium from axonally localized NMDARs at cortical L5, cerebellar stellate and parallel fiber, and hippocampal CA1 axons. Presently, no consensus has emerged as to whether functional NMDARs can be expressed in axons, however the present evidence favors axonal expression. In cerebellar stellate neurons which had been suggested to express axonal NMDARs (M. Glitsch & Marty, 1999), direct ionotophoresis of aspartate to the axon of these neurons failed to produce any calcium-mediated responses, although ionotophoresis onto dendritic sites produced axonal calcium transients which resulted from spreading depolarization through the neuron soma (Christie & Jahr, 2008). Similarly, bath application of AP5 did not change the stimulus-evoked calcium transients at cerebellar parallel fibers (Shin & Linden, 2005), a site which had also previously been hypothesized to express axonal NMDARs (Casado, Dieudonne, & Ascher, 2000; Casado, Isope, & Ascher, 2002). Since parallel fibers are believed to be able to activate cerebellar stellate interneurons (Shin & Linden, 2005), the proposed mechanism to reconcile these both of these findings was that subthreshold, dendritic NMDAR-mediated activity in cerebellar stellate interneurons was responsible for the observed effects on presynaptic release previously ascribed to axonal NMDARs (Christie & Jahr, 2008). However, a later study demonstrated that bath application of NMDA produced calcium influxes in cerebellar stellate axons even when the soma was hyperpolarized, arguing

against passive diffusion of a dendritic NMDAR-mediated currents into axons (Rossi et al., 2012). Additionally, Rossi *et al.* found that glutamate uncaging produced NMDAR-mediated axonal calcium transients at roughly thirty percent of cerebellar stellate axon sites, suggesting heterogeneous expression of axonal NMDARs (Rossi et al., 2012).

A similar controversy exists regarding the expression of NMDARs at L5 visual cortical axons. Similar to results from the cerebellum, direct application of aspartate failed to produce axonal calcium transients at L5 axons, but was capable of producing dendritic calcium responses (Christie & Jahr, 2009). However, these subthreshold NMDAR currents did not seem capable of reaching axonal sites, unlike what was observed in cerebellar stellate interneurons (Christie & Jahr, 2009). In response to these results, a later study paired 30 Hz action-potential firing with uncaging of NMDA at axonal sites and observed that at ~50% of axonal boutons, this protocol produced NMDAR antagonist-sensitive supralinear axonal calcium responses (Buchanan et al., 2012). As seen with NMDAR axonal calcium transients at cerebellar interneurons, this suggests that axonal NMDAR localization is heterogeneous. Indeed, it is known that presynaptic NMDARs only influence glutamate at a subset of synapses within the cortex such as at L4-L2/3 synapses, but not at L2/3-L2/3 synapses (Brasier & Feldman, 2008). If presynaptic NMDARs also express the less calcium permeable subunit GluN3A and have heterogeneous expression patterns, it may be especially difficult to regularly observe their activity using broad axonal calcium imaging methods.

4.3 Roles for presynaptic NMDARs in experience-dependent plasticity

Manipulations in the sensory environment are known to produce large changes in excitatory and inhibitory drive (Hensch, 2005a, 2005b), action potential firing properties (Lambo & Turrigiano, 2013; Nataraj & Turrigiano, 2011), synapse number (Wallace & Bear, 2004), and general functionality of the sensory cortex examined (Chapman & Stryker, 1993). Based on these changes it is important to consider that experience-dependent changes in presynaptic NMDAR function may drive, or be driven-by, other changes in circuit function that occur following visual deprivation. Based on that finding that two days of dark-rearing does not alter the ability to induce tLTD (Guo et al., 2012), but that dark-rearing from birth or ten days of LOVD can restore the ability to induce tLTD, it appears longer period of visual deprivation may be necessary restore the ability to induce tLTD. This raises the possibility that changes that occur in the first days following visual deprivation may drive the subsequent changes in presynaptic NMDAR function, although this is untested. However, it is known that during the critical period, tLTD at L2/3 synapses changes from a presynaptically-expressed form, to one that is expressed postsynaptically, but is gated by GABA(A)-mediated inhibition (Corlew et al., 2007). These results suggest that the development of postsynaptically-mediated tLTD at these synapses occurs simultaneously with increases in inhibitory drive. Since dark-rearing reverses the developmental increase in inhibitory drive that occurs in the visual cortex (Morales, Choi, & Kirkwood, 2002), one possibility is that changes in inhibitory transmission drive the switch in tLTD from a pre- to postsynaptic form. In this

model, dark-rearing would reverse the developmental loss in tLTD by first decreasing inhibitory tone. As such, one prediction of this is that chronic potentiation of GABA(A) transmission with diazepam early in development, as previously performed to prematurely begin the critical period (Fagiolini & Hensch, 2000), would prematurely result in the loss of presynaptic tLTD.

As mentioned, our results describing how visual experience alters presynaptic NMDAR function are overlaid on many other synaptic changes that occur following sensory deprivation. Indeed, we have observed that dark-rearing results in postsynaptic scaling of mEPSC amplitudes without affecting the mEPSC frequency, as has been previously described (Desai et al., 2002; Goel et al., 2006). While it may be initially surprising that dark-rearing doesn't increase mEPSC frequency since dark-rearing increases the contribution of presynaptic NMDARs to spontaneous glutamate release, this contribution is likely confined to a subset of synaptic inputs and likely is accompanied by decreases in the overall synapse number that occurs following dark-rearing (Valverde, 1971; Wallace & Bear, 2004). This reduction in synapse number following dark-rearing would result in a decrease in mEPSC frequency if these synapses were not "silent". Similarly, since I hypothesize that changes following dark-rearing are confined to a subset of synaptic inputs, it may be difficult to detect small increases in spontaneous presynaptic release at subsets of synapses due to the intrinsic variability of spontaneous release (note the considerable, typical variation in baseline mEPSC frequencies throughout Chapters 2 and 3).

Visual deprivation also results in the increased expression of GluN3A at visual cortical synapses, and loss of this NMDAR subunit occludes the effects of visual deprivation on tLTD and presynaptic glutamate release at high frequencies. In combination with the findings of Chapter 2 that the GluN3A subunit is required for the contribution of presynaptic NMDARs to tLTD and glutamate release early in development, our results strongly suggest that presynaptic GluN3A expression may be regulated by sensory experience. The cellular mechanisms underlying the increased expression of GluN3A in visual deprived mice are unknown, but may involve the sustained expression of GluN3A through development.

If presynaptic NMDARs are modified by sensory experience has not been thoroughly explored at many synapses, at L4 unitary connections presynaptic NMDARs may be involved in the experience-dependent switch in the polarity of slow-wave plasticity that occurs during the visual critical period (L. Wang et al., 2012). Before postnatal day 20, repetitive stimulation consisting of 20 bursts of 10 action potentials at 50 Hz, with each burst separated by 10 seconds causes “slow-wave” LTD that depends on putatively presynaptic NMDARs. However, during the critical period (P25-28), this same plasticity protocol results in potentiation, which also depends on presynaptic NMDARs. This developmental switch in the polarity of plasticity at visual cortical L4 unitary connections can be prevented if mice are monocularly-deprived. These results suggest that presynaptic NMDARs may produce different plasticity outcomes based on sensory experience. These results add to the conclusions presented in Chapter

4, namely that developmental changes occurring near the critical period alter the function of presynaptic NMDARs in an experience-dependent manner.

4.4 Functional significance of presynaptic NMDAR expression

While few *in vivo* studies have attempted to address the contribution of presynaptic NMDARs to visual cortical development, based on their functions *ex vivo*, several hypotheses can be formulated. Perhaps most importantly, presynaptic NMDARs enable a form of spike timing-dependent tLTD that is not gated by inhibition, unlike tLTD later in development (Corlew et al., 2007). As spike timing-dependent plasticity paradigms are sufficient to alter receptive fields (Meliza & Dan, 2006), presynaptically-expressed tLTD may assist in the development of receptive fields in the first weeks of life prior to significant increases in inhibitory tone. Interestingly, presynaptic NMDARs also enable a form of “self-depression” in which the firing pattern of the presynaptic neuron alone, independent of postsynaptic activity, can result in long-term decreases in glutamate release (Rodriguez-Moreno et al., 2013). This functional significance of this is unknown, however it may allow for presynaptic neurons to select for certain activity patterns without the need for postsynaptic retrograde interaction. Presynaptic NMDARs also increase spontaneous and evoked glutamate release in the developing visual cortex and following sensory deprivation (Chapters 2-3). This may ensure reliable synaptic transmission at nascent synapses to allow for Hebbian mechanisms to act to regulate synaptic strength and connectivity. Similarly, spontaneous neurotransmitter release is important for the stabilization of synaptic function via the regulation of postsynaptic translation (Sutton, Wall,

Aakalu, & Schuman, 2004). Since presynaptic NMDARS also enhance spontaneous glutamate release early in development, they may especially important for similar processes which regulation postsynaptic stability via spontaneous release.

A unifying role for presynaptic NMDARs may be as frequency filters for evoked release. In many brain areas, presynaptic NMDARs selectively promote glutamate release at some frequencies and very little at other frequencies. As demonstrated following visual deprivation at L2/3 synapses (Chapter 3), presynaptic NMDARs act as high-pass frequency filters in the visual cortex (Buchanan et al., 2012; Sjostrom et al., 2003) and in the cerebellum (Bidoret et al., 2009) . How presynaptic NMDAR-mediated high-pass frequency filtering influences cortical circuit dynamics is just beginning to be understood. However, at least in one instance, presynaptic NMDARs have been shown to be integral for the maintenance of frequency-dependent disynaptic inhibition (FDDI) mediated by cortical L5 Martinotti cells (Buchanan et al., 2012). FDDI occurs when which high-frequency firing of pyramidal neurons activates L5 Martinotti neurons, which then project to many excitatory neurons to inhibit them (Silberberg & Markram, 2007). Since Martinoitti cells project into many cortical layers throughout a cortical column (Y. Wang et al., 2004), it suggests that presynaptic NMDARs may be critical in regulating information flow though the cortex via their involvement in FDDI.

Due to their nearly ubiquitous expression in the brain, NMDARs are involved in many neurological and psychiatric disorders. The wide range of

diseases NMDAR dysfunction has been linked to is reviewed elsewhere, however it includes diseases that affect millions of people including schizophrenia, depression, pain, Alzheimer's disease, white-matter injury, cerebral ischaemia, Parkinsons's disease, Huntington's disease (Paoletti et al., 2013). Indeed, basic science studies of NMDARs have broad impacts on translational medicine because they may reveal cellular disease etiologies that are presently unknown. While roles for presynaptic NMDARs in particular in disease states has just started to be explored, there is evidence that presynaptic NMDARs are upregulated following cortical injury or in epilepsy models (Yan et al., 2012; J. Yang et al., 2006). Given that presynaptic NMDARs are likely to be expressed at subsets of presynaptic sites and likely express unique subunit compositions (including GluN3A), they may be particularly attractive pharmacological targets compared to more uniformly-expressed postsynaptic GluN2 subunits.

References

Agulhon, C., Fiacco, T. A., & McCarthy, K. D. (2010). Hippocampal short- and long-term plasticity are not modulated by astrocyte Ca2+ signaling. *Science, 327*(5970), 1250-1254. doi: 10.1126/science.1184821

Alle, H., & Geiger, J. R. (2006). Combined analog and action potential coding in hippocampal mossy fibers. *Science, 311*(5765), 1290-1293. doi: 10.1126/science.1119055

Allen, C. B., Celikel, T., & Feldman, D. E. (2003). Long-term depression induced by sensory deprivation during cortical map plasticity in vivo. *Nat Neurosci, 6*(3), 291-299. doi: 10.1038/nn1012

Aoki, C., Fujisawa, S., Mahadomrongkul, V., Shah, P. J., Nader, K., & Erisir, A. (2003). NMDA receptor blockade in intact adult cortex increases trafficking of NR2A subunits into spines, postsynaptic densities, and axon terminals. *Brain Res, 963*(1-2), 139-149.

Aoki, C., Lee, J., Nedelescu, H., Ahmed, T., Ho, A., & Shen, J. (2009). Increased levels of NMDA receptor NR2A subunits at pre- and postsynaptic sites of the hippocampal CA1: an early response to conditional double knockout of presenilin 1 and 2. *J Comp Neurol, 517*(4), 512-523. doi: 10.1002/cne.22151

Aoki, C., Venkatesan, C., Go, C. G., Mong, J. A., & Dawson, T. M. (1994). Cellular and subcellular localization of NMDA-R1 subunit immunoreactivity in the visual cortex of adult and neonatal rats. *J Neurosci, 14*(9), 5202-5222.

Aramakis, V. B., & Metherate, R. (1998). Nicotine selectively enhances NMDA receptor-mediated synaptic transmission during postnatal development in sensory neocortex. *J Neurosci, 18*(20), 8485-8495.

Awatramani, G. B., Price, G. D., & Trussell, L. O. (2005). Modulation of transmitter release by presynaptic resting potential and background calcium levels. *Neuron, 48*(1), 109-121. doi: 10.1016/j.neuron.2005.08.038

Bakin, J. S., & Weinberger, N. M. (1996). Induction of a physiological memory in the cerebral cortex by stimulation of the nucleus basalis. *Proc Natl Acad Sci U S A, 93*(20), 11219-11224.

Bandrowski, A. E., Ashe, J. H., & Crawford, C. A. (2001). Tetanic stimulation and metabotropic glutamate receptor agonists modify synaptic responses and protein kinase activity in rat auditory cortex. *Brain Res, 894*(2), 218-232. doi: S0006-8993(01)02052-2 [pii]

Banerjee, A., Meredith, R. M., Rodriguez-Moreno, A., Mierau, S. B., Auberson, Y. P., & Paulsen, O. (2009). Double dissociation of spike timing-dependent potentiation and depression by subunit-preferring NMDA receptor antagonists in mouse barrel cortex. *Cereb Cortex, 19*(12), 2959-2969. doi: bhp067 [pii]

Bao, S., Chan, V. T., & Merzenich, M. M. (2001). Cortical remodelling induced by activity of ventral tegmental dopamine neurons. *Nature, 412*(6842), 79-83. doi: 10.1038/35083586 [doi]

Bao, S., Chang, E. F., Woods, J., & Merzenich, M. M. (2004). Temporal plasticity in the primary auditory cortex induced by operant perceptual learning. *Nat Neurosci, 7*(9), 974-981. doi: 10.1038/nn1293 [doi]

Basura, G. J., Abbas, A. I., O'Donohue, H., Lauder, J. M., Roth, B. L., Walker, P. D., & Manis, P. B. (2008). Ontogeny of serotonin and serotonin2A receptors in rat auditory cortex. *Hear Res, 244*(1-2), 45-50. doi: S0378-5955(08)00153-6 [pii]

Bell, C. C., Han, V. Z., Sugawara, Y., & Grant, K. (1997). Synaptic plasticity in a cerebellum-like structure depends on temporal order. *Nature, 387*(6630), 278-281. doi: 10.1038/387278a0 [doi]

Bender, V. A., Bender, K. J., Brasier, D. J., & Feldman, D. E. (2006). Two coincidence detectors for spike timing-dependent plasticity in somatosensory cortex. *J Neurosci, 26*(16), 4166-4177. doi: 26/16/4166 [pii]

Berretta, N., & Jones, R. S. (1996). Tonic facilitation of glutamate release by presynaptic N-methyl-D-aspartate autoreceptors in the entorhinal cortex. *Neuroscience, 75*(2), 339-344.

Bi, G. Q., & Poo, M. M. (1998). Synaptic modifications in cultured hippocampal neurons: dependence on spike timing, synaptic strength, and postsynaptic cell type. *J Neurosci, 18*(24), 10464-10472.

Bidoret, C., Ayon, A., Barbour, B., & Casado, M. (2009). Presynaptic NR2A-containing NMDA receptors implement a high-pass filter synaptic plasticity rule. *Proc Natl Acad Sci U S A, 106*(33), 14126-14131. doi: 0904284106 [pii]

Bienenstock, E. L., Cooper, L. N., & Munro, P. W. (1982). Theory for the development of neuron selectivity: orientation specificity and binocular interaction in visual cortex. *J Neurosci, 2*(1), 32-48.

Binshtok, A. M., Fleidervish, I. A., Sprengel, R., & Gutnick, M. J. (2006). NMDA receptors in layer 4 spiny stellate cells of the mouse barrel cortex contain the NR2C subunit. *J Neurosci, 26*(2), 708-715. doi: 26/2/708 [pii]

Bliss, T. V., & Lomo, T. (1973). Long-lasting potentiation of synaptic transmission in the dentate area of the anaesthetized rabbit following stimulation of the perforant path. *J Physiol, 232*(2), 331-356.

Blue, M. E., Martin, L. J., Brennan, E. M., & Johnston, M. V. (1997). Ontogeny of non-NMDA glutamate receptors in rat barrel field cortex: I. Metabotropic receptors. *J Comp Neurol, 386*(1), 16-28. doi: 10.1002/(SICI)1096-9861(19970915)386:1<16::AID-CNE4>3.0.CO;2-G [pii]

Bodor, A. L., Katona, I., Nyiri, G., Mackie, K., Ledent, C., Hajos, N., & Freund, T. F. (2005). Endocannabinoid signaling in rat somatosensory cortex: laminar differences and involvement of specific interneuron types. *J Neurosci, 25*(29), 6845-6856. doi: 25/29/6845 [pii]

Boyden, E. S., Zhang, F., Bamberg, E., Nagel, G., & Deisseroth, K. (2005). Millisecond-timescale, genetically targeted optical control of neural activity. *Nat Neurosci, 8*(9), 1263-1268. doi: nn1525 [pii]

Brasier, D. J., & Feldman, D. E. (2008). Synapse-specific expression of functional presynaptic NMDA receptors in rat somatosensory cortex. *J Neurosci, 28*(9), 2199-2211. doi: 28/9/2199 [pii]

Brocher, S., Artola, A., & Singer, W. (1992). Agonists of cholinergic and noradrenergic receptors facilitate synergistically the induction of long-term potentiation in slices of rat visual cortex. *Brain Res, 573*(1), 27-36. doi: 0006-8993(92)90110-U [pii]

Brody, S. A., Nakanishi, N., Tu, S., Lipton, S. A., & Geyer, M. A. (2005). A developmental influence of the N-methyl-D-aspartate receptor NR3A subunit on prepulse inhibition of startle. *Biological Psychiatry, 57*(10), 1147-1152. doi: DOI 10.1016/j.biopsych.2005.01.024

Broide, R. S., O'Connor, L. T., Smith, M. A., Smith, J. A., & Leslie, F. M. (1995). Developmental expression of alpha 7 neuronal nicotinic receptor messenger RNA in rat sensory cortex and thalamus. *Neuroscience, 67*(1), 83-94. doi: 030645229400623D [pii]

Broide, R. S., Robertson, R. T., & Leslie, F. M. (1996). Regulation of alpha7 nicotinic acetylcholine receptors in the developing rat somatosensory cortex by thalamocortical afferents. *J Neurosci, 16*(9), 2956-2971.

Buchanan, K. A., Blackman, A. V., Moreau, A. W., Elgar, D., Costa, R. P., Lalanne, T., . . . Sjostrom, P. J. (2012). Target-specific expression of

presynaptic NMDA receptors in neocortical microcircuits. *Neuron, 75*(3), 451-466. doi: 10.1016/j.neuron.2012.06.017

Burnashev, N., Zhou, Z., Neher, E., & Sakmann, B. (1995). Fractional calcium currents through recombinant GluR channels of the NMDA, AMPA and kainate receptor subtypes. *J Physiol, 485 (Pt 2)*, 403-418.

Carandini, M., & Ferster, D. (2000). Membrane potential and firing rate in cat primary visual cortex. *J Neurosci, 20*(1), 470-484.

Casado, M., Dieudonne, S., & Ascher, P. (2000). Presynaptic N-methyl-D-aspartate receptors at the parallel fiber-Purkinje cell synapse. *Proc Natl Acad Sci U S A, 97*(21), 11593-11597. doi: 10.1073/pnas.200354297

Casado, M., Isope, P., & Ascher, P. (2002). Involvement of presynaptic N-methyl-D-aspartate receptors in cerebellar long-term depression. *Neuron, 33*(1), 123-130.

Celikel, T., Szostak, V. A., & Feldman, D. E. (2004). Modulation of spike timing by sensory deprivation during induction of cortical map plasticity. *Nat Neurosci, 7*(5), 534-541. doi: 10.1038/nn1222 [doi]

Chan, S. F., & Sucher, N. J. (2001). An NMDA receptor signaling complex with protein phosphatase 2A. *J Neurosci, 21*(20), 7985-7992.

Chapman, B., & Stryker, M. P. (1993). Development of orientation selectivity in ferret visual cortex and effects of deprivation. *J Neurosci, 13*(12), 5251-5262.

Charton, J. P., Herkert, M., Becker, C. M., & Schroder, H. (1999). Cellular and subcellular localization of the 2B-subunit of the NMDA receptor in the adult rat telencephalon. *Brain Res, 816*(2), 609-617. doi: S0006-8993(98)01243-8 [pii]

Chatterton, J. E., Awobuluyi, M., Premkumar, L. S., Takahashi, H., Talantova, M., Shin, Y., . . . Zhang, D. (2002). Excitatory glycine receptors containing the NR3 family of NMDA receptor subunits. *Nature, 415*(6873), 793-798. doi: 10.1038/nature715 [doi]

Cheetham, C. E., & Fox, K. (2010). Presynaptic development at L4 to l2/3 excitatory synapses follows different time courses in visual and somatosensory cortex. *J Neurosci, 30*(38), 12566-12571. doi: 30/38/12566 [pii]

Chen, L., Cooper, N. G., & Mower, G. D. (2000). Developmental changes in the expression of NMDA receptor subunits (NR1, NR2A, NR2B) in the cat

visual cortex and the effects of dark rearing. *Brain Res Mol Brain Res, 78*(1-2), 196-200.

Chow, B. Y., Han, X., Dobry, A. S., Qian, X., Chuong, A. S., Li, M., . . . Boyden, E. S. (2010). High-performance genetically targetable optical neural silencing by light-driven proton pumps. *Nature, 463*(7277), 98-102. doi: nature08652 [pii]

Chowdhury, D., Marco, S., Brooks, I. M., Zandueta, A., Rao, Y., Haucke, V., . . . Perez-Otano, I. (2013). Tyrosine phosphorylation regulates the endocytosis and surface expression of GluN3A-containing NMDA receptors. *J Neurosci, 33*(9), 4151-4164. doi: 10.1523/JNEUROSCI.2721-12.2013

Christie, J. M., Chiu, D. N., & Jahr, C. E. (2011). Ca(2+)-dependent enhancement of release by subthreshold somatic depolarization. *Nat Neurosci, 14*(1), 62-68. doi: 10.1038/nn.2718

Christie, J. M., & Jahr, C. E. (2008). Dendritic NMDA receptors activate axonal calcium channels. *Neuron, 60*(2), 298-307. doi: S0896-6273(08)00771-X [pii]

Christie, J. M., & Jahr, C. E. (2009). Selective expression of ligand-gated ion channels in L5 pyramidal cell axons. *J Neurosci, 29*(37), 11441-11450. doi: 29/37/11441 [pii]

Clark, S. A., Allard, T., Jenkins, W. M., & Merzenich, M. M. (1988). Receptive fields in the body-surface map in adult cortex defined by temporally correlated inputs. *Nature, 332*(6163), 444-445. doi: 10.1038/332444a0 [doi]

Clarke, R. J., & Johnson, J. W. (2006). NMDA receptor NR2 subunit dependence of the slow component of magnesium unblock. *J Neurosci, 26*(21), 5825-5834. doi: 26/21/5825 [pii]

Clopath, C., Busing, L., Vasilaki, E., & Gerstner, W. (2010). Connectivity reflects coding: a model of voltage-based STDP with homeostasis. *Nat Neurosci, 13*(3), 344-352. doi: nn.2479 [pii]

Cochilla, A. J., & Alford, S. (1999). NMDA receptor-mediated control of presynaptic calcium and neurotransmitter release. *J Neurosci, 19*(1), 193-205.

Cooper, L. N., & Bear, M. F. (2012). The BCM theory of synapse modification at 30: interaction of theory with experiment. *Nat Rev Neurosci, 13*(11), 798-810. doi: 10.1038/nrn3353

Corlew, R., Brasier, D. J., Feldman, D. E., & Philpot, B. D. (2008). Presynaptic NMDA receptors: newly appreciated roles in cortical synaptic function and plasticity. *Neuroscientist, 14*(6), 609-625. doi: 14/6/609 [pii]

Corlew, R., Wang, Y., Ghermazien, H., Erisir, A., & Philpot, B. D. (2007). Developmental switch in the contribution of presynaptic and postsynaptic NMDA receptors to long-term depression. *J Neurosci, 27*(37), 9835-9845. doi: 27/37/9835 [pii]

Costa, B. M., Feng, B., Tsintsadze, T. S., Morley, R. M., Irvine, M. W., Tsintsadze, V., . . . Monaghan, D. T. (2009). N-methyl-D-aspartate (NMDA) receptor NR2 subunit selectivity of a series of novel piperazine-2,3-dicarboxylate derivatives: preferential blockade of extrasynaptic NMDA receptors in the rat hippocampal CA3-CA1 synapse. *J Pharmacol Exp Ther, 331*(2), 618-626. doi: jpet.109.156752 [pii]

Couey, J. J., Meredith, R. M., Spijker, S., Poorthuis, R. B., Smit, A. B., Brussaard, A. B., & Mansvelder, H. D. (2007). Distributed network actions by nicotine increase the threshold for spike-timing-dependent plasticity in prefrontal cortex. *Neuron, 54*(1), 73-87. doi: S0896-6273(07)00184-5 [pii]

Cousin, M. A., & Robinson, P. J. (2001). The dephosphins: dephosphorylation by calcineurin triggers synaptic vesicle endocytosis. *Trends Neurosci, 24*(11), 659-665.

Crair, M. C., & Malenka, R. C. (1995). A critical period for long-term potentiation at thalamocortical synapses. *Nature, 375*(6529), 325-328. doi: 10.1038/375325a0 [doi]

Csicsvari, J., Hirase, H., Czurko, A., Mamiya, A., & Buzsaki, G. (1999). Oscillatory coupling of hippocampal pyramidal cells and interneurons in the behaving rat. *Journal of Neuroscience, 19*(1), 274-287.

Cull-Candy, S. G., & Leszkiewicz, D. N. (2004). Role of distinct NMDA receptor subtypes at central synapses. *Sci STKE, 2004*(255), re16. doi: stke.2552004re16 [pii]

Czepita, D., Reid, S. N., & Daw, N. W. (1994). Effect of longer periods of dark rearing on NMDA receptors in cat visual cortex. *J Neurophysiol, 72*(3), 1220-1226.

Dahmen, J. C., Hartley, D. E., & King, A. J. (2008). Stimulus-timing-dependent plasticity of cortical frequency representation. *J Neurosci, 28*(50), 13629-13639. doi: 28/50/13629 [pii]

Dan, Y., & Poo, M. M. (2006). Spike timing-dependent plasticity: from synapse to perception. *Physiol Rev, 86*(3), 1033-1048. doi: 86/3/1033 [pii]

Das, S., Sasaki, Y. F., Rothe, T., Premkumar, L. S., Takasu, M., Crandall, J. E., . . . Nakanishi, N. (1998). Increased NMDA current and spine density in mice lacking the NMDA receptor subunit NR3A. *Nature, 393*(6683), 377-381. doi: 10.1038/30748 [doi]

de Marchena, J., Roberts, A. C., Middlebrooks, P. G., Valakh, V., Yashiro, K., Wilfley, L. R., & Philpot, B. D. (2008). NMDA receptor antagonists reveal age-dependent differences in the properties of visual cortical plasticity. *J Neurophysiol, 100*(4), 1936-1948. doi: 10.1152/jn.90290.2008

Debanne, D., Gahwiler, B. H., & Thompson, S. M. (1998). Long-term synaptic plasticity between pairs of individual CA3 pyramidal cells in rat hippocampal slice cultures. *J Physiol, 507 (Pt 1)*, 237-247.

DeBiasi, S., Minelli, A., Melone, M., & Conti, F. (1996). Presynaptic NMDA receptors in the neocortex are both auto- and heteroreceptors. *Neuroreport, 7*(15-17), 2773-2776.

Desai, N. S., Cudmore, R. H., Nelson, S. B., & Turrigiano, G. G. (2002). Critical periods for experience-dependent synaptic scaling in visual cortex. *Nat Neurosci, 5*(8), 783-789. doi: 10.1038/nn878

Deshmukh, S., Onozuka, K., Bender, K. J., Bender, V. A., Lutz, B., Mackie, K., & Feldman, D. E. (2007). Postnatal development of cannabinoid receptor type 1 expression in rodent somatosensory cortex. *Neuroscience, 145*(1), 279-287. doi: S0306-4522(06)01642-3 [pii]

Diamond, M. E., Huang, W., & Ebner, F. F. (1994). Laminar comparison of somatosensory cortical plasticity. *Science, 265*(5180), 1885-1888.

Dittman, J. S., & Regehr, W. G. (1998). Calcium dependence and recovery kinetics of presynaptic depression at the climbing fiber to Purkinje cell synapse. *J Neurosci, 18*(16), 6147-6162.

Drew, P. J., & Feldman, D. E. (2009). Intrinsic signal imaging of deprivation-induced contraction of whisker representations in rat somatosensory cortex. *Cereb Cortex, 19*(2), 331-348. doi: bhn085 [pii]

Dudek, S. M., & Bear, M. F. (1992). Homosynaptic long-term depression in area CA1 of hippocampus and effects of N-methyl-D-aspartate receptor blockade. *Proc Natl Acad Sci U S A, 89*(10), 4363-4367.

Dudek, S. M., & Bear, M. F. (1993). Bidirectional long-term modification of synaptic effectiveness in the adult and immature hippocampus. *J Neurosci, 13*(7), 2910-2918.

Duguid, I. C. (2013). Presynaptic NMDA receptors: are they dendritic receptors in disguise? *Brain Res Bull, 93*, 4-9. doi: 10.1016/j.brainresbull.2012.12.004

Egger, V., Feldmeyer, D., & Sakmann, B. (1999). Coincidence detection and changes of synaptic efficacy in spiny stellate neurons in rat barrel cortex. *Nat Neurosci, 2*(12), 1098-1105. doi: 10.1038/16026 [doi]

Erreger, K., Dravid, S. M., Banke, T. G., Wyllie, D. J., & Traynelis, S. F. (2005). Subunit-specific gating controls rat NR1/NR2A and NR1/NR2B NMDA channel kinetics and synaptic signalling profiles. *J Physiol, 563*(Pt 2), 345-358. doi: 10.1113/jphysiol.2004.080028

Espinosa, J. S., & Stryker, M. P. (2012). Development and plasticity of the primary visual cortex. *Neuron, 75*(2), 230-249. doi: 10.1016/j.neuron.2012.06.009

Fagiolini, M., & Hensch, T. K. (2000). Inhibitory threshold for critical-period activation in primary visual cortex. *Nature, 404*(6774), 183-186. doi: 10.1038/35004582

Fagiolini, M., Pizzorusso, T., Berardi, N., Domenici, L., & Maffei, L. (1994). Functional postnatal development of the rat primary visual cortex and the role of visual experience: dark rearing and monocular deprivation. *Vision Res, 34*(6), 709-720.

Farb, C. R., Aoki, C., & Ledoux, J. E. (1995). Differential localization of NMDA and AMPA receptor subunits in the lateral and basal nuclei of the amygdala: a light and electron microscopic study. *J Comp Neurol, 362*(1), 86-108. doi: 10.1002/cne.903620106

Fatt, P., & Katz, B. (1952). Spontaneous subthreshold activity at motor nerve endings. *J Physiol, 117*(1), 109-128.

Featherstone, D. E., & Shippy, S. A. (2008). Regulation of synaptic transmission by ambient extracellular glutamate. *Neuroscientist, 14*(2), 171-181. doi: 10.1177/1073858407308518

Feldman, D. E. (2000). Timing-based LTP and LTD at vertical inputs to layer II/III pyramidal cells in rat barrel cortex. *Neuron, 27*(1), 45-56. doi: S0896-6273(00)00008-8 [pii]

Feldman, D. E. (2009). Synaptic mechanisms for plasticity in neocortex. *Annu Rev Neurosci, 32*, 33-55. doi: 10.1146/annurev.neuro.051508.135516 [doi]

Feldman, D. E. (2012). The spike-timing dependence of plasticity. *Neuron, 75*(4), 556-571. doi: 10.1016/j.neuron.2012.08.001

Ferraro, T. N., & Hare, T. A. (1985). Free and conjugated amino acids in human CSF: influence of age and sex. *Brain Res, 338*(1), 53-60.

Fiacco, T. A., Agulhon, C., Taves, S. R., Petravicz, J., Casper, K. B., Dong, X., . . . McCarthy, K. D. (2007). Selective stimulation of astrocyte calcium in situ does not affect neuronal excitatory synaptic activity. *Neuron, 54*(4), 611-626. doi: 10.1016/j.neuron.2007.04.032

Flint, A. C., Maisch, U. S., Weishaupt, J. H., Kriegstein, A. R., & Monyer, H. (1997). NR2A subunit expression shortens NMDA receptor synaptic currents in developing neocortex. *J Neurosci, 17*(7), 2469-2476.

Fox, K. (2002). Anatomical pathways and molecular mechanisms for plasticity in the barrel cortex. *Neuroscience, 111*(4), 799-814. doi: S0306452202000271 [pii]

Fox, K., & Wong, R. O. (2005). A comparison of experience-dependent plasticity in the visual and somatosensory systems. *Neuron, 48*(3), 465-477. doi: S0896-6273(05)00877-9 [pii]

Frey, M. C., Sprengel, R., & Nevian, T. (2009). Activity pattern-dependent long-term potentiation in neocortex and hippocampus of GluA1 (GluR-A) subunit-deficient mice. *J Neurosci, 29*(17), 5587-5596. doi: 29/17/5587 [pii]

Froemke, R. C., & Dan, Y. (2002). Spike-timing-dependent synaptic modification induced by natural spike trains. *Nature, 416*(6879), 433-438. doi: 10.1038/416433a [doi]

Froemke, R. C., Merzenich, M. M., & Schreiner, C. E. (2007). A synaptic memory trace for cortical receptive field plasticity. *Nature, 450*(7168), 425-429. doi: nature06289 [pii]

Froemke, R. C., Poo, M. M., & Dan, Y. (2005). Spike-timing-dependent synaptic plasticity depends on dendritic location. *Nature, 434*(7030), 221-225. doi: nature03366 [pii]

Froemke, R. C., Tsay, I. A., Raad, M., Long, J. D., & Dan, Y. (2006). Contribution of individual spikes in burst-induced long-term synaptic modification. *J Neurophysiol, 95*(3), 1620-1629. doi: 00910.2005 [pii]

Fu, Y. X., Djupsund, K., Gao, H., Hayden, B., Shen, K., & Dan, Y. (2002). Temporal specificity in the cortical plasticity of visual space representation. *Science, 296*(5575), 1999-2003. doi: 10.1126/science.1070521 [doi]

Galindo-Leon, E. E., Lin, F. G., & Liu, R. C. (2009). Inhibitory plasticity in a lateral band improves cortical detection of natural vocalizations. *Neuron, 62*(5), 705-716. doi: S0896-6273(09)00352-3 [pii]

Gerkin, R. C., Lau, P. M., Nauen, D. W., Wang, Y. T., & Bi, G. Q. (2007). Modular competition driven by NMDA receptor subtypes in spike-timing-dependent plasticity. *J Neurophysiol, 97*(4), 2851-2862. doi: 00860.2006 [pii]

Gerstner, W., Kempter, R., van Hemmen, J. L., & Wagner, H. (1996). A neuronal learning rule for sub-millisecond temporal coding. *Nature, 383*(6595), 76-81. doi: 10.1038/383076a0 [doi]

Glazewski, S., & Fox, K. (1996). Time course of experience-dependent synaptic potentiation and depression in barrel cortex of adolescent rats. *J Neurophysiol, 75*(4), 1714-1729.

Glitsch, M., & Marty, A. (1999). Presynaptic effects of NMDA in cerebellar Purkinje cells and interneurons. *J Neurosci, 19*(2), 511-519.

Glitsch, M. D. (2008). Spontaneous neurotransmitter release and Ca2+--how spontaneous is spontaneous neurotransmitter release? *Cell Calcium, 43*(1), 9-15. doi: 10.1016/j.ceca.2007.02.008

Goel, A., Jiang, B., Xu, L. W., Song, L., Kirkwood, A., & Lee, H. K. (2006). Cross-modal regulation of synaptic AMPA receptors in primary sensory cortices by visual experience. *Nat Neurosci, 9*(8), 1001-1003. doi: 10.1038/nn1725

Goutagny, R., Jackson, J., & Williams, S. (2009). Self-generated theta oscillations in the hippocampus. *Nature Neuroscience, 12*(12), 1491-1493. doi: Doi 10.1038/Nn.2440

Gray, J. A., Shi, Y., Usui, H., During, M. J., Sakimura, K., & Nicoll, R. A. (2011). Distinct Modes of AMPA Receptor Suppression at Developing Synapses by GluN2A and GluN2B: Single-Cell NMDA Receptor Subunit Deletion In Vivo. *Neuron, 71*(6), 1085-1101. doi: DOI 10.1016/j.neuron.2011.08.007

Gunaydin, L. A., Yizhar, O., Berndt, A., Sohal, V. S., Deisseroth, K., & Hegemann, P. (2010). Ultrafast optogenetic control. *Nat Neurosci*. doi: nn.2495 [pii]

Guo, Y., Huang, S., de Pasquale, R., McGehrin, K., Lee, H. K., Zhao, K., & Kirkwood, A. (2012). Dark exposure extends the integration window for spike-timing-dependent plasticity. *J Neurosci, 32*(43), 15027-15035. doi: 10.1523/JNEUROSCI.2545-12.2012

Haas, J. S., Nowotny, T., & Abarbanel, H. D. (2006). Spike-timing-dependent plasticity of inhibitory synapses in the entorhinal cortex. *J Neurophysiol, 96*(6), 3305-3313. doi: 00551.2006 [pii]

Hannan, A. J., Blakemore, C., Katsnelson, A., Vitalis, T., Huber, K. M., Bear, M., . . . Kind, P. C. (2001). PLC-beta1, activated via mGluRs, mediates activity-

dependent differentiation in cerebral cortex. *Nat Neurosci, 4*(3), 282-288. doi: 10.1038/85132 [doi]

Hannan, A. J., Kind, P. C., & Blakemore, C. (1998). Phospholipase C-beta1 expression correlates with neuronal differentiation and synaptic plasticity in rat somatosensory cortex. *Neuropharmacology, 37*(4-5), 593-605.

Hardingham, N., Wright, N., Dachtler, J., & Fox, K. (2008). Sensory deprivation unmasks a PKA-dependent synaptic plasticity mechanism that operates in parallel with CaMKII. *Neuron, 60*(5), 861-874. doi: S0896-6273(08)00891-X [pii]

Hatton, C. J., & Paoletti, P. (2005). Modulation of triheteromeric NMDA receptors by N-terminal domain ligands. *Neuron, 46*(2), 261-274. doi: S0896-6273(05)00200-X [pii]

Heifets, B. D., & Castillo, P. E. (2009). Endocannabinoid signaling and long-term synaptic plasticity. *Annu Rev Physiol, 71*, 283-306. doi: 10.1146/annurev.physiol.010908.163149

Hensch, T. K. (2005a). Critical period mechanisms in developing visual cortex. *Curr Top Dev Biol, 69*, 215-237. doi: S0070-2153(05)69008-4 [pii]

Hensch, T. K. (2005b). Critical period plasticity in local cortical circuits. *Nat Rev Neurosci, 6*(11), 877-888. doi: nrn1787 [pii]

Henson, M. A., Larsen, R. S., Lawson, S. N., Perez-Otano, I., Nakanishi, N., Lipton, S. A., & Philpot, B. D. (2012). Genetic deletion of NR3A accelerates glutamatergic synapse maturation. *PLoS One, 7*(8), e42327. doi: 10.1371/journal.pone.0042327

Henson, M. A., Roberts, A. C., Perez-Otano, I., & Philpot, B. D. (2010). Influence of the NR3A subunit on NMDA receptor functions. *Prog Neurobiol, 91*(1), 23-37. doi: S0301-0082(10)00015-8 [pii]

Herkert, M., Rottger, S., & Becker, C. M. (1998). The NMDA receptor subunit NR2B of neonatal rat brain: complex formation and enrichment in axonal growth cones. *Eur J Neurosci, 10*(5), 1553-1562.

Herman, M. A., & Jahr, C. E. (2007). Extracellular glutamate concentration in hippocampal slice. *J Neurosci, 27*(36), 9736-9741. doi: 10.1523/JNEUROSCI.3009-07.2007

Hestrin, S. (1992). Developmental Regulation of Nmda Receptor-Mediated Synaptic Currents at a Central Synapse. *Nature, 357*(6380), 686-689. doi: Doi 10.1038/357686a0

Hirai, H., Kirsch, J., Laube, B., Betz, H., & Kuhse, J. (1996). The glycine binding site of the N-methyl-D-aspartate receptor subunit NR1: identification of

novel determinants of co-agonist potentiation in the extracellular M3-M4 loop region. *Proc Natl Acad Sci U S A, 93*(12), 6031-6036.

Hoffman, D. A., & Johnston, D. (1998). Downregulation of transient K+ channels in dendrites of hippocampal CA1 pyramidal neurons by activation of PKA and PKC. *J Neurosci, 18*(10), 3521-3528.

Hoffman, D. A., & Johnston, D. (1999). Neuromodulation of dendritic action potentials. *J Neurophysiol, 81*(1), 408-411.

Hoffman, D. A., Magee, J. C., Colbert, C. M., & Johnston, D. (1997). K+ channel regulation of signal propagation in dendrites of hippocampal pyramidal neurons. *Nature, 387*(6636), 869-875. doi: 10.1038/43119 [doi]

Hoffman, D. A., Sprengel, R., & Sakmann, B. (2002). Molecular dissection of hippocampal theta-burst pairing potentiation. *Proceedings of the National Academy of Sciences of the United States of America, 99*(11), 7740-7745. doi: DOI 10.1073/pnas.092157999

Holmgren, C. D., & Zilberter, Y. (2001). Coincident spiking activity induces long-term changes in inhibition of neocortical pyramidal cells. *J Neurosci, 21*(20), 8270-8277. doi: 21/20/8270 [pii]

Huang, Y. H., Ishikawa, M., Lee, B. R., Nakanishi, N., Schluter, O. M., & Dong, Y. (2011). Searching for presynaptic NMDA receptors in the nucleus accumbens. *J Neurosci, 31*(50), 18453-18463. doi: 10.1523/JNEUROSCI.3824-11.2011

Hubel, D. H., & Wiesel, T. N. (1965). Binocular interaction in striate cortex of kittens reared with artificial squint. *J Neurophysiol, 28*(6), 1041-1059.

Husi, H., Ward, M. A., Choudhary, J. S., Blackstock, W. P., & Grant, S. G. (2000). Proteomic analysis of NMDA receptor-adhesion protein signaling complexes. *Nat Neurosci, 3*(7), 661-669. doi: 10.1038/76615

Ikeda, K., Araki, K., Takayama, C., Inoue, Y., Yagi, T., Aizawa, S., & Mishina, M. (1995). Reduced spontaneous activity of mice defective in the epsilon 4 subunit of the NMDA receptor channel. *Brain Res Mol Brain Res, 33*(1), 61-71. doi: 0169328X95001074 [pii]

Izhikevich, E. M., & Desai, N. S. (2003). Relating STDP to BCM. *Neural Comput, 15*(7), 1511-1523. doi: 10.1162/089976603321891783

Jacob, A. L., Jordan, B. A., & Weinberg, R. J. (2010). Organization of amyloid-beta protein precursor intracellular domain-associated protein-1 in the rat brain. *J Comp Neurol, 518*(16), 3221-3236. doi: 10.1002/cne.22394 [doi]

Jacob, V., Brasier, D. J., Erchova, I., Feldman, D., & Shulz, D. E. (2007). Spike timing-dependent synaptic depression in the in vivo barrel cortex of the rat. *J Neurosci, 27*(6), 1271-1284. doi: 27/6/1271 [pii]

Johnson, J. W., & Ascher, P. (1987). Glycine potentiates the NMDA response in cultured mouse brain neurons. *Nature, 325*(6104), 529-531. doi: 10.1038/325529a0

Jourdain, P., Bergersen, L. H., Bhaukaurally, K., Bezzi, P., Santello, M., Domercq, M., . . . Volterra, A. (2007). Glutamate exocytosis from astrocytes controls synaptic strength. *Nat Neurosci, 10*(3), 331-339. doi: 10.1038/nn1849

Kampa, B. M., & Stuart, G. J. (2006). Calcium spikes in basal dendrites of layer 5 pyramidal neurons during action potential bursts. *J Neurosci, 26*(28), 7424-7432. doi: 26/28/7424 [pii]

Kanold, P. O., & Shatz, C. J. (2006). Subplate neurons regulate maturation of cortical inhibition and outcome of ocular dominance plasticity. *Neuron, 51*(5), 627-638. doi: S0896-6273(06)00548-4 [pii]

Karavanova, I., Vasudevan, K., Cheng, J., & Buonanno, A. (2007). Novel regional and developmental NMDA receptor expression patterns uncovered in NR2C subunit-beta-galactosidase knock-in mice. *Mol Cell Neurosci, 34*(3), 468-480. doi: S1044-7431(06)00277-6 [pii]

Karmarkar, U. R., & Buonomano, D. V. (2002). A model of spike-timing dependent plasticity: one or two coincidence detectors? *J Neurophysiol, 88*(1), 507-513.

Kemp, J. A., & McKernan, R. M. (2002). NMDA receptor pathways as drug targets. *Nat Neurosci, 5 Suppl*, 1039-1042. doi: 10.1038/nn936 [doi]

Kirkwood, A., Rioult, M. C., & Bear, M. F. (1996). Experience-dependent modification of synaptic plasticity in visual cortex. *Nature, 381*(6582), 526-528. doi: 10.1038/381526a0 [doi]

Kirkwood, A., Rozas, C., Kirkwood, J., Perez, F., & Bear, M. F. (1999). Modulation of long-term synaptic depression in visual cortex by acetylcholine and norepinephrine. *J Neurosci, 19*(5), 1599-1609.

Kleckner, N. W., & Dingledine, R. (1988). Requirement for glycine in activation of NMDA-receptors expressed in Xenopus oocytes. *Science, 241*(4867), 835-837.

Koester, H. J., & Sakmann, B. (1998). Calcium dynamics in single spines during coincident pre- and postsynaptic activity depend on relative timing of back-

propagating action potentials and subthreshold excitatory postsynaptic potentials. *Proc Natl Acad Sci U S A, 95*(16), 9596-9601.

Komai, S., Licznerski, P., Cetin, A., Waters, J., Denk, W., Brecht, M., & Osten, P. (2006). Postsynaptic excitability is necessary for strengthening of cortical sensory responses during experience-dependent development. *Nat Neurosci, 9*(9), 1125-1133. doi: nn1752 [pii]

Kudoh, M., & Shibuki, K. (1994). Long-term potentiation in the auditory cortex of adult rats. *Neurosci Lett, 171*(1-2), 21-23. doi: 0304-3940(94)90594-0 [pii]

Kudoh, M., & Shibuki, K. (1996). Long-term potentiation of supragranular pyramidal outputs in the rat auditory cortex. *Exp Brain Res, 110*(1), 21-27.

Kudoh, M., & Shibuki, K. (1997). Importance of polysynaptic inputs and horizontal connectivity in the generation of tetanus-induced long-term potentiation in the rat auditory cortex. *J Neurosci, 17*(24), 9458-9465.

Kuner, T., & Schoepfer, R. (1996). Multiple structural elements determine subunit specificity of Mg2+ block in NMDA receptor channels. *J Neurosci, 16*(11), 3549-3558.

Kunz, P. A., Roberts, A. C., & Philpot, B. D. (2013). Presynaptic NMDA receptor mechanisms for enhancing spontaneous neurotransmitter release. *J Neurosci, 33*(18), 7762-7769. doi: 10.1523/JNEUROSCI.2482-12.2013

Kvist, T., Greenwood, J. R., Hansen, K. B., Traynelis, S. F., & Brauner-Osborne, H. (2013). Structure-based discovery of antagonists for GluN3-containing N-methyl-d-aspartate receptors. *Neuropharmacology, 75C*, 324-336. doi: 10.1016/j.neuropharm.2013.08.003

Lambo, M. E., & Turrigiano, G. G. (2013). Synaptic and intrinsic homeostatic mechanisms cooperate to increase L2/3 pyramidal neuron excitability during a late phase of critical period plasticity. *J Neurosci, 33*(20), 8810-8819. doi: 10.1523/JNEUROSCI.4502-12.2013

Larsen, R. S., Corlew, R. J., Henson, M. A., Roberts, A. C., Mishina, M., Watanabe, M., . . . Philpot, B. D. (2011). NR3A-containing NMDARs promote neurotransmitter release and spike timing-dependent plasticity. *Nat Neurosci, 14*(3), 338-344. doi: 10.1038/nn.2750

Larsen, R. S., Rao, D., Manis, P. B., & Philpot, B. D. (2010). STDP in the Developing Sensory Neocortex. *Front Synaptic Neurosci, 2*, 9. doi: 10.3389/fnsyn.2010.00009

Lau, C. G., & Zukin, R. S. (2007). NMDA receptor trafficking in synaptic plasticity and neuropsychiatric disorders. *Nat Rev Neurosci, 8*(6), 413-426. doi: 10.1038/nrn2153

Laube, B., Hirai, H., Sturgess, M., Betz, H., & Kuhse, J. (1997). Molecular determinants of agonist discrimination by NMDA receptor subunits: analysis of the glutamate binding site on the NR2B subunit. *Neuron, 18*(3), 493-503. doi: S0896-6273(00)81249-0 [pii]

Laurie, D. J., & Seeburg, P. H. (1994). Ligand affinities at recombinant N-methyl-D-aspartate receptors depend on subunit composition. *Eur J Pharmacol, 268*(3), 335-345.

Lefort, S., Tomm, C., Floyd Sarria, J. C., & Petersen, C. C. (2009). The excitatory neuronal network of the C2 barrel column in mouse primary somatosensory cortex. *Neuron, 61*(2), 301-316. doi: 10.1016/j.neuron.2008.12.020

Letzkus, J. J., Kampa, B. M., & Stuart, G. J. (2006). Learning rules for spike timing-dependent plasticity depend on dendritic synapse location. *J Neurosci, 26*(41), 10420-10429. doi: 26/41/10420 [pii]

Levy, W. B., & Steward, O. (1983). Temporal contiguity requirements for long-term associative potentiation/depression in the hippocampus. *Neuroscience, 8*(4), 791-797. doi: 0306-4522(83)90010-6 [pii]

Li, L., Bender, K. J., Drew, P. J., Jadhav, S. P., Sylwestrak, E., & Feldman, D. E. (2009). Endocannabinoid signaling is required for development and critical period plasticity of the whisker map in somatosensory cortex. *Neuron, 64*(4), 537-549. doi: S0896-6273(09)00806-X [pii]

Li, Y. H., & Han, T. Z. (2007). Glycine binding sites of presynaptic NMDA receptors may tonically regulate glutamate release in the rat visual cortex. *J Neurophysiol, 97*(1), 817-823. doi: 00980.2006 [pii]

Li, Y. H., Han, T. Z., & Meng, K. (2008). Tonic facilitation of glutamate release by glycine binding sites on presynaptic NR2B-containing NMDA autoreceptors in the rat visual cortex. *Neurosci Lett, 432*(3), 212-216. doi: S0304-3940(07)01296-7 [pii]

Li, Y. H., Wang, J., & Zhang, G. (2009). Presynaptic NR2B-containing NMDA autoreceptors mediate gluta-matergic synaptic transmission in the rat visual cortex. *Curr Neurovasc Res, 6*(2), 104-109.

Lin, H., Vicini, S., Hsu, F. C., Doshi, S., Takano, H., Coulter, D. A., & Lynch, D. R. (2010). Axonal {alpha}7 nicotinic ACh receptors modulate presynaptic NMDA receptor expression and structural plasticity of glutamatergic

presynaptic boutons. *Proc Natl Acad Sci U S A, 107*(38), 16661-16666. doi: 1007397107 [pii]

Lin, Y. W., Min, M. Y., Chiu, T. H., & Yang, H. W. (2003). Enhancement of associative long-term potentiation by activation of beta-adrenergic receptors at CA1 synapses in rat hippocampal slices. *J Neurosci, 23*(10), 4173-4181. doi: 23/10/4173 [pii]

Liu, X. B., Murray, K. D., & Jones, E. G. (2004). Switching of NMDA receptor 2A and 2B subunits at thalamic and cortical synapses during early postnatal development. *J Neurosci, 24*(40), 8885-8895. doi: 24/40/8885 [pii]

Lu, J. T., Li, C. Y., Zhao, J. P., Poo, M. M., & Zhang, X. H. (2007). Spike-timing-dependent plasticity of neocortical excitatory synapses on inhibitory interneurons depends on target cell type. *J Neurosci, 27*(36), 9711-9720. doi: 27/36/9711 [pii]

Lubke, J., Egger, V., Sakmann, B., & Feldmeyer, D. (2000). Columnar organization of dendrites and axons of single and synaptically coupled excitatory spiny neurons in layer 4 of the rat barrel cortex. *J Neurosci, 20*(14), 5300-5311.

Ma, O. K., & Sucher, N. J. (2004). Molecular interaction of NMDA receptor subunit NR3A with protein phosphatase 2A. *Neuroreport, 15*(9), 1447-1450.

Madisen, L., Mao, T., Koch, H., Zhuo, J. M., Berenyi, A., Fujisawa, S., . . . Zeng, H. (2012). A toolbox of Cre-dependent optogenetic transgenic mice for light-induced activation and silencing. *Nat Neurosci, 15*(5), 793-802. doi: 10.1038/nn.3078

Madisen, L., Zwingman, T. A., Sunkin, S. M., Oh, S. W., Zariwala, H. A., Gu, H., . . . Zeng, H. (2010). A robust and high-throughput Cre reporting and characterization system for the whole mouse brain. *Nat Neurosci, 13*(1), 133-140. doi: 10.1038/nn.2467

Maffei, A., & Turrigiano, G. G. (2008). Multiple modes of network homeostasis in visual cortical layer 2/3. *J Neurosci, 28*(17), 4377-4384. doi: 10.1523/JNEUROSCI.5298-07.2008

Magee, J. C., & Johnston, D. (1997). A synaptically controlled, associative signal for Hebbian plasticity in hippocampal neurons. *Science, 275*(5297), 209-213.

Malenka, R. C., & Bear, M. F. (2004). LTP and LTD: an embarrassment of riches. *Neuron, 44*(1), 5-21. doi: 10.1016/j.neuron.2004.09.012 [doi]

Mameli, M., Carta, M., Partridge, L. D., & Valenzuela, C. F. (2005). Neurosteroid-induced plasticity of immature synapses via retrograde modulation of presynaptic NMDA receptors. *J Neurosci, 25*(9), 2285-2294. doi: 25/9/2285 [pii]

Markram, H., Lubke, J., Frotscher, M., & Sakmann, B. (1997). Regulation of synaptic efficacy by coincidence of postsynaptic APs and EPSPs. *Science, 275*(5297), 213-215.

Mayer, M. L., & Westbrook, G. L. (1987). Permeation and block of N-methyl-D-aspartic acid receptor channels by divalent cations in mouse cultured central neurones. *J Physiol, 394*, 501-527.

Mayford, M., Bach, M. E., Huang, Y. Y., Wang, L., Hawkins, R. D., & Kandel, E. R. (1996). Control of memory formation through regulated expression of a CaMKII transgene. *Science, 274*(5293), 1678-1683.

McGuinness, L., Taylor, C., Taylor, R. D., Yau, C., Langenhan, T., Hart, M. L., . . . Emptage, N. J. (2010). Presynaptic NMDARs in the Hippocampus Facilitate Transmitter Release at Theta Frequency. *Neuron, 68*(6), 1109-1127. doi: S0896-6273(10)00939-6 [pii]

McIlhinney, R. A., Molnar, E., Atack, J. R., & Whiting, P. J. (1996). Cell surface expression of the human N-methyl-D-aspartate receptor subunit 1a requires the co-expression of the NR2A subunit in transfected cells. *Neuroscience, 70*(4), 989-997.

McKinney, R. A., Capogna, M., Durr, R., Gahwiler, B. H., & Thompson, S. M. (1999). Miniature synaptic events maintain dendritic spines via AMPA receptor activation. *Nat Neurosci, 2*(1), 44-49. doi: 10.1038/4548 [doi]

Meliza, C. D., & Dan, Y. (2006). Receptive-field modification in rat visual cortex induced by paired visual stimulation and single-cell spiking. *Neuron, 49*(2), 183-189. doi: S0896-6273(05)01057-3 [pii]

Meredith, R. M., Floyer-Lea, A. M., & Paulsen, O. (2003). Maturation of long-term potentiation induction rules in rodent hippocampus: role of GABAergic inhibition. *J Neurosci, 23*(35), 11142-11146. doi: 23/35/11142 [pii]

Min, R., & Nevian, T. (2012). Astrocyte signaling controls spike timing-dependent depression at neocortical synapses. *Nat Neurosci, 15*(5), 746-753. doi: 10.1038/nn.3075

Mohamad, O., Song, M. K., Wei, L., & Yu, S. P. (2013). Regulatory roles of the NMDA receptor GluN3A subunit in locomotion, pain perception and

cognitive functions in adult mice. *Journal of Physiology-London, 591*(1), 149-168. doi: DOI 10.1113/jphysiol.2012.239251

Monyer, H., Burnashev, N., Laurie, D. J., Sakmann, B., & Seeburg, P. H. (1994). Developmental and regional expression in the rat brain and functional properties of four NMDA receptors. *Neuron, 12*(3), 529-540.

Morales, B., Choi, S. Y., & Kirkwood, A. (2002). Dark rearing alters the development of GABAergic transmission in visual cortex. *J Neurosci, 22*(18), 8084-8090.

Morley, R. M., Tse, H. W., Feng, B., Miller, J. C., Monaghan, D. T., & Jane, D. E. (2005). Synthesis and pharmacology of N1-substituted piperazine-2,3-dicarboxylic acid derivatives acting as NMDA receptor antagonists. *J Med Chem, 48*(7), 2627-2637. doi: 10.1021/jm0492498 [doi]

Mullasseril, P., Hansen, K. B., Vance, K. M., Ogden, K. K., Yuan, H., Kurtkaya, N. L., . . . Traynelis, S. F. (2010). A subunit-selective potentiator of NR2C- and NR2D-containing NMDA receptors. *Nat Commun, 1*, 90. doi: 10.1038/ncomms1085

Nataraj, K., & Turrigiano, G. (2011). Regional and temporal specificity of intrinsic plasticity mechanisms in rodent primary visual cortex. *J Neurosci, 31*(49), 17932-17940. doi: 10.1523/JNEUROSCI.4455-11.2011

Navarrete, M., & Araque, A. (2010). Endocannabinoids potentiate synaptic transmission through stimulation of astrocytes. *Neuron, 68*(1), 113-126. doi: 10.1016/j.neuron.2010.08.043

Nelson, S. B., Sjostrom, P. J., & Turrigiano, G. G. (2002). Rate and timing in cortical synaptic plasticity. *Philos Trans R Soc Lond B Biol Sci, 357*(1428), 1851-1857. doi: 10.1098/rstb.2002.1162

Nevian, T., & Sakmann, B. (2006). Spine Ca2+ signaling in spike-timing-dependent plasticity. *J Neurosci, 26*(43), 11001-11013. doi: 26/43/11001 [pii]

Nimchinsky, E. A., Yasuda, R., Oertner, T. G., & Svoboda, K. (2004). The number of glutamate receptors opened by synaptic stimulation in single hippocampal spines. *J Neurosci, 24*(8), 2054-2064. doi: 10.1523/JNEUROSCI.5066-03.2004

Nishiyama, M., Hong, K., Mikoshiba, K., Poo, M. M., & Kato, K. (2000). Calcium stores regulate the polarity and input specificity of synaptic modification. *Nature, 408*(6812), 584-588. doi: 10.1038/35046067 [doi]

Paoletti, P., Bellone, C., & Zhou, Q. (2013). NMDA receptor subunit diversity: impact on receptor properties, synaptic plasticity and disease. *Nature Reviews Neuroscience, 14*(6), 383-400. doi: Doi 10.1038/Nrn3504

Paoletti, P., & Neyton, J. (2007). NMDA receptor subunits: function and pharmacology. *Curr Opin Pharmacol, 7*(1), 39-47. doi: 10.1016/j.coph.2006.08.011

Papouin, T., Ladepeche, L., Ruel, J., Sacchi, S., Labasque, M., Hanini, M., . . . Oliet, S. H. (2012). Synaptic and extrasynaptic NMDA receptors are gated by different endogenous coagonists. *Cell, 150*(3), 633-646. doi: 10.1016/j.cell.2012.06.029

Pellicciari, M. C., Miniussi, C., Rossini, P. M., & De Gennaro, L. (2009). Increased cortical plasticity in the elderly: changes in the somatosensory cortex after paired associative stimulation. *Neuroscience, 163*(1), 266-276. doi: S0306-4522(09)01000-8 [pii]

Perez-Otano, I., Lujan, R., Tavalin, S. J., Plomann, M., Modregger, J., Liu, X. B., . . . Ehlers, M. D. (2006). Endocytosis and synaptic removal of NR3A-containing NMDA receptors by PACSIN1/syndapin1. *Nat Neurosci, 9*(5), 611-621. doi: nn1680 [pii]

Pérez-Otaño, I., Schulteis, C. T., Contractor, A., Lipton, S. A., Trimmer, J. S., Sucher, N. J., & Heinemann, S. F. (2001). Assembly with the NR1 subunit is required for surface expression of NR3A-containing NMDA receptors. *J Neurosci, 21*(4), 1228-1237. doi: 21/4/1228 [pii]

Philpot, B. D., Sekhar, A. K., Shouval, H. Z., & Bear, M. F. (2001). Visual experience and deprivation bidirectionally modify the composition and function of NMDA receptors in visual cortex. *Neuron, 29*(1), 157-169. doi: S0896-6273(01)00187-8 [pii]

Piña-Créspo, J. C., Talantova, M., Micu, I., States, B., Chen, H. S., Tu, S., . . . Lipton, S. A. (2010). Excitatory glycine responses of CNS myelin mediated by NR1/NR3 "NMDA" receptor subunits. *J Neurosci, 30*(34), 11501-11505. doi: 30/34/11501 [pii]

Qu, Y., Arckens, L., Vandenbussche, E., Geeraerts, S., & Vandesande, F. (1998). Simultaneous determination of total and extracellular concentrations of the amino acid neurotransmitters in cat visual cortex by microbore liquid chromatography and electrochemical detection. *J Chromatogr A, 798*(1-2), 19-26.

Quinlan, E. M., Olstein, D. H., & Bear, M. F. (1999). Bidirectional, experience-dependent regulation of N-methyl-D-aspartate receptor subunit

composition in the rat visual cortex during postnatal development. *Proc Natl Acad Sci U S A, 96*(22), 12876-12880.

Quinlan, E. M., Philpot, B. D., Huganir, R. L., & Bear, M. F. (1999). Rapid, experience-dependent expression of synaptic NMDA receptors in visual cortex in vivo. *Nat Neurosci, 2*(4), 352-357. doi: 10.1038/7263

Rauner, C., & Kohr, G. (2011). Triheteromeric NR1/NR2A/NR2B Receptors Constitute the Major N-Methyl-D-aspartate Receptor Population in Adult Hippocampal Synapses. *Journal of Biological Chemistry, 286*(9), 7558-7566. doi: DOI 10.1074/jbc.M110.182600

Recanzone, G. H., Schreiner, C. E., & Merzenich, M. M. (1993). Plasticity in the frequency representation of primary auditory cortex following discrimination training in adult owl monkeys. *J Neurosci, 13*(1), 87-103.

Ribrault, C., Sekimoto, K., & Triller, A. (2011). From the stochasticity of molecular processes to the variability of synaptic transmission. *Nat Rev Neurosci, 12*(7), 375-387. doi: 10.1038/nrn3025

Roberts, A. C., Diez-Garcia, J., Rodriguiz, R. M., Lopez, I. P., Lujan, R., Martinez-Turrillas, R., . . . Perez-Otano, I. (2009). Downregulation of NR3A-containing NMDARs is required for synapse maturation and memory consolidation. *Neuron, 63*(3), 342-356. doi: S0896-6273(09)00471-1 [pii]

Rodríguez-Moreno, A., Banerjee, A., & Paulsen, O. (2010). Presynaptic NMDA receptors and spike timing-dependent long-term depression at cortical synapses. *Frontiers in Synaptic Neuroscience, 2*, 12. doi: 10.3389/fnsyn.2010.00018

Rodriguez-Moreno, A., Gonzalez-Rueda, A., Banerjee, A., Upton, A. L., Craig, M. T., & Paulsen, O. (2013). Presynaptic self-depression at developing neocortical synapses. *Neuron, 77*(1), 35-42. doi: 10.1016/j.neuron.2012.10.035

Rodriguez-Moreno, A., Kohl, M. M., Reeve, J. E., Eaton, T. R., Collins, H. A., Anderson, H. L., & Paulsen, O. (2011). Presynaptic induction and expression of timing-dependent long-term depression demonstrated by compartment-specific photorelease of a use-dependent NMDA receptor antagonist. *J Neurosci, 31*(23), 8564-8569. doi: 10.1523/JNEUROSCI.0274-11.2011

Rodriguez-Moreno, A., & Paulsen, O. (2008). Spike timing-dependent long-term depression requires presynaptic NMDA receptors. *Nat Neurosci, 11*(7), 744-745. doi: nn.2125 [pii]

Rossi, B., Ogden, D., Llano, I., Tan, Y. P., Marty, A., & Collin, T. (2012). Current and calcium responses to local activation of axonal NMDA receptors in developing cerebellar molecular layer interneurons. *PLoS One, 7*(6), e39983. doi: 10.1371/journal.pone.0039983

Sabatini, B. L., & Svoboda, K. (2000). Analysis of calcium channels in single spines using optical fluctuation analysis. *Nature, 408*(6812), 589-593. doi: 10.1038/35046076

Salter, M. W., & Kalia, L. V. (2004). Src kinases: a hub for NMDA receptor regulation. *Nat Rev Neurosci, 5*(4), 317-328. doi: 10.1038/nrn1368

Sasaki, Y. F., Rothe, T., Premkumar, L. S., Das, S., Cui, J., Talantova, M. V., . . . Lipton, S. A. (2002). Characterization and comparison of the NR3A subunit of the NMDA receptor in recombinant systems and primary cortical neurons. *J Neurophysiol, 87*(4), 2052-2063. doi: 10.1152/jn.00531.2001 [doi]

Schnupp, J. W., Hall, T. M., Kokelaar, R. F., & Ahmed, B. (2006). Plasticity of temporal pattern codes for vocalization stimuli in primary auditory cortex. *J Neurosci, 26*(18), 4785-4795. doi: 26/18/4785 [pii]

Schuett, S., Bonhoeffer, T., & Hubener, M. (2001). Pairing-induced changes of orientation maps in cat visual cortex. *Neuron, 32*(2), 325-337. doi: S0896-6273(01)00472-X [pii]

Seol, G. H., Ziburkus, J., Huang, S., Song, L., Kim, I. T., Takamiya, K., . . . Kirkwood, A. (2007). Neuromodulators control the polarity of spike-timing-dependent synaptic plasticity. *Neuron, 55*(6), 919-929. doi: S0896-6273(07)00626-5 [pii]

Shin, J. H., & Linden, D. J. (2005). An NMDA receptor/nitric oxide cascade is involved in cerebellar LTD but is not localized to the parallel fiber terminal. *J Neurophysiol, 94*(6), 4281-4289. doi: 10.1152/jn.00661.2005

Shouval, H. Z., Bear, M. F., & Cooper, L. N. (2002). A unified model of NMDA receptor-dependent bidirectional synaptic plasticity. *Proc Natl Acad Sci U S A, 99*(16), 10831-10836. doi: 10.1073/pnas.152343099 [doi]

Shu, Y., Hasenstaub, A., Duque, A., Yu, Y., & McCormick, D. A. (2006). Modulation of intracortical synaptic potentials by presynaptic somatic membrane potential. *Nature, 441*(7094), 761-765. doi: 10.1038/nature04720

Siegel, S. J., Brose, N., Janssen, W. G., Gasic, G. P., Jahn, R., Heinemann, S. F., & Morrison, J. H. (1994). Regional, cellular, and ultrastructural

distribution of N-methyl-D-aspartate receptor subunit 1 in monkey hippocampus. *Proc Natl Acad Sci U S A, 91*(2), 564-568.

Silberberg, G., & Markram, H. (2007). Disynaptic inhibition between neocortical pyramidal cells mediated by Martinotti cells. *Neuron, 53*(5), 735-746. doi: 10.1016/j.neuron.2007.02.012

Siucinska, E., & Kossut, M. (2004). Experience-dependent changes in cortical whisker representation in the adult mouse: a 2-deoxyglucose study. *Neuroscience, 127*(4), 961-971. doi: 10.1016/j.neuroscience.2004.06.004 [doi]

Sjostrom, P. J., & Hausser, M. (2006). A cooperative switch determines the sign of synaptic plasticity in distal dendrites of neocortical pyramidal neurons. *Neuron, 51*(2), 227-238. doi: S0896-6273(06)00471-5 [pii]

Sjostrom, P. J., Turrigiano, G. G., & Nelson, S. B. (2001). Rate, timing, and cooperativity jointly determine cortical synaptic plasticity. *Neuron, 32*(6), 1149-1164. doi: S0896-6273(01)00542-6 [pii]

Sjostrom, P. J., Turrigiano, G. G., & Nelson, S. B. (2003). Neocortical LTD via coincident activation of presynaptic NMDA and cannabinoid receptors. *Neuron, 39*(4), 641-654. doi: S0896627303004768 [pii]

Sjostrom, P. J., Turrigiano, G. G., & Nelson, S. B. (2004). Endocannabinoid-dependent neocortical layer-5 LTD in the absence of postsynaptic spiking. *J Neurophysiol, 92*(6), 3338-3343. doi: 10.1152/jn.00376.2004

Sjöström, P. J., Turrigiano, G. G., & Nelson, S. B. (2001). Rate, timing, and cooperativity jointly determine cortical synaptic plasticity. *Neuron, 32*(6), 1149-1164. doi: S0896-6273(01)00542-6 [pii]

Sjöström, P. J., Turrigiano, G. G., & Nelson, S. B. (2003). Neocortical LTD via coincident activation of presynaptic NMDA and cannabinoid receptors. *Neuron, 39*(4), 641-654. doi: S0896627303004768 [pii]

Smith, S. L., & Trachtenberg, J. T. (2007). Experience-dependent binocular competition in the visual cortex begins at eye opening. *Nat Neurosci, 10*(3), 370-375. doi: nn1844 [pii]

Smothers, C. T., & Woodward, J. J. (2003). Effect of the NR3 subunit on ethanol inhibition of recombinant NMDA receptors. *Brain Res, 987*(1), 117-121. doi: S0006899303033158 [pii]

Sobczyk, A., Scheuss, V., & Svoboda, K. (2005). NMDA receptor subunit-dependent [Ca2+] signaling in individual hippocampal dendritic spines. *J Neurosci, 25*(26), 6037-6046. doi: 10.1523/JNEUROSCI.1221-05.2005

Song, S., & Abbott, L. F. (2001). Cortical development and remapping through spike timing-dependent plasticity. *Neuron, 32*(2), 339-350. doi: S0896-6273(01)00451-2 [pii]

Speechley, W. J., Hogsden, J. L., & Dringenberg, H. C. (2007). Continuous white noise exposure during and after auditory critical period differentially alters bidirectional thalamocortical plasticity in rat auditory cortex in vivo. *Eur J Neurosci, 26*(9), 2576-2584. doi: EJN5857 [pii]

Spehlmann, R. (1971). Acetylcholine and the synaptic transmission of non-specific impulses to the visual cortex. *Brain, 94*(1), 139-150.

Sutton, M. A., Wall, N. R., Aakalu, G. N., & Schuman, E. M. (2004). Regulation of dendritic protein synthesis by miniature synaptic events. *Science, 304*(5679), 1979-1983. doi: 10.1126/science.1096202 [doi]

Tovar, K. R., McGinley, M. J., & Westbrook, G. L. (2013). Triheteromeric NMDA Receptors at Hippocampal Synapses. *Journal of Neuroscience, 33*(21), 9150-9160. doi: Doi 10.1523/Jneurosci.0829-13.2013

Tovar, K. R., & Westbrook, G. L. (1999). The incorporation of NMDA receptors with a distinct subunit composition at nascent hippocampal synapses in vitro. *Journal of Neuroscience, 19*(10), 4180-4188.

Traynelis, S. F., Wollmuth, L. P., McBain, C. J., Menniti, F. S., Vance, K. M., Ogden, K. K., . . . Dingledine, R. (2010). Glutamate receptor ion channels: structure, regulation, and function. *Pharmacol Rev, 62*(3), 405-496. doi: 10.1124/pr.109.002451

Tropea, D., Kreiman, G., Lyckman, A., Mukherjee, S., Yu, H., Horng, S., & Sur, M. (2006). Gene expression changes and molecular pathways mediating activity-dependent plasticity in visual cortex. *Nat Neurosci, 9*(5), 660-668. doi: 10.1038/nn1689

Tsien, J. Z., Huerta, P. T., & Tonegawa, S. (1996). The essential role of hippocampal CA1 NMDA receptor-dependent synaptic plasticity in spatial memory. *Cell, 87*(7), 1327-1338.

Tsubokawa, H., & Ross, W. N. (1997). Muscarinic modulation of spike backpropagation in the apical dendrites of hippocampal CA1 pyramidal neurons. *J Neurosci, 17*(15), 5782-5791

.

Tzounopoulos, T., Kim, Y., Oertel, D., & Trussell, L. O. (2004). Cell-specific, spike timing-dependent plasticities in the dorsal cochlear nucleus. *Nat Neurosci, 7*(7), 719-725. doi: 10.1038/nn1272 [doi]nn1272 [pii]

Ulbrich, M. H., & Isacoff, E. Y. (2008). Rules of engagement for NMDA receptor subunits. *Proc Natl Acad Sci U S A, 105*(37), 14163-14168. doi: 10.1073/pnas.0802075105

Urakubo, H., Honda, M., Froemke, R. C., & Kuroda, S. (2008). Requirement of an allosteric kinetics of NMDA receptors for spike timing-dependent plasticity. *J Neurosci, 28*(13), 3310-3323. doi: 28/13/3310 [pii]10.1523/JNEUROSCI.0303-08.2008 [doi]

Valverde, F. (1971). Rate and extent of recovery from dark rearing in the visual cortex of the mouse. *Brain Res, 33*(1), 1-11.

Vicini, S., Wang, J. F., Li, J. H., Zhu, W. J., Wang, Y. H., Luo, J. H., . . . Grayson, D. R. (1998). Functional and pharmacological differences between recombinant N-methyl-D-aspartate receptors. *J Neurophysiol, 79*(2), 555-566.

Wallace, W., & Bear, M. F. (2004). A morphological correlate of synaptic scaling in visual cortex. *J Neurosci, 24*(31), 6928-6938. doi: 10.1523/JNEUROSCI.1110-04.2004

Wang, L., Fontanini, A., & Maffei, A. (2012). Experience-dependent switch in sign and mechanisms for plasticity in layer 4 of primary visual cortex. *J Neurosci, 32*(31), 10562-10573. doi: 10.1523/JNEUROSCI.0622-12.2012

Wang, Y., Toledo-Rodriguez, M., Gupta, A., Wu, C., Silberberg, G., Luo, J., & Markram, H. (2004). Anatomical, physiological and molecular properties of Martinotti cells in the somatosensory cortex of the juvenile rat. *J Physiol, 561*(Pt 1), 65-90. doi: 10.1113/jphysiol.2004.073353

Watanabe, S., Hoffman, D. A., Migliore, M., & Johnston, D. (2002). Dendritic K+ channels contribute to spike-timing dependent long-term potentiation in hippocampal pyramidal neurons. *Proc Natl Acad Sci U S A, 99*(12), 8366-8371. doi: 10.1073/pnas.122210599 [doi]122210599 [pii]

Weinberger, N. M. (2003). The nucleus basalis and memory codes: auditory cortical plasticity and the induction of specific, associative behavioral memory. *Neurobiol Learn Mem, 80*(3), 268-284. doi: S1074742703000728 [pii]

Weinberger, N. M., Miasnikov, A. A., & Chen, J. C. (2006). The level of cholinergic nucleus basalis activation controls the specificity of auditory associative memory. *Neurobiol Learn Mem, 86*(3), 270-285. doi: S1074-7427(06)00052-9 [pii]10.1016/j.nlm.2006.04.004 [doi]

Wespatat, V., Tennigkeit, F., & Singer, W. (2004). Phase sensitivity of synaptic modifications in oscillating cells of rat visual cortex. *J Neurosci, 24*(41), 9067-9075. doi: 24/41/9067 [pii]10.1523/JNEUROSCI.2221-04.2004 [doi]

Whitfield, I. C. (1980). Auditory cortex and the pitch of complex tones. *J Acoust Soc Am, 67*(2), 644-647.

Wiesel, T. N., & Hubel, D. H. (1963). Single-Cell Responses in Striate Cortex of Kittens Deprived of Vision in One Eye. *J Neurophysiol, 26*, 1003-1017.

Wong, H. K., Liu, X. B., Matos, M. F., Chan, S. F., Perez-Otano, I., Boysen, M., . . . Sucher, N. J. (2002). Temporal and regional expression of NMDA receptor subunit NR3A in the mammalian brain. *J Comp Neurol, 450*(4), 303-317. doi: 10.1002/cne.10314 [doi]

Woodhall, G., Evans, D. I., Cunningham, M. O., & Jones, R. S. (2001). NR2B-containing NMDA autoreceptors at synapses on entorhinal cortical neurons. *J Neurophysiol, 86*(4), 1644-1651.

Xu, J., Pang, Z. P., Shin, O. H., & Sudhof, T. C. (2009). Synaptotagmin-1 functions as a Ca2+ sensor for spontaneous release. *Nat Neurosci, 12*(6), 759-766. doi: 10.1038/nn.2320

Yan, L., Imbrosci, B., Zhang, W., Neubacher, U., Hatt, H., Eysel, U. T., & Mittmann, T. (2012). Changes in NMDA-receptor function in the first week following laser-induced lesions in rat visual cortex. *Cereb Cortex, 22*(10), 2392-2403. doi: 10.1093/cercor/bhr318

Yang, J., Woodhall, G. L., & Jones, R. S. (2006). Tonic facilitation of glutamate release by presynaptic NR2B-containing NMDA receptors is increased in the entorhinal cortex of chronically epileptic rats. *J Neurosci, 26*(2), 406-410. doi: 26/2/406 [pii]10.1523/JNEUROSCI.4413-05.2006 [doi]

Yang, Y., DeWeese, M. R., Otazu, G. H., & Zador, A. M. (2008). Millisecond-scale differences in neural activity in auditory cortex can drive decisions. *Nat Neurosci, 11*(11), 1262-1263. doi: nn.2211 [pii]10.1038/nn.2211 [doi]

Yao, H., & Dan, Y. (2001). Stimulus timing-dependent plasticity in cortical processing of orientation. *Neuron, 32*(2), 315-323. doi: S0896-6273(01)00460-3 [pii]

Yao, Y., & Mayer, M. L. (2006). Characterization of a soluble ligand binding domain of the NMDA receptor regulatory subunit NR3A. *J Neurosci, 26*(17), 4559-4566. doi: 26/17/4559 [pii]10.1523/JNEUROSCI.0560-06.2006 [doi]

Yashiro, K., Corlew, R., & Philpot, B. D. (2005). Visual deprivation modifies both presynaptic glutamate release and the composition of

perisynaptic/extrasynaptic NMDA receptors in adult visual cortex. *J Neurosci, 25*(50), 11684-11692. doi: 25/50/11684 [pii]10.1523/JNEUROSCI.4362-05.2005 [doi]

Yazaki-Sugiyama, Y., Kang, S., Cateau, H., Fukai, T., & Hensch, T. K. (2009). Bidirectional plasticity in fast-spiking GABA circuits by visual experience. *Nature, 462*(7270), 218-221. doi: nature08485 [pii]10.1038/nature08485 [doi]

Zhang, J. C., Lau, P. M., & Bi, G. Q. (2009). Gain in sensitivity and loss in temporal contrast of STDP by dopaminergic modulation at hippocampal synapses. *Proc Natl Acad Sci U S A, 106*(31), 13028-13033. doi: 0900546106 [pii]10.1073/pnas.0900546106 [doi]

Zhou, Q., Tao, H. W., & Poo, M. M. (2003). Reversal and stabilization of synaptic modifications in a developing visual system. *Science, 300*(5627), 1953-1957. doi: 10.1126/science.1082212300/5627/1953 [pii]

Zilberter, M., Holmgren, C., Shemer, I., Silberberg, G., Grillner, S., Harkany, T., & Zilberter, Y. (2009). Input specificity and dependence of spike timing-dependent plasticity on preceding postsynaptic activity at unitary connections between neocortical layer 2/3 pyramidal cells. *Cereb Cortex, 19*(10), 2308-2320. doi: 10.1093/cercor/bhn247

Zucker, R. S., & Regehr, W. G. (2002). Short-term synaptic plasticity. *Annu Rev Physiol, 64*, 355-405. doi: 10.1146/annurev.physiol.64.092501.114547